AFGL-TR-82-0205

A FOURTH ORDER ENERGY AND POTENTIAL ENSTROPHY CONSERVING DIFFERENCE SCHEME

Kenji Takano
M.G. Wurtele

Department of Atmospheric Sciences
University of California, Los Angeles
405 Hilgard Avenue
Los Angeles, California 90024

Final Report
Sept. 1978-Sept. 1981

June 1982

AD A126626

Approved for public release; distribution unlimited

DTIC
APR 1 1 1983
H

AIR FORCE GEOPHYSICS LABORATORY
AIR FORCE SYSTEMS COMMAND
UNITED STATES AIR FORCE
HANSCOM AFB, MASSACHUSETTS 01731

DTIC FILE COPY

83 04 11 092

REPORT DOCUMENTATION PAGE

READ INSTRUCTIONS BEFORE COMPLETING FORM

1. REPORT NUMBER: AFGL-TR-82-0205	2. GOVT ACCESSION NO.: AD-A126626
3. RECIPIENT'S CATALOG NUMBER:	
4. TITLE (and Subtitle): A FOURTH ORDER ENERGY AND POTENTIAL ENSTROPHY CONSERVING DIFFERENCE SCHEME	5. TYPE OF REPORT & PERIOD COVERED: Final Report Sept. 1978-Sept. 1981
	6. PERFORMING ORG. REPORT NUMBER:
7. AUTHOR(s): Kenji Takano M. G. Wurtele	8. CONTRACT OR GRANT NUMBER(s): F19628-78-C-0129
9. PERFORMING ORGANIZATION NAME AND ADDRESS: University of California, Los Angeles 405 Hilgard Avenue Los Angeles, California 90024	10. PROGRAM ELEMENT, PROJECT, TASK AREA & WORK UNIT NUMBERS: 61102F 2310G2AK
11. CONTROLLING OFFICE NAME AND ADDRESS: Air Force Geophysics Laboratory Hanscom AFB, Massachusetts 01731 Monitor/C. H. Yang/LYD	12. REPORT DATE: June 1982
	13. NUMBER OF PAGES: 85
14. MONITORING AGENCY NAME & ADDRESS (if different from Controlling Office)	15. SECURITY CLASS. (of this report): Unclassified
	15a. DECLASSIFICATION DOWNGRADING SCHEDULE

16. DISTRIBUTION STATEMENT (of this Report)

Approved for public release; distribution unlimited

17. DISTRIBUTION STATEMENT (of the abstract entered in Block 20, if different from Report)

18. SUPPLEMENTARY NOTES

19. KEY WORDS (Continue on reverse side if necessary and identify by block number)

1. Difference schemes, fourth order
2. Shallow water equations, numerical integration of
3. General circulation model, difference scheme for

20. ABSTRACT (Continue on reverse side if necessary and identify by block number)

A horizontal difference scheme that conserves both potential enstrophy and energy for general flow and, in addition, yields fourth-order accuracy for the advection of potential vorticity in case of non-divergent flow, is derived for the shallow water equations on the staggered grid as a simple extension of the second-order potential enstrophy and energy conserving scheme presented by Arakawa and Lamb (1981). This fourth-order scheme is derived both for a Cartesian grid and for a spherical grid.

Comparison by means of numerical experiments between the newly derived scheme

DD FORM 1 JAN 73 1473

20. (continued)

and the second-order scheme showed the distinct advantage of the new scheme in giving better development and faster moving speed of the low.

ABSTRACT

A horizontal difference scheme that conserves both potential enstrophy and energy for general flow and, in addition, yields fourth-order accuracy for the advection of potential vorticity in case of non-divergent flow, is derived for the shallow water equations on the staggered grid as a simple extension of the second-order potential enstrophy and energy conserving scheme presented by Arakawa and Lamb (1981). This fourth-order scheme is derived both for a Cartesian grid and for a spherical grid.

Comparison by means of numerical experiments between the newly derived scheme and the second-order scheme showed the distinct advantage of the new scheme in giving better development and faster moving speed of the law.

DTIC COPY INSPECTED

Accession For
NTIS GRA&I
DTIC TAB
Unannounced
Justification
By
Distribution/
Availability Codes
Dist | Avail and/or Special
A

I. Introduction

Recently Arakawa and Lamb (1981) (hereafter AL) derived a second-order potential enstrophy and energy conserving scheme for the shallow water equations in order to improve the simulation of nonlinear aspects of the flow over steep topography. Their numerical experiments showed the advantages of the scheme over the (potential) enstrophy conserving scheme for horizontal nondivergent flow, not only in suppressing a spurious energy cascade but also in determining the overall flow regime.

A new horizontal difference scheme presented in this paper was derived as a simple extension of their scheme focused on the increase of the finite difference accuracy. The scheme, of course, was designed to conserve both potential enstrophy and energy for general flow and, in addition, to give fourth-order accuracy for the advection of potential vorticity in case of non divergent flow; the advection term leads to a fourth-order Jacobian proposed by Arakawa (1966).

In Section 2, the shallow water equations are presented and derivation method of the fourth-order scheme is outlined. The method is much the same as used in AL. The derivation of the scheme is performed in Section 3. The advantage of this fourth-order scheme is demonstrated in Section 4 through a comparison, by means of numerical time integration, with the second-order scheme by AL. The appendix presents the scheme for a spherical grid that can be derived by analogy to the procedure in Section 3.

2. Outline of the derivation procedure.

The governing differential equations for quasi-static motion in a homogeneous incompressible fluid with a free surface can be written as

$$\frac{\partial \mathbf{V}}{\partial t} + q\mathbf{k}\times\mathbf{V}^* + \nabla(K+\Phi) = 0 \qquad (2.1)$$

$$\frac{\partial h}{\partial t} + \nabla \cdot \mathbf{V}^* = 0 \qquad (2.2)$$

Here t is the time, ∇ the horizontal del operator, $\mathbf{k}$ the vertical unit vector, $\mathbf{V}$ the horizontal velocity, h the vertical extent of a fluid column above the bottom surface and the (absolute) potential vorticity q, the mass flux $\mathbf{V}^*$, the kinetic energy per unit mass K and Φ are defined by

$$q \equiv (f + \zeta) h^{-1} \qquad (2.3)$$

$$\mathbf{V}^* \equiv h\mathbf{V} \qquad (2.4)$$

$$K \equiv \tfrac{1}{2} V^2 \qquad (2.5)$$

$$\Phi \equiv g(h + h_s) \qquad (2.6)$$

Here ζ is the vorticity, $\mathbf{k} \cdot \nabla \times \mathbf{V}$, f the Coriolis parameter, g the gravitational acceleration and h_s the bottom surface height.

After some multiplications the equations for the time change of total kinetic energy and potential energy in this fluid may be expressed as:

$$\frac{\partial}{\partial t}(hK) + \nabla \cdot (\mathbf{V}^* K) + \mathbf{V}^* \cdot \nabla \Phi = 0 \qquad (2.7)$$

and

$$\frac{\partial}{\partial t}(\tfrac{1}{2} g h^2 + g h h_s) + \nabla \cdot (\mathbf{V}^* \Phi) - \mathbf{V}^* \cdot \nabla \Phi = 0 \qquad (2.8)$$

The summation of (2.7) and (2.8) then yields a statement of the conservation of total energy.

$$\frac{\partial}{\partial t}\overline{[h(K+\tfrac{1}{2}gh+gh_s)]} = 0 \tag{2.9}$$

where the overbar denotes the mean over an infinite domain or a closed domain. Here it should be noted that the term in (2.1) involving q does not contribute to the change of total kinetic energy and the last term in (2.7) and (2.8) cancel in giving (2.9). These two points must be taken into account in the construction of the finite-difference scheme.

The vorticity equation for this fluid motion may be written in the form

$$\frac{\partial}{\partial t}(hq) + \nabla\cdot(V^* q) = 0 \tag{2.10}$$

and then we obtain the potential vorticity advection equation.

$$\frac{\partial q}{\partial t} + V\cdot\nabla q = 0 \tag{2.11}$$

Thus in the absence of spatial gradients of q there should be no time change of q. This condition will be also used to construct the finite-difference scheme.

Now hq times (2.11) plus 1/2 q^2 times (2.2) gives the equation for time change of potential enstrophy

$$\frac{\partial}{\partial t}(h\tfrac{1}{2}q^2) + \nabla\cdot(V^*\tfrac{1}{2}q^2) = 0 \tag{2.12}$$

which leads to a statement of the conservation of potential enstrophy,

$$\frac{\partial}{\partial t}\overline{(h\,\tfrac{1}{2}q^2)} = 0 \tag{2.13}$$

Our present purpose is to derive such a finite-difference scheme for the momentum equation (2.1) that i) it is consistent with a reasonable advection scheme for potential vorticity advection equation (2.11); ii) it guarantees conservation of total energy (2.9) and potential enstrophy (2.13) for the general case of divergent mass flux; and iii) it has fourth-order accuracy for the advection of potential vorticity when flow is horizontal and nondivergent.

The derivation of the scheme is performed along the following line. First, we can derive the same constraint as in AL for the total energy conservation, by the application of requirements discussed in this section to a general difference scheme for (2.1). Then, since the scheme still retains a high degree of freedom, we further impose the following requirements to fix the scheme.

1) When q in the finite-difference analog of (2.11) is constant in space, there is no time change of q.

2) To guarantee conservation of potential enstrophy the finite-difference analog of (2.13) must hold.

3) In case of the nondivergent mass flux advection scheme for (2.1) leads to the Arakawa fourth-order Jacobian (Arakawa, 1966).

4) The symmetry between the Cartesian components of the momentum equations for the case of a square grid must be retained.

3. Derivation of the fourth-order scheme

The arrangement of the variables and the indices on the square grid to be used in this derivation, called the C grid, is shown in Fig. 1. Here u and v are the Cartesian components of $\mathbf{V}$ in x and y directions, respectively.

The second-order differencing for the continuity equation (2.2) can be written

$$\frac{\partial}{\partial t} h_{i+\frac{1}{2},j+\frac{1}{2}} + (\nabla \cdot \mathbf{V}^*)_{i+\frac{1}{2},j+\frac{1}{2}} = 0 \tag{3.1}$$

where

$$(\nabla \cdot \mathbf{V}^*)_{i+\frac{1}{2},j+\frac{1}{2}} \equiv \frac{1}{d}\left[u^*_{i+1,j+\frac{1}{2}} - u^*_{i,j+\frac{1}{2}} + v^*_{i+\frac{1}{2},j+1} - v^*_{i+\frac{1}{2},j} \right] \tag{3.2}$$

$$u^*_{i,j+\frac{1}{2}} \equiv \left[h^{(u)} u \right]_{i,j+\frac{1}{2}} \tag{3.3}$$

$$v^*_{i+\frac{1}{2},j} \equiv \left[h^{(v)} v \right]_{i+\frac{1}{2},j} \tag{3.4}$$

and we choose

$$h^{(u)}_{i,j+\frac{1}{2}} \equiv \left(\bar{h}^{i} \right)_{i,j+\frac{1}{2}} \tag{3.5}$$

$$h^{(v)}_{i+\frac{1}{2},j} \equiv \left(\bar{h}^{j} \right)_{i+\frac{1}{2},j} \tag{3.6}$$

here overbars - i and - j denote the arithmetic average of two neighboring points in x and y directions respectively.

The general fourth-order scheme for the Cartesian components of the momentum equation (2.1) may be written.

$$\frac{\partial}{\partial t} u_{i,j+\frac{1}{2}} - \alpha_{i,j+\frac{1}{2}} v^*_{i+\frac{1}{2},j+1} - \beta_{i,j+\frac{1}{2}} v^*_{i-\frac{1}{2},j+1} - \gamma_{i,j+\frac{1}{2}} v^*_{i-\frac{1}{2},j}$$
$$- \delta_{i,j+\frac{1}{2}} v^*_{i+\frac{1}{2},j} + \varepsilon_{i+\frac{1}{2},j+\frac{1}{2}} u^*_{i+1,j+\frac{1}{2}} - \varepsilon_{i-\frac{1}{2},j+\frac{1}{2}} u^*_{i-1,j+\frac{1}{2}}$$
$$+ \lambda_{i,j+1} u^*_{i,j+1\frac{1}{2}} - \lambda_{i,j} u^*_{i,j-\frac{1}{2}} + d^{-1}[(K+\Phi)_{i+\frac{1}{2},j+\frac{1}{2}}$$
$$- (K+\Phi)_{i-\frac{1}{2},j+\frac{1}{2}}] = 0 \quad . \tag{3.7}$$

$$\frac{\partial}{\partial t} v_{i+\frac{1}{2},j} + \gamma_{i+1,j+\frac{1}{2}} u^*_{i+1,j+\frac{1}{2}} + \delta_{i,j+\frac{1}{2}} u^*_{i,j+\frac{1}{2}} + \alpha_{i,j-\frac{1}{2}} u^*_{i,j-\frac{1}{2}}$$
$$+ \beta_{i+1,j-\frac{1}{2}} u^*_{i+1/j-\frac{1}{2}} + \phi_{i+\frac{1}{2},j+\frac{1}{2}} v^*_{i+\frac{1}{2},j+1} - \phi_{i+\frac{1}{2},j-\frac{1}{2}} v^*_{i+\frac{1}{2},j-1}$$
$$+ \mu_{i+1,j} v^*_{i+1\frac{1}{2},j} - \mu_{i,j} v^*_{i-\frac{1}{2},j} + d^{-1}[(K+\Phi)_{i+\frac{1}{2},j+\frac{1}{2}}$$
$$- (K+\Phi)_{i+\frac{1}{2},j-\frac{1}{2}}] = 0 , \tag{3.8}$$

where K defined at the h points is specified by

$$K_{i+\frac{1}{2},j+\frac{1}{2}} = [\overline{\overline{1/2\, u^2}^{\,i}} + \overline{\overline{1/2\, v^2}^{\,j}})_{i+\frac{1}{2},j+\frac{1}{2}} \tag{3.9}$$

Equations (3.5), (3.6), and (3.9) are designed to maintain conservation of total kinetic energy for the divergent mass flux (AL). The symbols α, β, γ, δ, ε, ϕ, λ and μ are linear combinations of the q. λ and μ give additional generality to the fourth-order scheme. Note that the terms involving q cancel by virtue of their form when we derive the equation for the time change of total kinetic energy.

Application of (3.7) and (3.8) at the points surrounding a ζ

point gives the finite-difference vorticity equation consistent with this scheme

$$\begin{aligned}\frac{\partial}{\partial t}(h^{(q)}q)_{i,j} = \frac{1}{d}\Big[&-v^*_{i+\frac12,j+1}(\alpha_{i,j+\frac12}+\phi_{i+\frac12,j+\frac12})-v^*_{i-\frac12,j+1}(\beta_{i,j+\frac12}-\phi_{i-\frac12,j+\frac12})\\&+v^*_{i+\frac12,j}(\alpha_{i,j-\frac12}-\delta_{i,j+\frac12}+\mu_{i,j})+v^*_{i-\frac12,j}(\beta_{i,j-\frac12}-\gamma_{i,j+\frac12}+\mu_{i,j})\\&+v^*_{i+\frac12,j-1}(\delta_{i,j-\frac12}+\phi_{i+\frac12,j-\frac12})+v^*_{i-\frac12,j-1}(\gamma_{i,j-\frac12}-\phi_{i-\frac12,j-\frac12})\\&-v^*_{i-1\frac12,j}(\mu_{i-1,j})-v^*_{i+1\frac12,j}(\mu_{i+1,j})\\&-u^*_{i+1,j+\frac12}(\gamma_{i+1,j+\frac12}-\varepsilon_{i+\frac12,j+\frac12})-u^*_{i,j+\frac12}(\delta_{i,j+\frac12}-\gamma_{i,j+\frac12}+\lambda_{i,j})\\&+u^*_{i-1,j+\frac12}(\delta_{i-1,j+\frac12}-\varepsilon_{i-\frac12,j+\frac12})-u^*_{i+1,j-\frac12}(\beta_{i+1,j-\frac12}+\varepsilon_{i+\frac12,j-\frac12})\\&-u^*_{i,j-\frac12}(\alpha_{i,j-\frac12}-\beta_{i,j-\frac12}+\lambda_{i,j})+u^*_{i-1,j-\frac12}(\alpha_{i-1,j-\frac12}+\varepsilon_{i-\frac12,j-\frac12})\\&+u^*_{i,j-1\frac12}(\lambda_{i,j-1})+u^*_{i,j+1\frac12}(\lambda_{i,j+1})\Big],\end{aligned} \tag{3.10}$$

where the vorticity change has been expressed $\frac{\partial}{\partial t}(h^{(q)}q)_{i,j}$ with

$$q_{i,j} \equiv \frac{(f+\zeta)_{i,j}}{h^{(q)}_{i,j}} \tag{3.11}$$

$$\zeta_{i,j} \equiv d^{-1}\left[u_{i,j-\frac12}-u_{i,j+\frac12}+v_{i+\frac12,j}-v_{i-\frac12,j}\right] \tag{3.12}$$

and $h^{(q)}$ is a linear combination of h, as yet unspecified.

Now we impose the first requirement, to wit, that $\partial q/\partial t$ vanish when q is formally set equal to a constant on the right-hand side of (3.10), regardless of the constant. If we write α, β, γ, δ, ε, ϕ, λ, and μ in general form as linear combination of the surrounding q:

$$
\left.
\begin{aligned}
\begin{pmatrix}\alpha\\ \beta\\ \gamma\\ \delta\end{pmatrix}_{i,j+\frac{1}{2}} &= \begin{pmatrix}\alpha\\ \beta\\ \gamma\\ \delta\end{pmatrix}^{(1)} q_{i+1,j+1} + \begin{pmatrix}\alpha\\ \beta\\ \gamma\\ \delta\end{pmatrix}^{(2)} q_{i,j+1} + \begin{pmatrix}\alpha\\ \beta\\ \gamma\\ \delta\end{pmatrix}^{(3)} q_{i-1,j+1} + \begin{pmatrix}\alpha\\ \beta\\ \gamma\\ \delta\end{pmatrix}^{(4)} q_{i-1,j} \\
&\quad + \begin{pmatrix}\alpha\\ \beta\\ \gamma\\ \delta\end{pmatrix}^{(5)} q_{i,j} + \begin{pmatrix}\alpha\\ \beta\\ \gamma\\ \delta\end{pmatrix}^{(6)} q_{i+1,j} + \begin{pmatrix}\alpha\\ \beta\\ \gamma\\ \delta\end{pmatrix}^{(7)} q_{i,j+2} + \begin{pmatrix}\alpha\\ \beta\\ \gamma\\ \delta\end{pmatrix}^{(8)} q_{i,j-1} \\
\begin{pmatrix}\varepsilon\\ \phi\end{pmatrix}_{i+\frac{1}{2},j+\frac{1}{2}} &= \begin{pmatrix}\varepsilon\\ \phi\end{pmatrix}^{(1)} q_{i+1,j+1} + \begin{pmatrix}\varepsilon\\ \phi\end{pmatrix}^{(2)} q_{i,j+1} + \begin{pmatrix}\varepsilon\\ \phi\end{pmatrix}^{(3)} q_{i,j} + \begin{pmatrix}\varepsilon\\ \phi\end{pmatrix}^{(4)} q_{i+1,j} \\
\begin{pmatrix}\lambda\\ \mu\end{pmatrix}_{i,j} &= \begin{pmatrix}\lambda\\ \mu\end{pmatrix}^{(1)} q_{i,j+1} + \begin{pmatrix}\lambda\\ \mu\end{pmatrix}^{(2)} q_{i-1,j} + \begin{pmatrix}\lambda\\ \mu\end{pmatrix}^{(3)} q_{i,j-1} + \begin{pmatrix}\lambda\\ \mu\end{pmatrix}^{(4)} q_{i+1,j}
\end{aligned}
\right\} \quad (3.13)
$$

then when q is formally set equal to a constant, (3.10) can be written as

$$
\begin{aligned}
\frac{\partial}{\partial t} h_{i,j}^{(8)} = -\frac{1}{d}\big[&(A+F)(v^*_{i+\frac{1}{2},j+1} - v^*_{i+\frac{1}{2},j}) + (C-E)(u^*_{i+1,j+\frac{1}{2}} - u^*_{i,j+\frac{1}{2}}) \\
&+ (B-F)(v^*_{i-\frac{1}{2},j+1} - v^*_{i-\frac{1}{2},j}) + (D-E)(u^*_{i,j+\frac{1}{2}} - u^*_{i-1,j+\frac{1}{2}}) \\
&+ (C-F)(v^*_{i-\frac{1}{2},j} - v^*_{i-\frac{1}{2},j-1}) + (A+E)(u^*_{i,j-\frac{1}{2}} - u^*_{i-1,j-\frac{1}{2}}) \\
&+ (D+F)(v^*_{i+\frac{1}{2},j} - v^*_{i+\frac{1}{2},j-1}) + (B+E)(u^*_{i+1,j-\frac{1}{2}} - u^*_{i,j-\frac{1}{2}}) \\
&+ M(v^*_{i+\frac{1}{2},j} + v^*_{i-\frac{1}{2},j} - v^*_{i-1\frac{1}{2},j} - v^*_{i+1\frac{1}{2},j}) \\
&- L(u^*_{i,j+\frac{1}{2}} + u^*_{i,j-\frac{1}{2}} - u^*_{i,j-1\frac{1}{2}} - u^*_{i,j+1\frac{1}{2}})\big]
\end{aligned}
\quad (3.14)
$$

where $A \equiv \sum_K \alpha^{(K)}$, $B \equiv \sum_K \beta^{(K)}$, etc.

In the case of a square grid, for simplicity and geometrical symmetry, $h^{(q)}$ is defined as

$$h^{(q)}_{i,j} = \frac{1}{4}\left(h_{i+\frac{1}{2},j+\frac{1}{2}} + h_{i-\frac{1}{2},j+\frac{1}{2}} + h_{i-\frac{1}{2},j-\frac{1}{2}} + h_{i+\frac{1}{2},j+\frac{1}{2}} \right) \tag{3.15}$$

Then from (3.1) and (3.15) we can write

$$\begin{aligned} \frac{\partial}{\partial t} h^{(q)}_{i,j} = -\frac{1}{4d}\Big[& \left(v^*_{i+\frac{1}{2},j+1} - v^*_{i+\frac{1}{2},j} + u^*_{i+1,j+\frac{1}{2}} - u^*_{i,j+\frac{1}{2}} \right) \\ & + \left(v^*_{i-\frac{1}{2},j+1} - v^*_{i-\frac{1}{2},j} + u^*_{i,j+\frac{1}{2}} - u^*_{i-1,j+\frac{1}{2}} \right) \\ & + \left(v^*_{i-\frac{1}{2},j} - v^*_{i-\frac{1}{2},j-1} + u^*_{i,j-\frac{1}{2}} - u^*_{i-1,j+\frac{1}{2}} \right) \\ & + \left(v^*_{i+\frac{1}{2},j} - v^*_{i+\frac{1}{2},j+1} + u^*_{i+1,j-\frac{1}{2}} - u^*_{i,j-\frac{1}{2}} \right) \Big] \end{aligned} \tag{3.16}$$

Comparison of (3.14) and (3.16) yields the constraints,

$$A = B = C = D = 1/4,\ E = F = L = M = 0 \tag{3.17}$$

For the requirements 2), that potential enstrophy be conserved in finite difference form, we formally rewrite the vorticity equation as:

$$\frac{\partial}{\partial t}(h^{(q)} q)_{i,j} + \sum_{i',j' \neq 0} a_{i,j:\,i+i',j+j'}\, q_{i+i',j+j'} + b_{i,j}\, q_{i,j} = 0 \tag{3.18}$$

where $a_{i,j}$ and $b_{i,j}$ are linear combination of U^* and V^*. Then according to AL the necessary and sufficient conditions for the conservation of potential enstrophy in divergent flow can be formulated as

$$a_{i,j:\,i+i',j+j'} = -\,a_{i+i',j+j':\,i,j} \tag{3.19}$$

$$b_{i,j} = \sum_{i',j' \neq 0} a_{i,j:\,i+i',j+j'} \tag{3.20}$$

To impose these constraints we use (3.13) to rewrite (3.10) explicitly in the form given by (3.18) and obtain the following:

$$
\begin{aligned}
b_{i,j} = {} & (\alpha^{(2)} - \delta^{(5)})\, v^*_{i+\frac{1}{2},j} + (\beta^{(2)} - \gamma^{(5)})\, v^*_{i-\frac{1}{2},j} + (\delta^{(2)} + \phi^{(2)})\, v^*_{i+\frac{1}{2},j-1} \\
& + (\gamma^{(2)} - \phi^{(1)})\, v^*_{i-\frac{1}{2},j-1} - (\alpha^{(5)} + \phi^{(3)})\, v^*_{i+\frac{1}{2},j+1} - (\beta^{(5)} - \phi^{(4)})\, v^*_{i-\frac{1}{2},j+1} \\
& - \mu^{(4)} v^*_{i-1\frac{1}{2},j} - \mu^{(2)} v^*_{i+1\frac{1}{2},j} \\
& - (\gamma^{(4)} - \varepsilon^{(3)})\, u^*_{i+1,j+\frac{1}{2}} - (\delta^{(5)} - \gamma^{(5)})\, u^*_{i,j+\frac{1}{2}} + (\delta^{(6)} - \varepsilon^{(4)})\, u^*_{i-1,j+\frac{1}{2}} \\
& - (\beta^{(3)} + \varepsilon^{(2)})\, u^*_{i+1,j-\frac{1}{2}} - (\alpha^{(2)} - \beta^{(2)})\, u^*_{i,j-\frac{1}{2}} + (\alpha^{(1)} + \varepsilon^{(1)})\, u^*_{i-1,j-\frac{1}{2}} \\
& + \lambda^{(1)} u^*_{i,j-1\frac{1}{2}} + \lambda^{(3)} u^*_{i,j+1\frac{1}{2}}
\end{aligned}
\tag{3.21}
$$

$$
\left.
\begin{aligned}
a_{i,j:i+1,j} = {} & (\alpha^{(1)} - \delta^{(6)} + \mu^{(4)})\, v^*_{i+\frac{1}{2},j} + (\beta^{(1)} - \gamma^{(6)} + \mu^{(6)})\, v^*_{i-\frac{1}{2},j} \\
& + (\delta^{(1)} + \phi^{(1)})\, v^*_{i+\frac{1}{2},j-1} + \gamma^{(1)} v^*_{i-\frac{1}{2},j-1} - (\alpha^{(6)} + \phi^{(4)})\, v^*_{i+\frac{1}{2},j+1} \\
& - \beta^{(6)} v^*_{i-\frac{1}{2},j+1} - (\gamma^{(5)} - \varepsilon^{(4)})\, u^*_{i+1,j+\frac{1}{2}} - (\delta^{(6)} - \gamma^{(6)} + \lambda^{(4)})\, u^*_{i,j+\frac{1}{2}} \\
& - (\beta^{(2)} + \varepsilon^{(1)})\, u^*_{i+1,j-\frac{1}{2}} - (\alpha^{(1)} - \beta^{(1)} + \lambda^{(4)})\, u^*_{i,j-\frac{1}{2}} \\
a_{i,j:i-1,j} = {} & (\alpha^{(3)} - \delta^{(4)} + \mu^{(2)})\, v^*_{i+\frac{1}{2},j} + (\beta^{(3)} - \gamma^{(4)} + \mu^{(2)})\, v^*_{i-\frac{1}{2},j} \\
& + \delta^{(3)} v^*_{i+\frac{1}{2},j-1} + (\gamma^{(3)} - \phi^{(2)})\, v^*_{i-\frac{1}{2},j-1} - \alpha^{(4)} v^*_{i+\frac{1}{2},j+1} \\
& - (\beta^{(4)} - \phi^{(3)})\, v^*_{i-\frac{1}{2},j+1} - (\delta^{(4)} - \gamma^{(4)} + \lambda^{(2)})\, u^*_{i,j+\frac{1}{2}} + (\delta^{(5)} - \varepsilon^{(3)})\, u^*_{i-1,j+\frac{1}{2}} \\
& - (\alpha^{(3)} - \beta^{(3)} + \lambda^{(2)})\, u^*_{i,j-\frac{1}{2}} + (\alpha^{(2)} - \varepsilon^{(2)})\, u^*_{i-1,j+\frac{1}{2}} \\
a_{i,j:i,j+1} = {} & (\alpha^{(7)} - \delta^{(2)} + \mu^{(1)})\, v^*_{i+\frac{1}{2},j} + (\beta^{(7)} - \gamma^{(2)} + \mu^{(1)})\, v^*_{i-\frac{1}{2},j} \\
& + \delta^{(7)} v^*_{i+\frac{1}{2},j-1} + \gamma^{(7)} v^*_{i-\frac{1}{2},j-1} - (\alpha^{(2)} + \phi^{(2)})\, v^*_{i+\frac{1}{2},j+1} \\
& - (\beta^{(2)} - \phi^{(1)}) v^*_{i-\frac{1}{2},j+1} - (\gamma^{(3)} - \varepsilon^{(2)})\, u^*_{i+1,j+\frac{1}{2}} - (\delta^{(2)} - \gamma^{(2)} + \lambda^{(1)})\, u^*_{i,j+\frac{1}{2}} \\
& - (\alpha^{(9)} - \beta^{(9)} + \lambda^{(1)})\, u^*_{i,j-\frac{1}{2}} + (\delta^{(1)} - \varepsilon^{(1)})\, u^*_{i-1,j+\frac{1}{2}} \\
a_{i,j:i,j-1} = {} & (\alpha^{(5)} - \delta^{(8)} + \mu^{(3)})\, v^*_{i+\frac{1}{2},j} + (\beta^{(5)} - \gamma^{(8)} + \mu^{(3)})\, v^*_{i-\frac{1}{2},j} \\
& + (\delta^{(5)} + \phi^{(3)})\, v^*_{i+\frac{1}{2},j-1} + (\gamma^{(5)} - \phi^{(\infty)})\, v^*_{i-\frac{1}{2},j-1} - \alpha^{(8)} v^*_{i+\frac{1}{2},j+1} \\
& - \beta^{(8)} v^*_{i-\frac{1}{2},j+1} - (\delta^{(8)} - \gamma^{(8)} + \lambda^{(3)})\, u^*_{i,j+\frac{1}{2}} - (\beta^{(4)} + \varepsilon^{(3)})\, u^*_{i+1,j-\frac{1}{2}} \\
& - (\alpha^{(5)} - \beta^{(5)} + \lambda^{(3)})\, u^*_{i,j-\frac{1}{2}} + (\alpha^{(6)} + \varepsilon^{(4)})\, u^*_{i-1,j-\frac{1}{2}}
\end{aligned}
\right\}
\tag{3.22}
$$

$$
\begin{aligned}
a_{i,j:\,i+1,j+1} &= -\delta^{(1)} v^*_{i+\frac{1}{2},j} - \gamma^{(1)} v^*_{i-\frac{1}{2},j} - (\alpha^{(1)} + \phi^{(1)}) v^*_{i+\frac{1}{2},j+1} \\
&\quad - \beta^{(1)} v^*_{i-\frac{1}{2},j+1} - \mu^{(1)} v^*_{i+1\frac{1}{2},j} - (\gamma^{(2)} - \varepsilon^{(1)}) u^*_{i+1,j+\frac{1}{2}} \\
&\quad - (\delta^{(1)} - \gamma^{(1)}) u^*_{i,j+\frac{1}{2}} - \beta^{(7)} u^*_{i+1,j-\frac{1}{2}} + \lambda^{(4)} u^*_{i,j+1\frac{1}{2}} \\
a_{i,j:\,i-1,j-1} &= \alpha^{(4)} v^*_{i+\frac{1}{2},j} + \beta^{(4)} v^*_{i-\frac{1}{2},j} + (\gamma^{(4)} - \phi^{(3)}) v^*_{i-\frac{1}{2},j-1} \\
&\quad + \delta^{(4)} v^*_{i+\frac{1}{2},j-1} - \mu^{(8)} v^*_{i-1\frac{1}{2},j} + (\alpha^{(5)} + \varepsilon^{(3)}) u^*_{i-1,j-\frac{1}{2}} \\
&\quad - (\alpha^{(4)} - \beta^{(4)}) u^*_{i,j-\frac{1}{2}} + \delta^{(8)} u^*_{i-1,j+\frac{1}{2}} + \lambda^{(2)} u^*_{i,j-1\frac{1}{2}} \\
a_{i,j:\,i-1,j+1} &= -\delta^{(3)} v^*_{i+\frac{1}{2},j} - \gamma^{(3)} v^*_{i-\frac{1}{2},j} - \alpha^{(3)} v^*_{i+\frac{1}{2},j+1} \\
&\quad - (\beta^{(3)} - \phi^{(2)}) v^*_{i-\frac{1}{2},j+1} - \mu^{(1)} v^*_{i-1\frac{1}{2},j} - (\delta^{(3)} - \gamma^{(3)}) u^*_{i,j+\frac{1}{2}} \\
&\quad + (\delta^{(2)} - \varepsilon^{(2)}) u^*_{i-1,j+\frac{1}{2}} + \alpha^{(7)} u^*_{i-1,j-\frac{1}{2}} + \lambda^{(2)} u^*_{i,j+1\frac{1}{2}} \\
a_{i,j:\,i+1,j-1} &= \alpha^{(6)} v^*_{i+\frac{1}{2},j} + \beta^{(6)} v^*_{i-\frac{1}{2},j} + (\delta^{(6)} + \phi^{(4)})_{i+\frac{1}{2},j-1} \\
&\quad + \gamma^{(4)} v^*_{i-\frac{1}{2},j-1} - \mu^{(3)} v^*_{i+1\frac{1}{2},j} - \delta^{(8)} u^*_{i+1,j+\frac{1}{2}} \\
&\quad - (\beta^{(5)} + \varepsilon^{(4)}) u^*_{i+1,j-\frac{1}{2}} - (\alpha^{(6)} - \beta^{(6)}) u^*_{i,j-\frac{1}{2}} + \lambda^{(4)} u^*_{i,j-1\frac{1}{2}} \\
a_{i,j:\,i+2,j} &= -\mu^{(4)} v^*_{i+1\frac{1}{2},j} - \gamma^{(6)} u^*_{i+1,j+\frac{1}{2}} - \beta^{(1)} u^*_{i+1,j-\frac{1}{2}} \\
a_{i,j:\,i-2,j} &= -\mu^{(2)} v^*_{i-1\frac{1}{2},j} + \alpha^{(3)} u^*_{i-1,j-\frac{1}{2}} + \delta^{(8)} u^*_{i-1,j+\frac{1}{2}} \\
a_{i,j:\,i,j+2} &= -\delta^{(7)} v^*_{i+\frac{1}{2},j} - \gamma^{(7)} v^*_{i-\frac{1}{2},j} - \beta^{(7)} v^*_{i-\frac{1}{2},j+1} - \alpha^{(7)} v^*_{i+\frac{1}{2},j+1} \\
&\quad - (\delta^{(7)} - \gamma^{(7)}) u^*_{i,j+\frac{1}{2}} + \lambda^{(1)} u^*_{i,j+1\frac{1}{2}} \\
a_{i,j:\,i,j-2} &= \alpha^{(8)} v^*_{i+\frac{1}{2},j} + \beta^{(8)} v^*_{i-\frac{1}{2},j} + \delta^{(8)} v^*_{i+\frac{1}{2},j-1} + \gamma^{(8)} v^*_{i-\frac{1}{2},j-1} \\
&\quad - (\alpha^{(8)} - \beta^{(8)}) u^*_{i,j-\frac{1}{2}} + \lambda^{(3)} u^*_{i,j-1\frac{1}{2}}
\end{aligned}
$$

$$
\begin{aligned}
a_{i,j:\,i+2,j+1} &= -\gamma^{(1)} u^*_{i+1,j+\frac{1}{2}} \quad , \quad a_{i,j:\,i-2,j-1} = \alpha^{(4)} u^*_{i-1,j-\frac{1}{2}} \\
a_{i,j:\,i+1,j+2} &= -\gamma^{(7)} u^*_{i+1,j+\frac{1}{2}} \quad , \quad a_{i,j:\,i-1,j-2} = \alpha^{(8)} u^*_{i-1,j-\frac{1}{2}} \\
a_{i,j:\,i+2,j-2} &= -\beta^{(6)} u^*_{i+1,j-\frac{1}{2}} \quad , \quad a_{i,j:\,i-2,j+1} = \delta^{(3)} u^*_{i-1,j+\frac{1}{2}} \\
a_{i,j:\,i-1,j+2} &= \delta^{(7)} u^*_{i-1,j+\frac{1}{2}} \quad , \quad a_{i,j:\,i+1,j-2} = -\beta^{(8)} u^*_{i+1,j-\frac{1}{2}}
\end{aligned}
\qquad (3.22)
$$

Applying first the constraint (3.20) for arbitrary U^* and V^*, and simplifying, using (3.17), requires

$$\left.\begin{aligned}
&\alpha^{(2)} = \beta^{(2)} = \gamma^{(5)} = \delta^{(5)} \\
&\delta^{(2)} + \phi^{(2)} = \gamma^{(2)} - \phi^{(1)} = 1/8 \\
&\alpha^{(5)} + \phi^{(3)} = \beta^{(5)} - \phi^{(4)} = 1/8 \\
&\gamma^{(4)} - \varepsilon^{(3)} = \delta^{(6)} - \varepsilon^{(4)} = 1/8 \\
&\beta^{(3)} + \varepsilon^{(2)} = \alpha^{(1)} + \varepsilon^{(1)} = 1/8 \\
&\lambda^{(1)} = \lambda^{(3)} = \mu^{(2)} = \mu^{(4)} = 0
\end{aligned}\right\} \qquad (3.23)$$

To apply the constraint (3.19), each $a_{i,j:\,i-i',\,j-j'}$ is required to equal $-a_{i,j:\,i+i',\,j+j'}$ when all pairs of indices appearing in the former are incremented by (i',j'). This gives the following conditions:

$$\left.\begin{aligned}
&\alpha^{(4)} = \alpha^{(8)} = \beta^{(6)} = \beta^{(8)} = \gamma^{(1)} = \gamma^{(7)} = \delta^{(3)} = \delta^{(7)} = 0 \\
&\alpha^{(3)} = \beta^{(1)} = \gamma^{(6)} = \delta^{(4)} = \mu^{(1)} = -\mu^{(3)} \\
&\alpha^{(7)} = \beta^{(7)} = \gamma^{(8)} = \delta^{(8)} = \lambda^{(2)} = -\lambda^{(4)} \\
&\alpha^{(2)} = \beta^{(2)} = \gamma^{(5)} = \delta^{(5)} = 1/24 - \lambda^{(2)} - \mu^{(1)}
\end{aligned}\right\} \qquad (3.24)$$

For the requirement (3), to wit, the reduction of the non-divergent mass-flux advection to the fourth-order Jacobian, we rewrite (3.22) for the case of no mass flux divergent introducing a stream function. By equating the resultant with the fourth-order approximation of the Jacobian (Arakawa, 1966), we can determine the following coefficients (See Appendix A)

$$\lambda^{(2)} = -\lambda^{(4)} = -\frac{1}{24}\,, \quad \mu^{(1)} = -\mu^{(3)} = -\frac{1}{24} \qquad (3.25)$$

and thus, from (3.24)

$$\left.\begin{aligned} \alpha^{(2)} &= \beta^{(2)} = \gamma^{(5)} = \delta^{(5)} = 1/8 \\ \alpha^{(3)} &= \beta^{(1)} = \gamma^{(6)} = \delta^{(4)} = -1/24 \\ \alpha^{(7)} &= \beta^{(7)} = \gamma^{(8)} = \delta^{(8)} = -1/24 \end{aligned}\right\} \quad (3.26)$$

Now (3.23) and (3.24) can be combined to express unspecified coefficients in terms of $\varepsilon^{(1)}$, $\varepsilon^{(3)}$, $\phi^{(1)}$ and $\phi^{(3)}$:

$$\left.\begin{aligned} &\alpha^{(1)} = 1/8 - \varepsilon^{(1)},\ \alpha^{(5)} = 1/8 - \phi^{(3)},\ \alpha^{(6)} = -1/24 + \varepsilon^{(1)} + \phi^{(3)} \\ &\beta^{(3)} = 1/24 + \varepsilon^{(1)},\ \beta^{(4)} = 1/8 - \varepsilon^{(1)} + \phi^{(1)},\ \beta^{(5)} = 1/24 - \phi^{(1)} \\ &\gamma^{(2)} = 1/8 + \phi^{(1)},\ \gamma^{(3)} = -1/24 - \varepsilon^{(3)} - \phi^{(1)},\ \gamma^{(4)} = 1/8 + \varepsilon^{(3)} \\ &\delta^{(1)} = 1/8 + \varepsilon^{(3)} - \phi^{(3)},\ \delta^{(2)} = 1/24 + \phi^{(3)},\ \delta^{(6)} = 1/24 - \varepsilon^{(3)} \\ &\varepsilon^{(2)} = 1/24 - \varepsilon^{(1)},\ \varepsilon^{(4)} = -1/12 - \varepsilon^{(3)},\ \phi^{(2)} = 1/12 - \phi^{(3)},\ \phi^{(4)} = -1/12 - \phi^{(1)} \end{aligned}\right\} \quad (3.27)$$

Finally the requirement of symmetry between the Cartesian components of the momentum equations for the case of a square grid yields

$$\left.\begin{aligned} &\alpha^{(1)} = \beta^{(5)},\ \alpha^{(2)} = \beta^{(2)},\ \alpha^{(5)} = \beta^{(3)},\ \alpha^{(6)} = \beta^{(4)} \\ &\delta^{(1)} = \alpha^{(6)},\ \delta^{(2)} = \alpha^{(1)},\ \delta^{(5)} = \alpha^{(2)},\ \delta^{(6)} = \alpha^{(5)} \end{aligned}\right\} \quad (3.28)$$

From (3.27) and (3.28), we obtain

$$\varepsilon^{(3)} = -\varepsilon^{(1)},\quad \phi^{(1)} = \varepsilon^{(1)} - 1/12,\quad \phi^{(3)} = 1/12 - \varepsilon^{(1)} \quad (3.29)$$

If we now choose, simply for reasons of symmetry between ε and ϕ

$$\varepsilon^{(1)} = 1/24 \quad (3.30)$$

the terms in (3.13) are completely specified as;

$$
\left.
\begin{aligned}
\alpha_{i,j+\frac{1}{2}} &= \frac{1}{24}\left[\, 2q_{i+1,j+1} + 3q_{i,j+1} + 2q_{i,j} + q_{i+1,j} - q_{i,j+2} - q_{i-1,j+1} \,\right] \\
\beta_{i,j+\frac{1}{2}} &= \frac{1}{24}\left[\, 3q_{i,j+1} + 2q_{i-1,j+1} + q_{i-1,j} + 2q_{i,j} - q_{i+1,j+1} - q_{i,j+2} \,\right] \\
\gamma_{i,j+\frac{1}{2}} &= \frac{1}{24}\left[\, 2q_{i,j+1} + q_{i-1,j+1} + 2q_{i-1,j} + 3q_{i,j} - q_{i,j-1} - q_{i+1,j} \,\right] \\
\delta_{i,j+\frac{1}{2}} &= \frac{1}{24}\left[\, q_{i+1,j+1} + 2q_{i,j+1} + 3q_{i,j} + 2q_{i+1,j} - q_{i-1,j} - q_{i,j-1} \,\right] \\
\varepsilon_{i+\frac{1}{2},j+\frac{1}{2}} &= \frac{1}{24}\left[\, q_{i+1,j+1} + q_{i,j+1} - q_{i,j} - q_{i+1,j} \,\right] \\
\phi_{i+\frac{1}{2},j+\frac{1}{2}} &= \frac{1}{24}\left[\, -q_{i+1,j+1} + q_{i,j+1} + q_{i,j} - q_{i+1,j} \,\right] \\
\lambda_{i,j} &= \frac{1}{24}\left[\, q_{i+1,j} - q_{i-1,j} \,\right] \\
\mu_{i,j} &= \frac{1}{24}\left[\, q_{i,j-1} - q_{i,j+1} \,\right]
\end{aligned}
\right\} \quad (3.31)
$$

When we disregard additional coefficients, λ and μ in the momentum equations, it is easily shown from (3.23) - (3.30) that the final forms of α, β, γ, δ, ε and ϕ coincide with those of the second-order scheme presented by Arakawa and Lamb (1981).

In summary, use of (3.5), (3.6), (3.9), (3.11), (3.12), (3.15) and (3.31) in (3.1) - (3.4), (3.7) and (3.8) give a fourth-order potential enstrophy and energy conserving scheme for the shallow water equations.

4. Numerical test of the fourth-order scheme

In this section the potential superiority of the newly derived scheme is examined by means of the numerical experiments comparing its results with those of the second-order scheme of Arakawa and Lamb. For this purpose, a two-layer, homogeneous, incompressible fluid system model was used. Quasi-static motion in the each layer of this fluid system may be described by (2.1) - (2.6), but replacing h in (2.6) by $rh_2 + h_1$; here (and hereafter) subscripts 1 and 2 denote the lower and upper layers, respectively; and r, equal to 1 in the upper layer and to the ratio of density of two layers ρ_2/ρ_1 in the lower layer, expresses the effect of stratification. In this fluid system, the summation of total energy for two layers is conserved, and mass and potential enstrophy are conserved in the each layer.

In the numerical experiments, X and Y are directed toward the east and the north, respectively. The computational domain is confined in a channel bounded by two parallel rigid wall at y = 0 and y = W = 7500 km; and by X = 0 and X = L = 13500 km, where cyclic boundary conditions are applied. The mean heights of each layer top, H_1 and H_2, are chosen to be 5 km and 10 km, respectively and grid size d = 500 km. The bottom topography is a circular mountain, placed at the center of the domain, of circular and parabolic cross section, and expressed by

$$h_s = h_m (1-D^2/R^2) \qquad \text{for} \qquad 0 \leqslant D \leqslant R$$

and

$$h_s = 0 \qquad \text{for} \qquad R < D$$

here D is the distance measured from the center of the mountain, R = 3 d so that the bottom diameter of the mountain is 3000 km and the maximum height, h_m, of 3 km is chosen (see Figure 2). The ratio of density r = 2/3, and

the acceleration of gravity $g = 9.8\ m\ s^{-2}$, are selected. Experiments were performed with two different Coriolis parameters: one is a constant $f = f_o = 10^{-4} s^{-1}$ (f-plane) and the other is variable $f = f_o + \beta\ (y-W/2)$ with $\beta = 1.62 \times 10^{-11} m^{-1}\ s^{-1}$ (β-plane). At the north and south boundaries, the rigid wall conditions, $v = 0$, and a computational boundary condition, $\zeta = 0$, are applied. The variable outside the boundaries involved in the fourth-order scheme are expressed by those of interior points using the conditions that u, h, f are symmetric, and v is anti-symmetric, with respect to the boundaries. The preliminary numerical integration with these conditions showed that they worked well within the acceptable accuracies for conservative quantities: 0.04% decrease in mass, 0.08% decrease in total energy, 0.04% and 0.03% increases in potential enstrophy for the lower and upper layers, respectively, after 10 days. However, a certain proportion of the accuracy may be attributable to round-off error from the use of single precision in the code. As initial wind fields, uniform westerly flows of 20 ms^{-1} and 30 ms^{-1} are prescribed for the lower and upper layers, respectively. The height fields are then obtained from the steady state solutions of the equations for the two layer fluid system in the absence of a mountain. The Matsuno scheme is used first for the initial time step, and then once in every five leapfrog time steps. A time interval of eight minutes is applied for all experiments, though the second-order scheme may allow use of a longer time interval than that acceptable for the fourth-order scheme (Gerrity et al., 1972). This time integration scheme is the same as that used in the UCLA-GCM, for reasons of convenience. The model time of

integration was 20 days.

Fig. 3 shows the relative time changes in potential enstrophy, total energy and mass to their initial values.

For all cases, total energy and total mass monotonously decrease almost at the same rate up to 20 days (0.15% and 0.08%, respectively). These rates of decrease are much smaller than those resulting from the fourth-order scheme presented by Navan and Riphagen (1979) (1.44% or 0.99% for total energy and 0.54% or 0.42% for mass, after 4 days). For potential enstrophy, the fourth-order scheme gives better conservation than the second-order scheme does.

Figs. 4-23 show the 24-hour changes of the wind vector based on $\bar{u}^i$ and $\bar{v}^i$ at h points and the differential height of the lower layer (height of interface) $h_1 \quad -H_1$, for a period up to 20 days, for the fourth- and second-order scheme on the f-plane. Comparison of these results shows that the fourth-order scheme yields a faster translating speed of the low (interfacial depression) produced by the mountain (the effect of truncation error in general being to reduce propagation speeds). The five-day average speed of the lows in the fourth- and second-order schemes are 19.1 ms^{-1} and 16.8 ms^{-1}, respectively, so that the difference of distance of low centers reaches about 1000 km after 6 days. The passing event over the mountain at Day 8 and the subsequent reformation of the traveling low on the lee side, consistent with potential vorticity conservation are dramatically reproduced in the fourth-order scheme, but not so distinctly done in the second-order scheme. In the second passing event after Day 15, which exhibited somewhat different behavior from the earlier one, the difference of the results of two schemes is also clearly seen. The deep traveling lows in the fourth-order scheme pass just north of the mountain, preserving their forms and in-

tensities, and also producing the jet stream near the boundary associated with the stationary high over the mountain(Day 16), while in the second-order scheme the weak low is absorbed by the relatively strong high as it approaches.

The results of the β-plane computations are shown in Figs. 24-43. In this case the initial height fields are not of course identical to those in the f-plane, but the differences are so small as to be negligible. Thus we can determine the effect of β, comparing the results in this case with those in the f-plane case. The evolution of whole pattern in the β-plane is much more complex and the intensities of the high and the low are greater than those in the f-plane case. One of the remarkable features is the occurrence of the splitting of the lee side low into a stationary low and a low traveling toward the northeast of the mountain, never seen in the f-plane case. Note that the occurrence time of the splitting in the fourth-order scheme is one day earlier than that in the second-order scheme (see Day 4 and Day 5). Here we can see the same advantages of the fourth-order scheme as noted in the previous f-plane computations. After 6 days, the difference of distance of the traveling low centers has increased to 2000 km, twice as much as that in the f-plane case. Later, the difference gradually decreases because the low in the second-order scheme is catching up, while the low in the fourth-order scheme is blocked by the strong blocking high over the mountain. The traveling lows can not easily pass over the mountain, but go around it until they combine with another low in the south, associated with the planetary wave. This splitting and the associated blocking phenomenon are not produced in the similar experiment by Kasahara (1966). The motion in the well-developed strong high over the mountain occasionally resembles a Taylor column, with a stagnation area just south of the mountain, although this effect is confined to the lower layer.

5. Summary and further comments

A horizontal difference scheme has been derived for the shallow water equations, conserving both potential enstrophy and total energy for general flow, and, in addition, yielding the fourth-order accuracy in the potential vorticity advection (in case of horizontal nondivergent flow), in the presence of bottom topography. This development may be considered as a straightforward (if complicated) extension of the second-order potential-enstrophy and energy conserving scheme of Arakawa and Lamb (1981). Comparisons by means of numerical experiments using the two-layer model with the second order scheme by Arakawa and Lamb showed the advantages of the newly derived scheme in better development, faster traveling speeds of the lows produced by the mountain, and better conservation of potential enstrophy. The increase of computation time by the fourth-order scheme is less than 10%. On the present model, the calculation code of the advection terms occupy the major part of the whole code, so that the increase in computation time may become negligibly small in more complex GCM or NWP models. The new scheme has been already incorpolated into the current UCLA-GCM with the SICK-proof kinetic energy for the scheme defined by

$$K_{i+1/2,j+1/2} = \overline{\left[1/3\, u^2_{j+1/2} + 1/24\, (u_{j+3/2} + u_{j-1/2})^2 \right]}^{i}_{i+1/2} + \overline{\left[1/3\, v^2_{i+1/2} + 1/24\, (v_{i+3/2} + v_{i-1/2})^2 \right]}^{j}_{j+1/2} \qquad (5.1)$$

This has practically eliminated the linear computational instability

of meridionally propagating inertia-gravity waves (Arakawa and Lamb (1981)), and has given good simulation results. GISS also has used the scheme for their climate model.

References

Arakawa, A., 1966: Computational design for long-term numerical integration of the equations of fluid motion: Two-dimensional incompressible flow. Part I. J. Comput. Phys. 1, 119-143.

Arakawa, A. and V. R. Lamb, 1981: A potential enstrophy and energy conserving scheme for the shallow water equations. Mon. Wea. Rev., 109, 18-36.

Gerrity, J. P., R. D. McPherson and P. D. Polger, 1972: On the efficient reduction of truncation error in numerical weather prediction models. Mon. Wea. Rev., 100, 637-643.

Kasahara, A., 1966: The dynamical influence of orography on the large-scale motion of the atmosphere. J. Atmos. Sci., 23, 259-271.

Navon, I. M. and H. A. Riphagen, 1979: An implicit compact fourth-order algorithm for solving the shallow-water equations in conservation-low form. Mon. Wea. Rev., 107, 1107-1127.

APPENDIX A

The fourth-order scheme for the case of no mass flux divergence

The finite-difference Arakawa fourth-order Jacobian $J_A^{(4)}$ (1966), which originally represents the advection term in the vorticity equation and guarantees the enstrophy and kinetic energy conservation for horizontal nondivergent flow, can be directly applied to the present case of potential vorticity and potential enstrophy because of its universal form. Thus the schemes for the momentum equations (3.7) and (3.8) conserve potential enstrophy and have fourth-order accuracy, if the finite-difference potential vorticity equation (3.10) derived from it reduces to this Jacobian form.

The Arakawa fourth-order Jacobian for the present case can be written as:

$$
\begin{aligned}
&\left[J_A^{(4)}(q,\psi^*)\right]_{i,j} \\
&= -\frac{1}{12d^2}\Big[(\psi^*_{i,j-1}+\psi^*_{i+1,j-1}-\psi^*_{i,j+1}-\psi^*_{i+1,j+1})(q_{i+1,j}+q_{i,j}) \\
&\quad -(\psi^*_{i-1,j-1}+\psi^*_{i,j-1}-\psi^*_{i-1,j+1}-\psi^*_{i,j+1})(q_{i,j}+q_{i-1,j}) \\
&\quad +(\psi^*_{i+1,j}+\psi^*_{i+1,j+1}-\psi^*_{i-1,j}-\psi^*_{i-1,j+1})(q_{i,j+1}+q_{i,j}) \\
&\quad -(\psi^*_{i+1,j-1}+\psi^*_{i+1,j}-\psi^*_{i-1,j-1}-\psi^*_{i-1,j})(q_{i,j}+q_{i,j-1}) \\
&\quad +(\psi^*_{i+1,j}-\psi^*_{i,j+1})(q_{i+1,j+1}+q_{i,j})-(\psi^*_{i,j-1}-\psi^*_{i-1,j})(q_{i,j}+q_{i-1,j-1}) \\
&\quad +(\psi^*_{i,j+1}-\psi^*_{i-1,j})(q_{i-1,j+1}+q_{i,j})-(\psi^*_{i+1,j}-\psi^*_{i,j-1})(q_{i,j}+q_{i+1,j-1})\Big] \\
&-\frac{1}{24d^2}\Big[(\psi^*_{i-1,j+1}-\psi^*_{i+1,j-1})(q_{i+1,j+1}-q_{i-1,j-1})-(\psi^*_{i+1,j+1}-\psi^*_{i-1,j-1})(q_{i-1,j+1}-q_{i+1,j-1}) \\
&\quad +(\psi^*_{i,j+2}-\psi^*_{i+2,j})q_{i+1,j+1}-(\psi^*_{i-2,j}-\psi^*_{i,j-2})q_{i-1,j-1} \\
&\quad -(\psi^*_{i,j+2}-\psi^*_{i-2,j})q_{i-1,j+1}+(\psi^*_{i+2,j}-\psi^*_{i,j-2})q_{i+1,j-1} \\
&\quad +(\psi^*_{i+1,j+1}-\psi^*_{i+1,j-1})q_{i+2,j}-(\psi^*_{i-1,j+1}-\psi^*_{i-1,j-1})q_{i-2,j} \\
&\quad -(\psi^*_{i+1,j+1}-\psi^*_{i-1,j+1})q_{i,j+2}+(\psi^*_{i+1,j-1}-\psi^*_{i-1,j-1})q_{i,j-2}\Big]
\end{aligned}
\tag{A.1}
$$

where ψ^* denotes a stream function for the mass flux.

With the definition of ψ^* as

$$u^*_{i,j+1/2} = \alpha^{-1}(\psi^*_{i,j} - \psi^*_{i,j+1}) \tag{A.2}$$

$$v^*_{i+1/2,j} = \alpha^{-1}(\psi^*_{i+1,j} - \psi_{i,j}) \tag{A.3}$$

the right-hand side of (3.10) can be rewritten as

$$\begin{aligned}
-\frac{1}{\alpha^2}\Big[& \psi^*_{i+1,j}(-\alpha_{i,j-1/2} + \delta_{i,j+1/2} + \gamma_{i+1,j+1/2} - \beta_{i+1,j-1/2} - \varepsilon_{i+1/2,j-1/2} - \varepsilon_{i+1/2,j+1/2} - \mu_{i+1,j} - \mu_{i,j}) \\
& + \psi^*_{i-1,j}(\beta_{i,j-1/2} - \gamma_{i,j+1/2} - \delta_{i-1,j+1/2} + \alpha_{i-1,j-1/2} + \varepsilon_{i-1/2,j-1/2} + \varepsilon_{i-1/2,j+1/2} + \mu_{i,j} + \mu_{i-1,j}) \\
& + \psi^*_{i,j+1}(-\alpha_{i,j+1/2} + \beta_{i,j+1/2} - \delta_{i,j+1/2} + \gamma_{i,j+1/2} - \phi_{i+1/2,j+1/2} - \phi_{i-1/2,j-1/2} - \lambda_{i,j} - \lambda_{i,j+1}) \\
& + \psi^*_{i,j-1}(-\gamma_{i,j-1/2} + \delta_{i,j-1/2} + \alpha_{i,j-1/2} - \beta_{i,j-1/2} + \phi_{i+1/2,j-1/2} + \phi_{i-1/2,j-1/2} + \lambda_{i,j-1} + \lambda_{i,j}) \\
& + \psi^*_{i+1,j+1}(\alpha_{i,j+1/2} - \gamma_{i+1,j+1/2} + \varepsilon_{i+1/2,j+1/2} + \phi_{i+1/2,j+1/2}) \\
& + \psi^*_{i-1,j+1}(-\beta_{i,j+1/2} + \delta_{i-1,j+1/2} - \varepsilon_{i-1/2,j+1/2} + \phi_{i-1/2,j+1/2}) \\
& + \psi^*_{i-1,j-1}(\gamma_{i,j-1/2} - \alpha_{i-1,j-1/2} - \varepsilon_{i-1/2,j-1/2} - \phi_{i-1/2,j-1/2}) \\
& + \psi^*_{i+1,j-1}(-\delta_{i,j-1/2} + \beta_{i+1,j-1/2} + \varepsilon_{i+1/2,j-1/2} - \phi_{i+1/2,j-1/2}) \\
& + \psi^*_{i,j-2}(-\lambda_{i,j-1}) + \psi^*_{i,j+2}(\lambda_{i,j+1}) \\
& + \psi^*_{i-2,j}(-\mu_{i-1,j}) + \psi^*_{i+2,j}(\mu_{i+1,j})\Big]
\end{aligned} \tag{A.4}$$

Equation (A.4) with the right-hand side of (A.1) gives the forms of λ and μ and four independent constraints on α, β, γ, δ, ε and ϕ as

functions of q:

$$\lambda_{i,j+1} = \frac{1}{24}\left(\varphi_{i+1,j+1} - \varphi_{i-1,j+1}\right)$$

$$\mu_{i-1,j} = \frac{1}{24}\left(\varphi_{i-1,j-1} - \varphi_{i-1,j+1}\right)$$

$$-\alpha_{i,j-1/2} + \delta_{i,j+1/2} + \gamma_{i+1,j+1/2} - \beta_{i+1,j-1/2} - \varepsilon_{i+1/2,j-1/2} - \varepsilon_{i+1/2,j+1/2} - \mu_{i,j} - \mu_{i+1,j}$$
$$= -\frac{1}{6}\left(\varphi_{i+1,j-1} + \varphi_{i,j-1} - \varphi_{i+1,j+1} - \varphi_{i,j+1}\right)$$

$$-\alpha_{i,j+1/2} + \beta_{i,j+1/2} - \delta_{i,j+1/2} + \gamma_{i,j+1/2} - \phi_{i+1/2,j+1/2} - \phi_{i-1/2,j+1/2} - \lambda_{i,j} - \lambda_{i,j+1}$$
$$= -\frac{1}{6}\left(\varphi_{i+1,j+1} + \varphi_{i+1,j} - \varphi_{i-1,j+1} - \varphi_{i-1,j}\right)$$

$$\alpha_{i,j+1/2} - \gamma_{i+1,j+1/2} + \varepsilon_{i+1/2,j+1/2} + \phi_{i+1/2,j+1/2}$$
$$= -\frac{1}{24}\left\{4\left(\varphi_{i+1,j} - \varphi_{i,j+1}\right) - \varphi_{i+1,j-1} + \varphi_{i-1,j+1} - \varphi_{i+2,j} + \varphi_{i,j+2}\right\}$$

$$-\beta_{i,j+1/2} + \delta_{i-1,j+1/2} - \varepsilon_{i-1/2,j+1/2} + \phi_{i-1/2,j+1/2}$$
$$= -\frac{1}{24}\left\{4\left(\varphi_{i,j+1} - \varphi_{i-1,j}\right) - \varphi_{i+1,j+1} + \varphi_{i-1,j-1} + \varphi_{i-2,j} - \varphi_{i,j+2}\right\} \qquad \text{(A.5)}$$

After some algebraic manipulations similar to those in AL, we obtain the final forms as:

$$\alpha_{i,j+\frac{1}{2}} = C_{i+\frac{1}{2},j+\frac{1}{2}} + \frac{1}{96}\left[16\,g_{i,j+1} + 8(g_{i,j} + g_{i+1,j+1}) - 3(g_{i-1,j+1} + g_{i,j+2}) + g_{i+1,j-1} + g_{i+2,j} - (g_{i-1,j} + g_{i,j-1} + g_{i+1,j+2} + g_{i+2,j+1})\right] - \frac{1}{2}(\xi+\phi)_{i+\frac{1}{2},j+\frac{1}{2}}$$

$$\beta_{i,j+\frac{1}{2}} = -C_{i-\frac{1}{2},j+\frac{1}{2}} + \frac{1}{96}\left[16\,g_{i,j+1} + 8(g_{i-1,j+1} + g_{i,j}) - 3(g_{i,j+2} + g_{i+1,j+1}) + g_{i-2,j} + g_{i-1,j-1} - (g_{i-2,j+1} + g_{i-1,j+2} + g_{i,j-1} + g_{i+1,j})\right] - \frac{1}{2}(\xi+\phi)_{i-\frac{1}{2},j+\frac{1}{2}}$$

$$\gamma_{i,j+\frac{1}{2}} = C_{i-\frac{1}{2},j+\frac{1}{2}} + \frac{1}{96}\left[16\,g_{i,j} + 8(g_{i-1,j} + g_{i,j+1}) - 3(g_{i,j-1} + g_{i+1,j}) + g_{i-2,j+1} + g_{i-1,j+2} - (g_{i-2,j} + g_{i-1,j-1} + g_{i,j+2} + g_{i+1,j+1})\right] + \frac{1}{2}(\xi+\phi)_{i-\frac{1}{2},j+\frac{1}{2}}$$

$$\delta_{i,j+\frac{1}{2}} = -C_{i+\frac{1}{2},j+\frac{1}{2}} + \frac{1}{96}\left[16\,g_{i,j} + 8(g_{i,j+1} + g_{i+1,j}) - 3(g_{i-1,j} + g_{i,j-1}) + g_{i+1,j+2} + g_{i+2,j+1} - (g_{i-1,j+1} + g_{i,j+2} + g_{i+1,j-1} + g_{i+2,j})\right] + \frac{1}{2}(\xi+\phi)_{i+\frac{1}{2},j+\frac{1}{2}}$$

$$\lambda_{i,j+1} = \frac{1}{24}(g_{i+1,j+1} - g_{i-1,j+1})$$

$$\mu_{i+1,j} = \frac{1}{24}(g_{i+1,j-1} - g_{i+1,j+1}) \qquad \text{(A.6)}$$

where the new variable C is defined by

$$C_{i+\frac{1}{2},j+\frac{1}{2}} = \frac{1}{4}(\alpha_{i,j+\frac{1}{2}} - \beta_{i+1,j+\frac{1}{2}} + \gamma_{i+1,j+\frac{1}{2}} - \delta_{i,j+\frac{1}{2}}) \qquad \text{(A.7)}$$

APPENDIX B

The fourth-order scheme for the shallow water equations on a spherical grid.

1. The governing equations in spherical coordinates.

The shallow water equations (2.1) and (2.2) on a spherical grid may be described as:

$$\frac{\partial}{\partial t}\left(\frac{u}{m}\right) - q\frac{hv}{m} + \frac{\partial}{\partial \xi}(K+\Phi) = 0 \tag{B.1}$$

$$\frac{\partial}{\partial t}\left(\frac{v}{n}\right) + q\frac{hu}{n} + \frac{\partial}{\partial \eta}(K+\Phi) = 0 \tag{B.2}$$

$$\frac{\partial}{\partial t}\left(\frac{h}{mn}\right) + \frac{\partial}{\partial \xi}\left(h\frac{u}{n}\right) + \frac{\partial}{\partial \eta}\left(h\frac{v}{m}\right) = 0 \tag{B.3}$$

where m and n are metric factors in the spherical coordinates $\xi = \lambda$ (longitude) and $\eta = \varphi$ (latitude) expressed by $1/m = a\cos\varphi$ and $1/n = a$ (the radius of the earth). U and V are the component of $\mathbf{V}$ in ξ and η, respectively and q, K and Φ are defined in Section 2. The vorticity $\zeta = \mathbf{k}\cdot\nabla\times\mathbf{V}$ can be expressed as

$$mn\left[\frac{\partial}{\partial \xi}\frac{v}{n} - \frac{\partial}{\partial \eta}\frac{u}{m}\right] \tag{B.4}$$

Then the equation for the time change of kinetic energy can be obtained as

$$\frac{\partial}{\partial t}\left(\frac{h}{mn}K\right) + \frac{\partial}{\partial \xi}\left(\frac{hu}{n}K\right) + \frac{\partial}{\partial \eta}\left(\frac{hv}{m}K\right) + \frac{hu}{n}\frac{\partial \Phi}{\partial \xi} + \frac{hv}{m}\frac{\partial \Phi}{\partial \eta} = 0 \tag{B.5}$$

2. The finite-difference scheme for interior points of the spherical grid.

A portion of the spherical grid with the variables staggered as in the C grid and the indices (i.j) centered at a q point is shown in Fig. B1. Here $\Delta\xi$ and $\Delta\eta$ are constant grid intervals in ξ and η, respectively, and m and n are assumed to vary only in j.

For the continuity equation (B.3) multiplied by $\Delta\xi\Delta\eta$, the following finite difference form is chosen:

$$\frac{\partial}{\partial t} H_{i+\frac{1}{2},j+\frac{1}{2}} + u^*_{i+\frac{1}{2},j+\frac{1}{2}} - u^*_{i,j+\frac{1}{2}} + v^*_{i+\frac{1}{2},j+1} - v^*_{i+\frac{1}{2},j} = 0 \tag{B.6}$$

$$H_{i+\frac{1}{2},j+\frac{1}{2}} \equiv \frac{\Delta\xi\Delta\eta}{(mn)_{j+\frac{1}{2}}} h_{i+\frac{1}{2},j+\frac{1}{2}} \tag{B.7}$$

$$\left.\begin{aligned} u^*_{i,j+\frac{1}{2}} &\equiv (h^{(u)}u)_{i,j+\frac{1}{2}} \frac{\Delta\eta}{m_{j+\frac{1}{2}}} \\ v^*_{i+\frac{1}{2},j} &\equiv (h^{(v)}v)_{i+\frac{1}{2},j} \frac{\Delta\xi}{m_j} \end{aligned}\right\} \tag{B.8}$$

Here $\Delta\xi\Delta\eta / (mn)_{j+\frac{1}{2}}$ is area of the stippled region in Fig. B1 and $h^{(u)}$, $h^{(v)}$ are as-yet-unspecified functions of h.

Ignoring pressure gradient forces, the remaining terms in (B.1) and (B.2) can be represented as in the square grid case,

$$\frac{\partial}{\partial t}\frac{\Delta\xi}{m_{j+1/2}}u_{i,j+1/2} - \alpha_{i,j+1/2}v^*_{i+1/2,j+1} - \beta_{i,j+1/2}v^*_{i-1/2,j+1} - \gamma_{i,j+1/2}v^*_{i-1/2,j} - \delta_{i,j+1/2}v^*_{i+1/2,j} + \varepsilon_{i+1/2,j+1/2}u^*_{i+1,j+1/2} - \varepsilon_{i-1/2,j+1/2}u^*_{i-1,j+1/2} + \lambda_{i,j+1}u^*_{i,j+1/2} - \lambda_{i,j}u^*_{i,j-1/2} + [K_{i+1/2,j+1/2} - K_{i-1/2,j+1/2}] = 0, \quad (B.9)$$

$$\frac{\partial}{\partial t}\frac{\Delta\eta}{n_j}v_{i+1/2,j} + \gamma_{i+1,j+1/2}u^*_{i+1,j+1/2} + \delta_{i,j+1/2}u^*_{i,j+1/2} + \alpha_{i,j-1/2}u^*_{i,j-1/2} + \beta_{i+1,j-1/2}u^*_{i+1,j-1/2} + \phi_{i+1/2,j+1/2}v^*_{i+1/2,j+1} + \phi_{i+1/2,j-1/2}v^*_{i+1/2,j-1} + \mu_{i+1,j}v^*_{i+1/2,j} - \mu_{i,j}v^*_{i-1/2,j} + [K_{i+1/2,j+1/2} - K_{i+1/2,j-1/2}] = 0 \quad (B.10)$$

but U^* and V^* are now defined by (B.8). The coefficients α, β, γ, δ, ϵ, ϕ, λ and μ are again functions of q to be determined, where $q_{i,j} \equiv (f+\zeta)_{i,j}/h^{(q)}_{i,j}$ and $h^{(q)}$ is an as-yet-unspecified function of h. The finite-difference form for ζ chosen is

$$\zeta_{i,j} = \frac{(mn)_j}{\Delta\xi\Delta\eta}\left[\left(v\frac{\Delta\eta}{n}\right)_{i+1/2,j} - \left(v\frac{\Delta\eta}{n}\right)_{i-1/2,j} + \left(u\frac{\Delta\xi}{m}\right)_{i,j-1/2} - \left(u\frac{\Delta\xi}{m}\right)_{i,j+1/2}\right] \quad (B.11)$$

As in the square grid case, $h^{(u)}$ and $h^{(v)}$ are chosen as

$$\left.\begin{aligned} h^{(u)} &\equiv \bar{h}^{i} \\ h^{(v)} &\equiv \bar{h}^{j} \end{aligned}\right\} \quad (B.12)$$

Then it is easily shown from the finite-difference analog of (B.5) that we must specify

$$K_{i+1/2,j+1/2} \equiv \frac{(mn)_{j+1/2}}{\Delta\xi\Delta\eta}\left[\overline{\frac{1}{2}\frac{\Delta\xi\Delta\eta}{m_{j+1/2}n_{j+1/2}}u^2}^{\,i} + \overline{\frac{1}{2}\frac{\Delta\xi\Delta\eta}{m_j n_j}v^2}^{\,j}\right]_{i+1/2,j+1/2} \quad (B.13)$$

to maintain conservation of total kinetic energy for divergent mass flux.

Since the procedure to determine α, β, γ, δ, ε, ϕ, λ and μ as functions of q is identical to that presented for the square grid, we can directly use the results of (3.31) with consistently determined $h^{(q)}$ in q for the spherical grid (AL);

$$g_{i,j} = \frac{f_i + S_{i,j}}{\frac{(mn)_j}{4}\left[\frac{h_{i+1/2,j+1/2}+h_{i-1/2,j+1/2}}{(mn)_{j+1/2}} + \frac{h_{i+1/2,j-1/2}+h_{i-1/2,j-1/2}}{(mn)_{j-1/2}}\right]}$$

$$= \frac{\frac{\Delta\xi\Delta\eta}{(mn)_j}(f_j + S_{i,j})}{1/4\left[H_{i+1/2,j+1/2} + H_{i-1/2,j+1/2} + H_{i+1/2,j-1/2} + H_{i-1/2,j-1/2}\right]} \qquad \text{(B.14)}$$

$$\frac{\Delta\xi\Delta\eta}{(mn)_j} = \frac{1}{2}\left(\frac{\Delta\xi\Delta\eta}{(mn)_{j-1/2}} + \frac{\Delta\xi\Delta\eta}{(mn)_{j+1/2}}\right) \qquad \text{(B.15)}$$

3. Modification of the scheme at the pole

The arrangement of the variables and the indices near the North Pole (NP) is shown in Fig. B2.

The continuity equation at j = NP-1/2 in the grid system can be expressed as

$$\frac{\partial}{\partial t} H_{i+1/2,NP-1/2} + u^*_{i+1,NP-1/2} - u^*_{i,NP-1/2} - v^*_{i+1/2,NP-1} = 0 \qquad (B.16)$$

$$H_{i+1/2,NP-1/2} = \frac{\Delta\xi\Delta\eta}{(mn)_{NP-1/2}} h_{i+1/2,NP-1/2}$$

The momentum equations for u at j = NP-1/2 and V at j = NP-1 can be written

$$\begin{aligned} &\frac{\partial}{\partial t}\left(\frac{u\Delta\xi}{m}\right)_{i,NP-1/2} - \gamma'_{i,NP-1/2} v^*_{i-1/2,NP-1} - \delta'_{i,NP-1/2} v^*_{i+1/2,NP-1} \\ &\quad + \varepsilon'_{i+1/2,NP-1/2} u^*_{i+1,NP-1/2} - \varepsilon'_{i-1/2,NP-1/2} u^*_{i-1,NP-1/2} - \lambda_{i,NP-1} u^*_{i,NP-3/2} \\ &\quad + [K'_{i+1/2,NP-1/2} - K'_{i-1/2,NP-1/2}] = 0 \end{aligned} \qquad (B.17)$$

$$\begin{aligned} &\frac{\partial}{\partial t}\left(\frac{v\Delta\eta}{n}\right)_{i+1/2,NP-1} + (\gamma' u^*)_{i+1,NP-1/2} + (\delta' u^*)_{i,NP-1/2} + (\alpha u^*)_{i,NP-3/2} \\ &\quad + (\beta u^*)_{i+1,NP-3/2} - \phi_{i+1/2,NP-2} v^*_{i+1/2,NP-2} + \mu_{i+1,NP-1} v^*_{i+3/2,NP-1} \\ &\quad - \mu_{i,NP-1} v^*_{i-1/2,NP-1} + [K'_{i+1/2,NP-1/2} - K_{i+1/2,NP-3/2}] = 0 \end{aligned} \qquad (B.18)$$

where the primed variables are to be determined and the others are defined as in (3.31).

At the North Pole, we define q through the circulation theorem

$$q_{NP} \equiv \frac{f_{NP} + \zeta_{NP}}{h^{(8)}_{NP}} \tag{B.19}$$

where

$$\zeta_{NP} = \frac{1}{A^{8}_{NP}} \sum_{i=1}^{IMAX} \left(\frac{u \Delta \xi}{m} \right)_{i, NP-1/2} \tag{B.20}$$

$$A^{8}_{NP} = IMAX \frac{\Delta \xi \Delta \eta}{(mn)_{NP}} \tag{B.21}$$

The factor $\Delta\xi\Delta\eta / (mn)_{NP}$ in (8.21) represents the area of the hatched region in Fig. B2, and IMAX is the total number of grid points in the ξ direction.

For the conservation of total kinetic energy in the divergent mass flux, K' at j = NP-1/2 must be given by

$$K'_{i+1/2, NP-1/2} \equiv \frac{1}{2} \frac{(mn)_{NP-1/2}}{\Delta\xi\Delta\eta} \left[\overline{\frac{\Delta\xi\Delta\eta}{(mn)_{NP-1/2}} u^2}^{\,i} + \frac{1}{2} \frac{\Delta\xi\Delta\eta}{(mn)_{NP-1}} v^2_{i+1/2, NP-1} \right] \tag{B.22}$$

After the application of requirement on potential vorticity advection and potential enstrophy conservation to (B.16)-(B.21), we obtain the constraint on the area-weighting factors, the form of $h_p^{(q)}$ and γ', δ' and ε' as functions of q.

$$\frac{\Delta\xi\Delta\eta}{(mn)_{NP-1}} = \frac{1}{2}\left[\frac{\Delta\xi\Delta\eta}{(mn)_{NP-1/2}} + \frac{\Delta\xi\Delta\eta}{(mn)_{NP-3/2}}\right] \tag{B.23}$$

$$h^{(g)}_{NP} \equiv \frac{1}{IMAX}\sum_{i=1}^{IMAX} h_{i+1/2,NP-1/2} \tag{B.24}$$

$$\frac{\Delta\xi\Delta\eta}{(mn)_{NP}} = \frac{1}{2}\frac{\Delta\xi\Delta\eta}{(mn)_{NP-1/2}} \tag{B.25}$$

$$\left.\begin{aligned}
\gamma'_{i,NP-1/2} &= \frac{1}{24}\left[3g_{NP} + 2g_{i-1,NP-1} + 3g_{i,NP-1/2} - g_{i,NP-2} - g_{i+1,NP-1}\right] \\
\delta'_{i,NP-1/2} &= \frac{1}{24}\left[3g_{NP} + 3g_{i,NP-1} + 2g_{i+1,NP-1} - g_{i-1,NP-1} - g_{i,NP-2}\right] \\
\varepsilon'_{i+1/2,NP-1/2} &= \frac{1}{24}\left[2g_{NP} - g_{i,NP-1} - g_{i+1,NP-1}\right]
\end{aligned}\right\} \tag{B.26}$$

and

$$\left.\begin{aligned}
\alpha_{i,NP-3/2} &= \frac{1}{24}\left[2g_{i+1,NP-1} + 3g_{i,NP-1} + 2g_{i,NP-2} + g_{i+1,NP-2} - g_{NP} - g_{i-1,NP-1}\right] \\
\beta_{i,NP-3/2} &= \frac{1}{24}\left[3g_{i,NP-1} + 2g_{i-1,NP-1} + g_{i-1,NP-2} + 2g_{i,NP-2} - g_{i+1,NP-1} - g_{NP}\right] \\
\mu_{i+1,NP-1} &= \frac{1}{24}\left[g_{i+1,NP-2} - g_{NP}\right]
\end{aligned}\right\} \tag{B.27}$$

The proceudre used for the North Pole can be directly applied to the South Pole (SP) taking into account geometrical symmetry, so that we give only the results here.

. The continuity equation at j = SP+1/2

$$\frac{\partial}{\partial t} H_{i+\frac{1}{2},SP+\frac{1}{2}} + u^*_{i+1,SP+\frac{1}{2}} - u^*_{i,SP+1} + v^*_{i+\frac{1}{2},SP+1} = 0 \qquad (B.28)$$

$$H_{i+\frac{1}{2},SP+\frac{1}{2}} = \frac{\Delta\xi\Delta\eta}{(mn)_{SP+\frac{1}{2}}} h_{i+\frac{1}{2},SP+\frac{1}{2}}$$

. The momentum equations for u at j = SP+1/2 and v at j = SP + 1

$$\frac{\partial}{\partial t}\left(\frac{u\Delta\xi}{m}\right)_{i,SP+\frac{1}{2}} - \alpha'_{i,SP+\frac{1}{2}} v^*_{i+\frac{1}{2},SP+1} - \beta'_{i,SP+\frac{1}{2}} v^*_{i-\frac{1}{2},SP+1}$$
$$+ \varepsilon'_{i+\frac{1}{2},SP+\frac{1}{2}} u^*_{i+1,SP+\frac{1}{2}} - \varepsilon'_{i-\frac{1}{2},SP+\frac{1}{2}} u^*_{i-1,SP+\frac{1}{2}} + \lambda_{i,SP+1} u^*_{i,SP+\frac{3}{2}}$$
$$+ \left[K'_{i+\frac{1}{2},SP+\frac{1}{2}} - K'_{i-\frac{1}{2},SP+\frac{1}{2}}\right] = 0 \qquad (B.29)$$

$$\frac{\partial}{\partial t}\left(\frac{v\Delta\eta}{n}\right)_{i+\frac{1}{2},SP+\frac{1}{2}} + (\gamma u^*)_{i+1,SP+\frac{3}{2}} + (\delta u^*)_{i,SP+\frac{3}{2}} + (\alpha' u^*)_{i,SP+\frac{1}{2}}$$
$$+ (\beta' u^*)_{i+1,SP+\frac{1}{2}} + \phi_{i+\frac{1}{2},SP+\frac{3}{2}} v^*_{i+\frac{1}{2},SP+2} + \mu_{i+1,SP+1} v^*_{i+\frac{3}{2},SP+1}$$
$$- \mu_{i,SP+1} v^*_{i-\frac{1}{2},SP+1} + \left[K_{i+\frac{1}{2},SP+\frac{3}{2}} - K'_{i+\frac{1}{2},SP+\frac{1}{2}}\right] = 0 \qquad (B.30)$$

here

$$K'_{i+\frac{1}{2},SP+\frac{1}{2}} \equiv \frac{1}{2}\frac{(mn)_{SP+\frac{1}{2}}}{\Delta\xi\Delta\eta}\left[\overline{\frac{\Delta\xi\Delta\eta}{(mn)_{SP+\frac{1}{2}}} u^2}^{\,i} + \frac{1}{2}\frac{\Delta\xi\Delta\eta}{(mn)_{SP+1}} v^2_{i+\frac{1}{2},SP+1}\right] \qquad (B.31)$$

and

$$\left.\begin{aligned}
\alpha'_{i,sp+1/2} &= \frac{1}{24}\left[2q_{i+1,sp+1}+3q_{i,sp+1}+3q_{sp}-q_{i,sp+2}-q_{i-1,sp+1}\right]\\
\beta'_{i,sp+1/2} &= \frac{1}{24}\left[3q_{i,sp+1}+2q_{i-1,sp+1}+3q_{sp}-q_{i+1,sp+1}-q_{i,sp+2}\right]\\
\varepsilon'_{i+1/2,sp+1/2} &= \frac{1}{24}\left[q_{i+1,sp+1}+q_{i,sp+1}-2q_{sp}\right]
\end{aligned}\right\} \quad (B.32)$$

$$\left.\begin{aligned}
\gamma_{i,sp+3/2} &= \frac{1}{24}\left[2q_{i,sp+2}+q_{i-1,sp+2}+2q_{i-1,sp+1}+3q_{i,sp+1}-q_{sp}-q_{i+1,sp+1}\right]\\
\delta_{i,sp+3/2} &= \frac{1}{24}\left[q_{i+1,sp+2}+2q_{i,sp+2}+3q_{i,sp+1}+2q_{i+1,sp+1}-q_{i-1,sp+1}-q_{sp}\right]\\
\mu_{i+1,sp+1} &= \frac{1}{24}\left[q_{sp}-q_{i+1,sp+2}\right]
\end{aligned}\right\} \quad (B.33)$$

Potential vorticity and vorticity are defined as

$$q_{sp} = \frac{f_{sp}+\zeta_{sp}}{h^{(q)}_{sp}} \quad (B.34)$$

$$\zeta_{sp} = -\frac{1}{A^q_{sp}}\sum_{i=1}^{IMAX}\left(\frac{u\Delta\xi}{m}\right)_{i,sp+1/2} \quad (B.35)$$

$$A^q_{sp} = IMAX\,\frac{\Delta\xi\Delta\eta}{(mn)_{sp}} \quad (B.36)$$

$$h^{(q)}_{sp} = \frac{1}{IMAX}\sum_{i=1}^{IMAX} h_{i+1/2,sp+1/2} \quad (B.37)$$

$$\frac{\Delta\xi\Delta\eta}{(mn)_{sp}} = \frac{1}{2}\,\frac{\Delta\xi\Delta\eta}{(mn)_{sp+1/2}} \quad (B.38)$$

$$\frac{\Delta\xi\Delta\eta}{(mn)_{sp+1}} = \frac{1}{2}\left[\frac{\Delta\xi\Delta\eta}{(mn)_{sp+1/2}}+\frac{\Delta\xi\Delta\eta}{(mn)_{sp+3/2}}\right] \quad (B.39)$$

LEGEND

Fig. 1 The staggering of the variable based on the C grid.

Fig. 2 A horizontal domain with a circular mountain and a vertical-section view of the two-layer fluid.

Fig. 3 Time change of the conservative quantities to their initial values expressed by the percentage. f_p : constant f case, β_p: variable f case, the solid line: the fourth-order scheme, the dashed line: the second-order scheme.

Fig.4-23 Results of the time integration for the constant f case. The arrows and contours represent the wind vectors and the differential heights of the lower layer, respectively.

Fig.24-43 As in Fig. 4-23, except for the variable f case (β-plane).

Fig.B1 A portion of the spherical grid. The area of the dotted region is represented by $(\Delta\xi\Delta\eta/mn)_{i+1/2,\,j+1/2}$.

Fig.B2 The spherical grid near the North Pole. The areas of the dotted and hatched regions respectively represent $(\Delta\xi\Delta\eta/mn)_{NP}$ and $(\Delta\xi\Delta\eta/mn)_{NP-1/2}$.

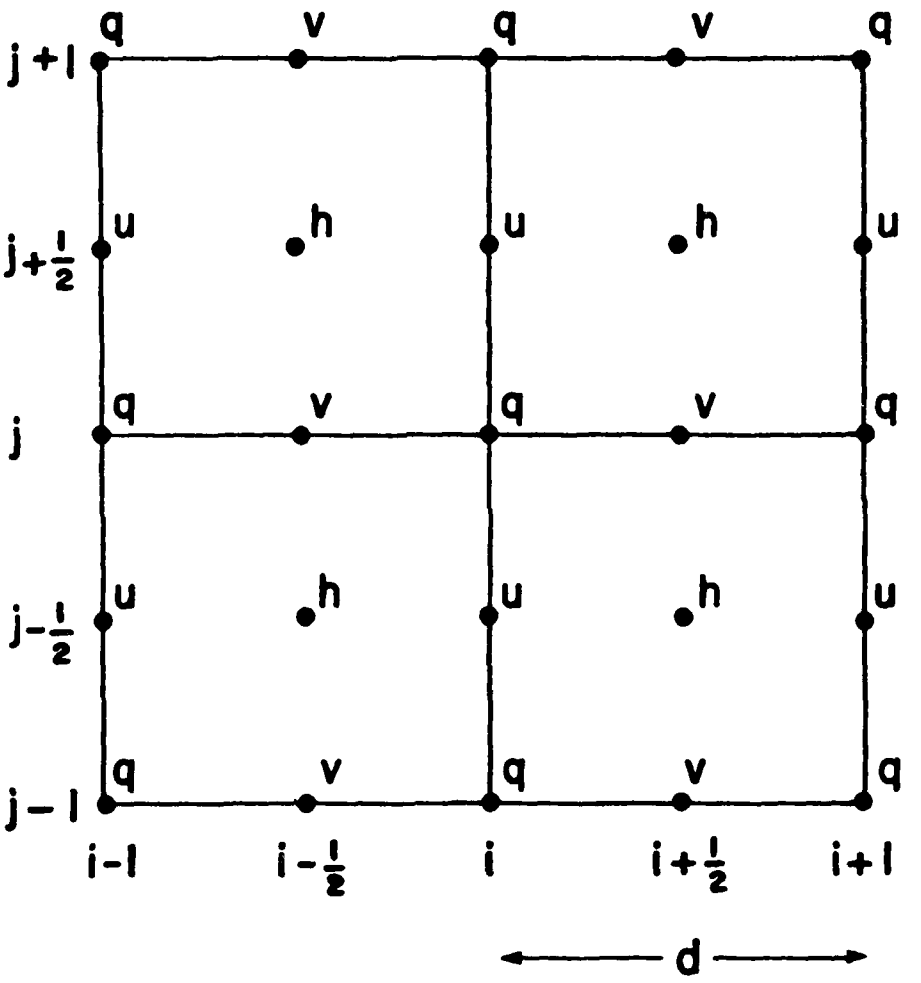

Figure 1

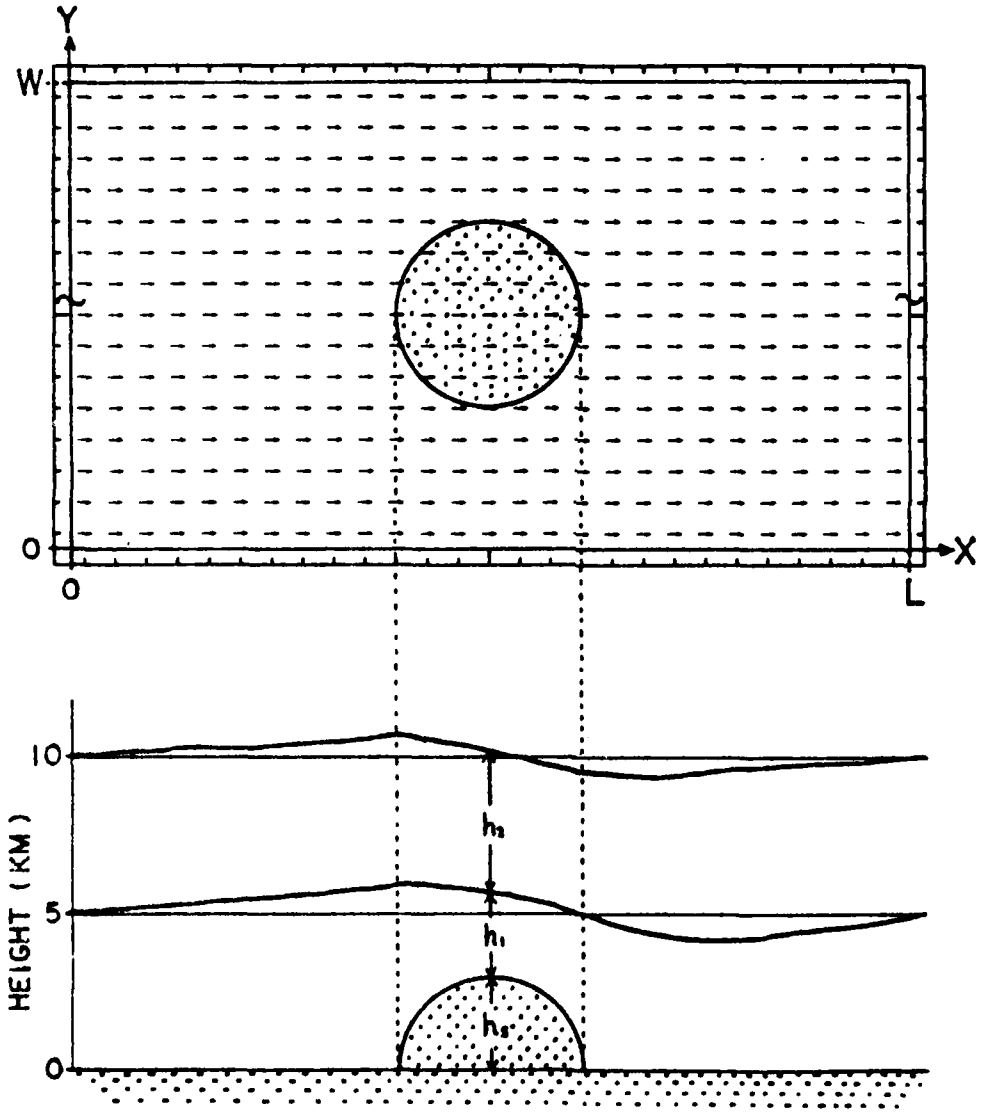

Figure 2

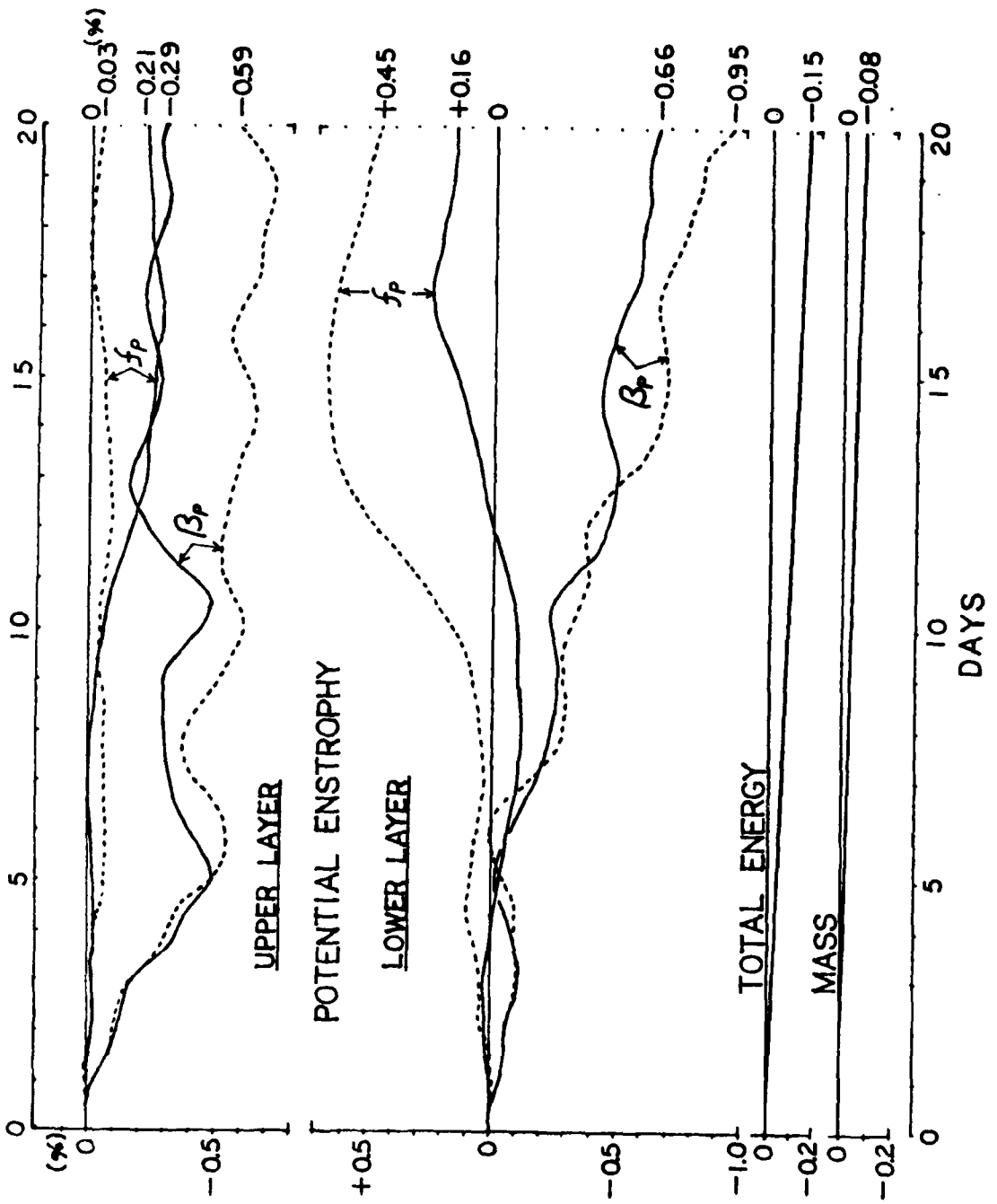
UPPER LAYER
POTENTIAL ENSTROPHY
LOWER LAYER
TOTAL ENERGY
MASS
DAYS
(%)
0
0.03
-0.21
-0.29
-0.59
+0.45
+0.16
-0.66
-0.95
-0.15
-0.08
f_p
β_p
0
5
10
15
20
+0.5
-0.5
-1.0
-0.2

Figure 3

The results of numerical experiments

on the f-plane

Figures 4-23:

Day 1, Hour 0 to Day 20, Hour 0.

Second- and Fourth-order Schemes

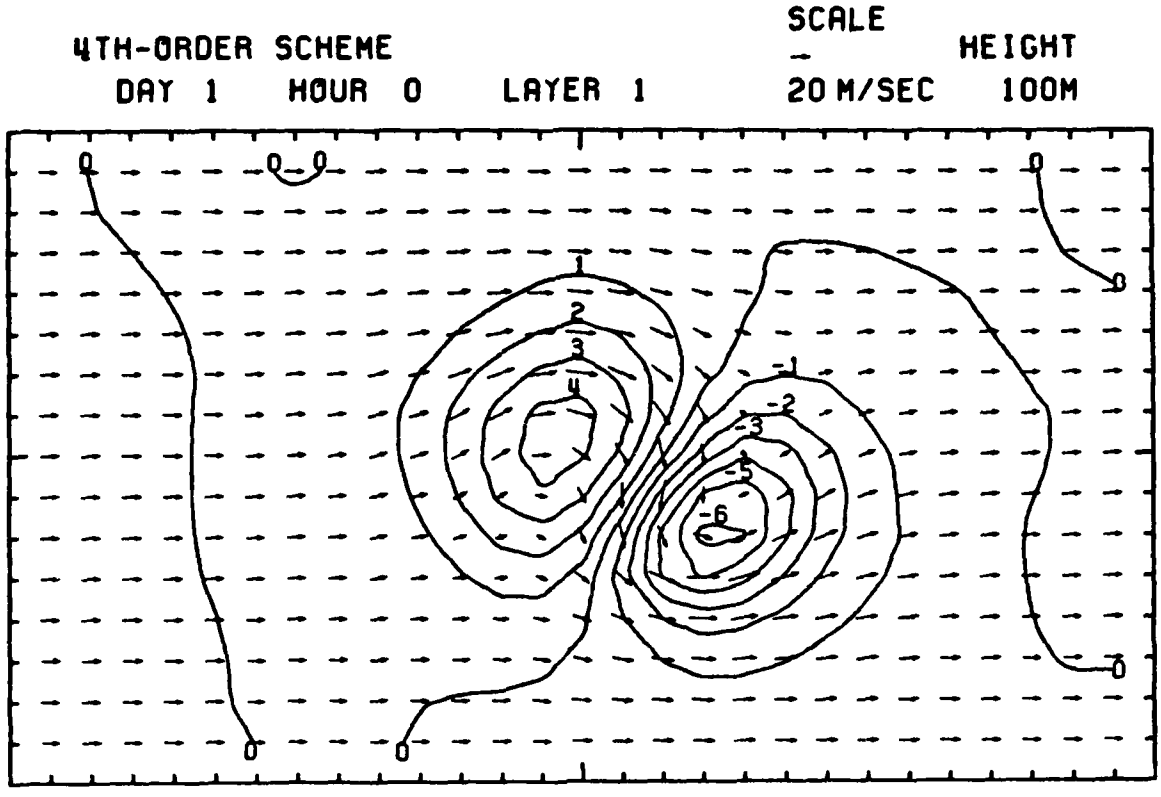
4TH-ORDER SCHEME
DAY 1 HOUR 0 LAYER 1
SCALE
20 M/SEC
HEIGHT
100M

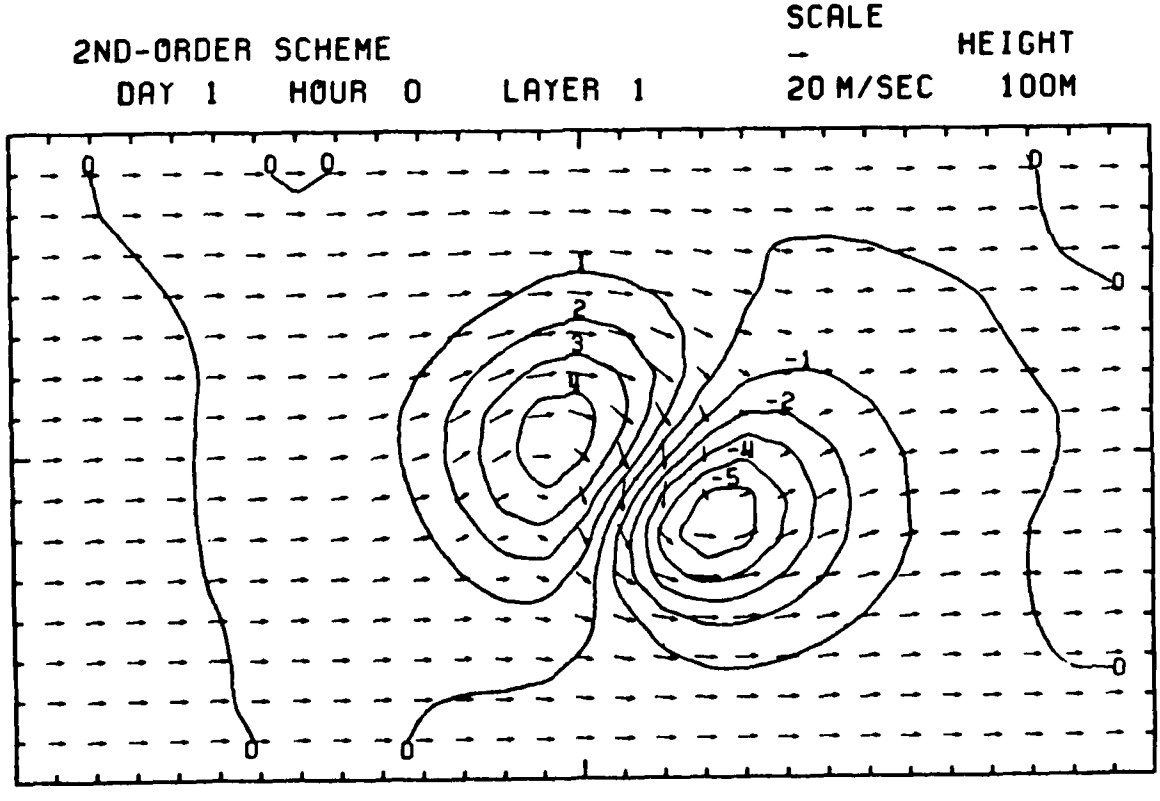
2ND-ORDER SCHEME
DAY 1 HOUR 0 LAYER 1
SCALE
20 M/SEC
HEIGHT
100M

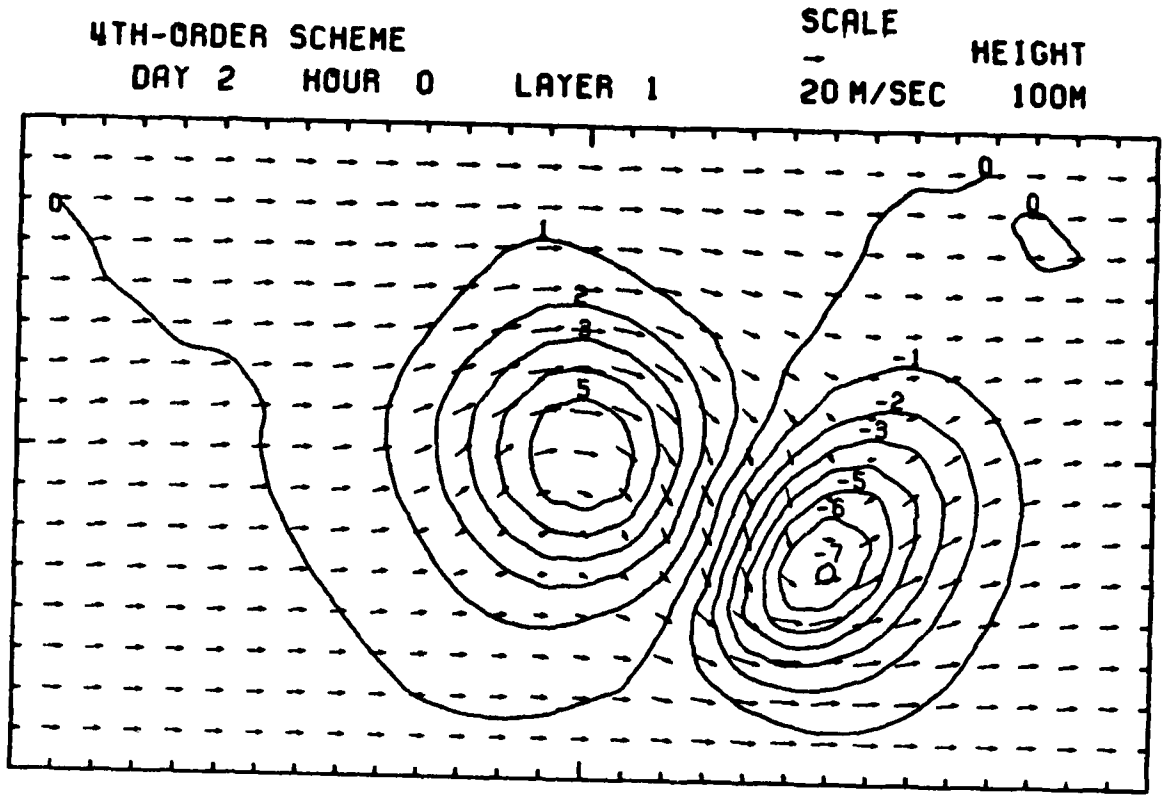
4TH-ORDER SCHEME
DAY 2 HOUR 0 LAYER 1
SCALE
20 M/SEC
HEIGHT
100M

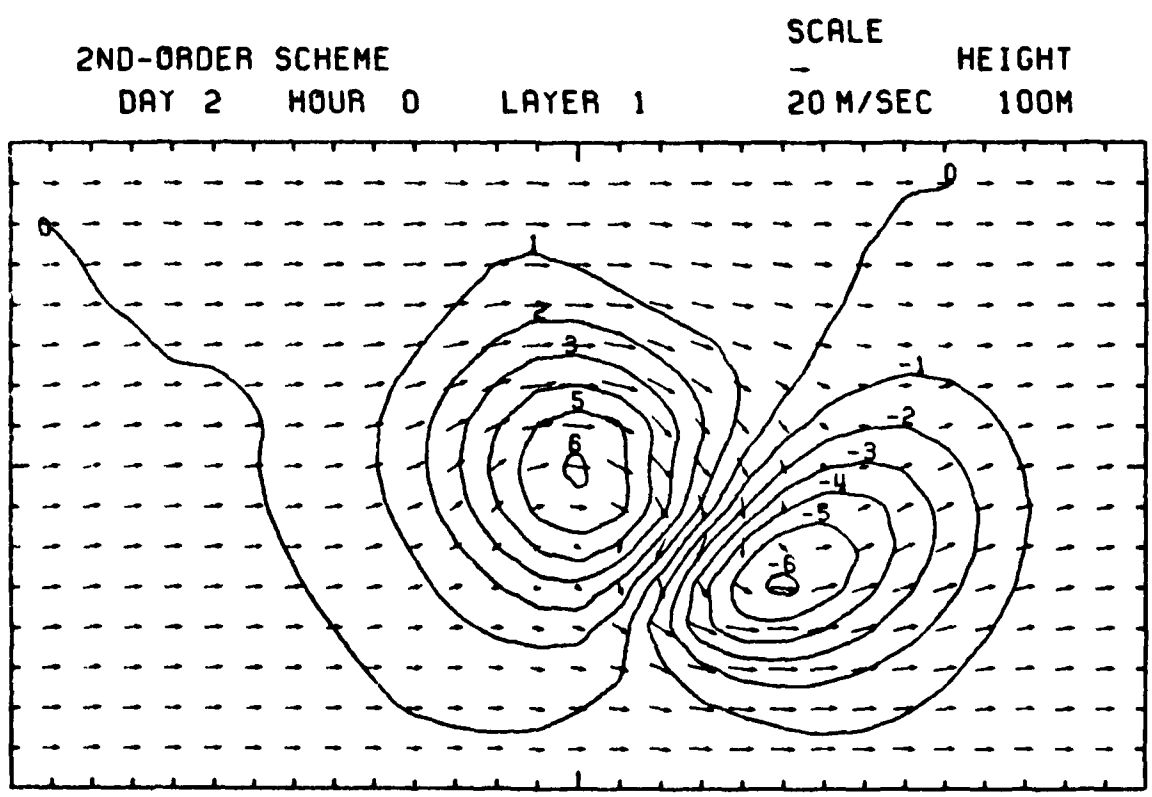
2ND-ORDER SCHEME
DAY 2 HOUR 0 LAYER 1
SCALE
20 M/SEC
HEIGHT
100M

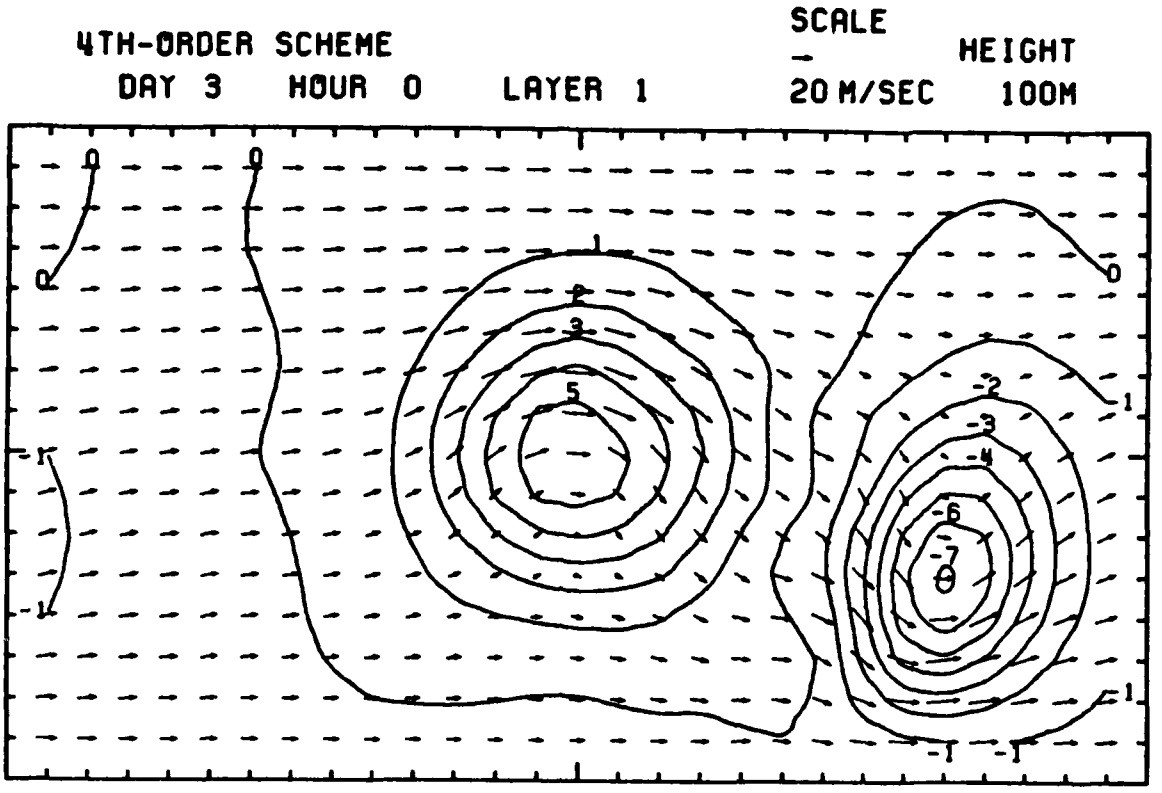
4TH-ORDER SCHEME
DAY 3 HOUR 0 LAYER 1
SCALE
–
20 M/SEC
HEIGHT
100M

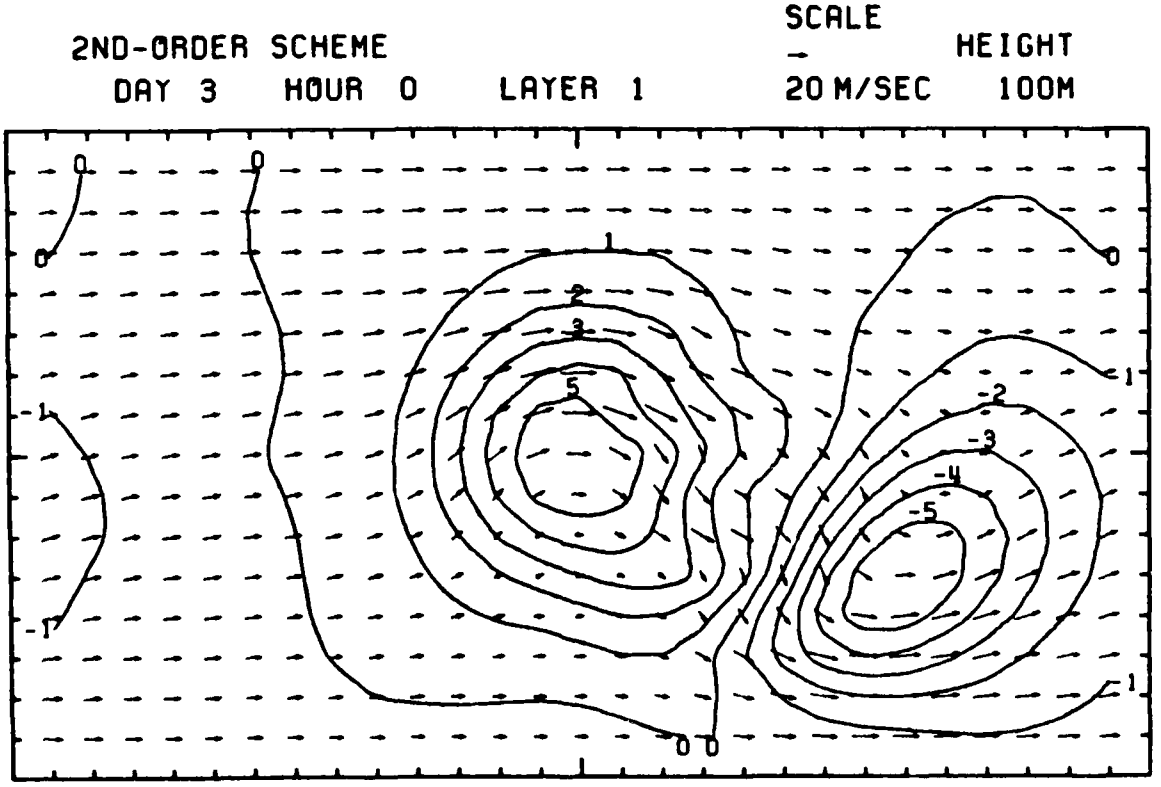
2ND-ORDER SCHEME
DAY 3 HOUR 0 LAYER 1
SCALE
–
20 M/SEC
HEIGHT
100M

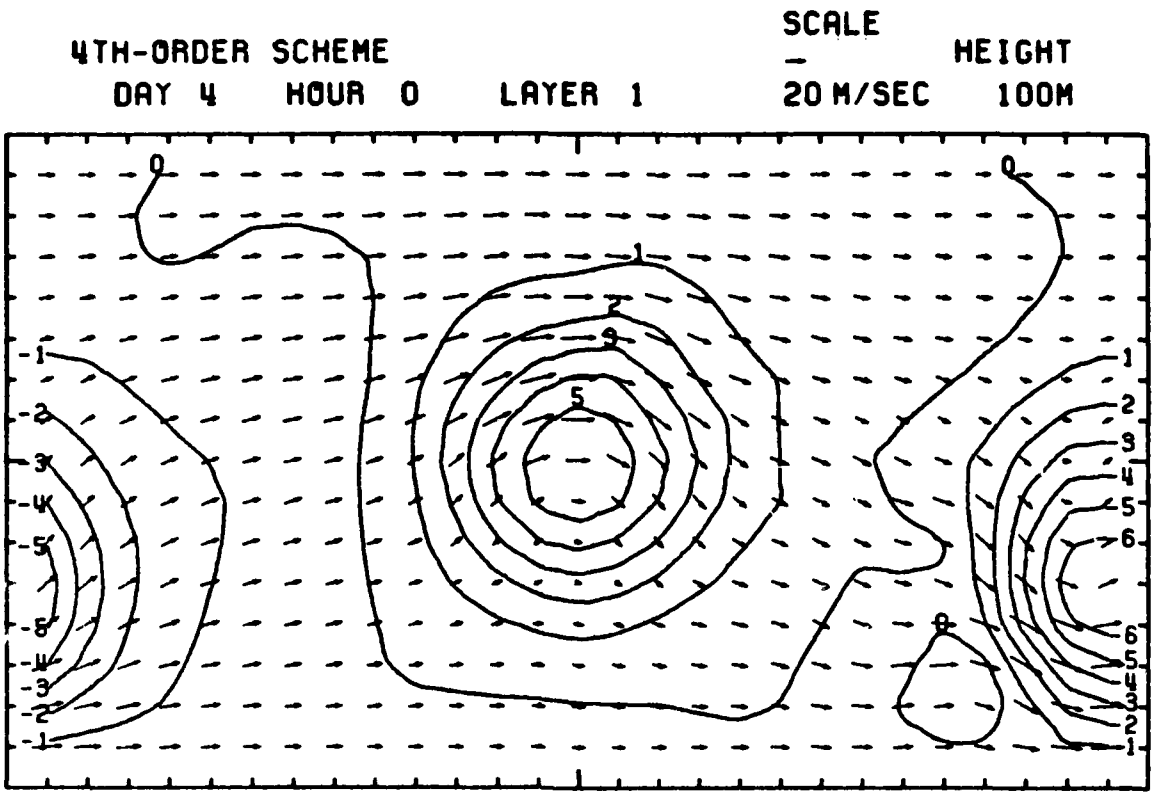
4TH-ORDER SCHEME
DAY 4 HOUR 0 LAYER 1
SCALE
20 M/SEC
HEIGHT
100M

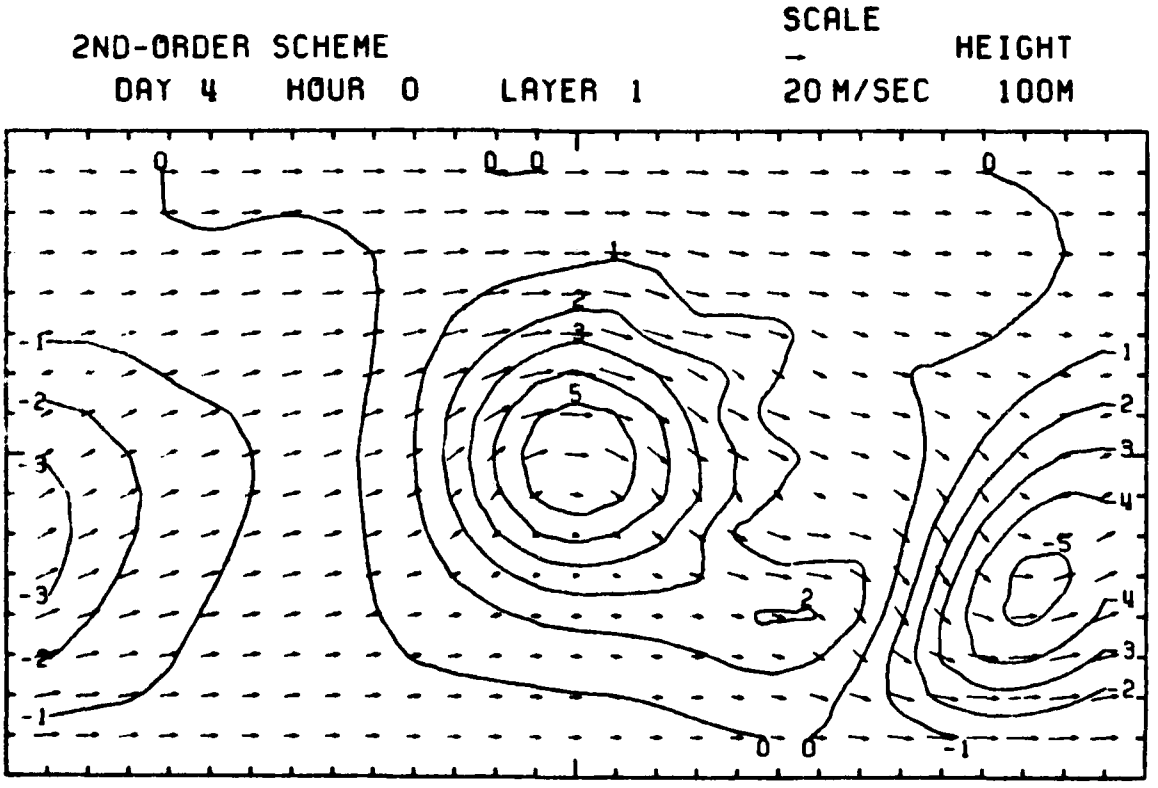
2ND-ORDER SCHEME
DAY 4 HOUR 0 LAYER 1
SCALE
20 M/SEC
HEIGHT
100M

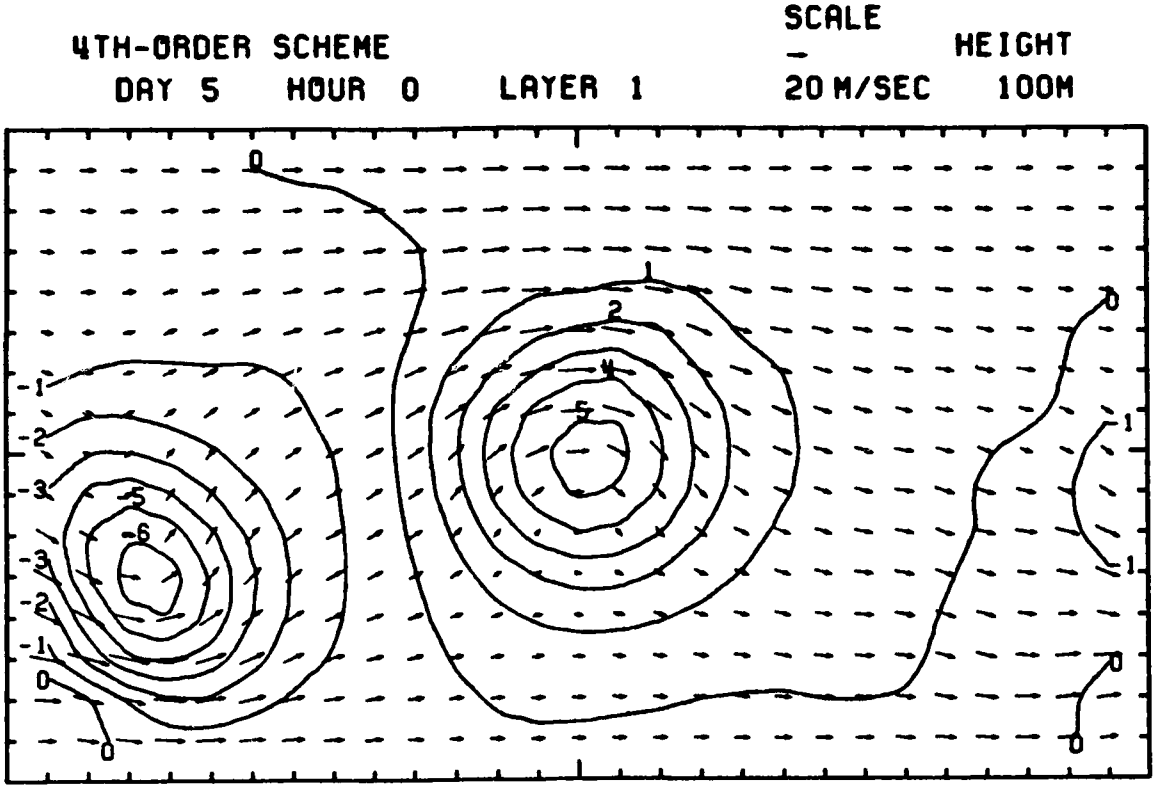
4TH-ORDER SCHEME
DAY 5 HOUR 0 LAYER 1
SCALE
20 M/SEC
HEIGHT
100M

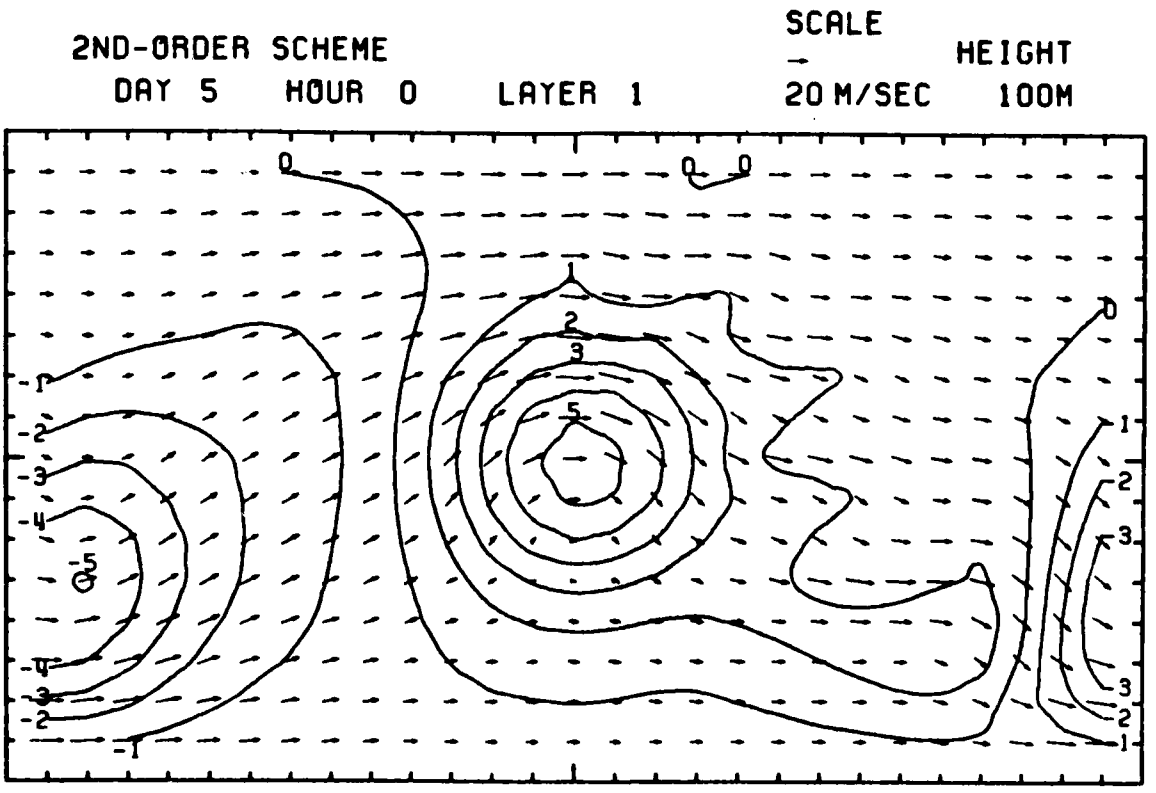
2ND-ORDER SCHEME
DAY 5 HOUR 0 LAYER 1
SCALE
20 M/SEC
HEIGHT
100M

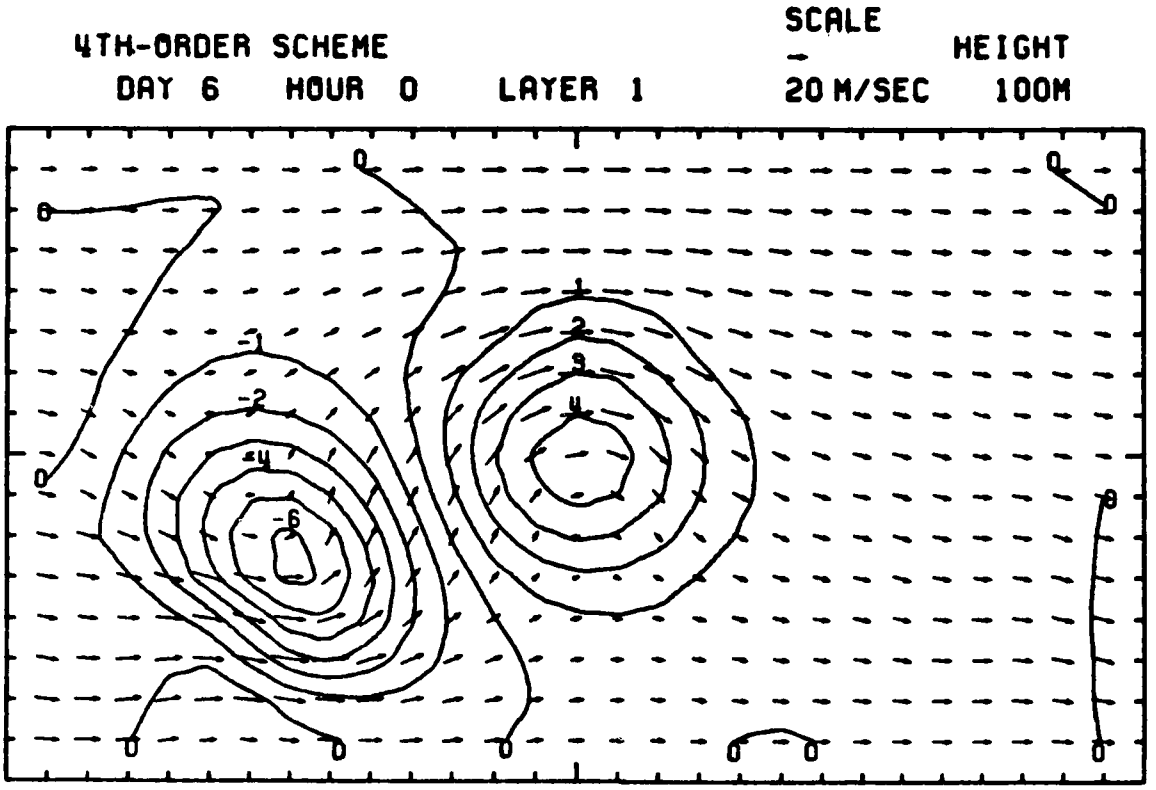
4TH-ORDER SCHEME
DAY 6 HOUR 0 LAYER 1
SCALE
20 M/SEC
HEIGHT
100M

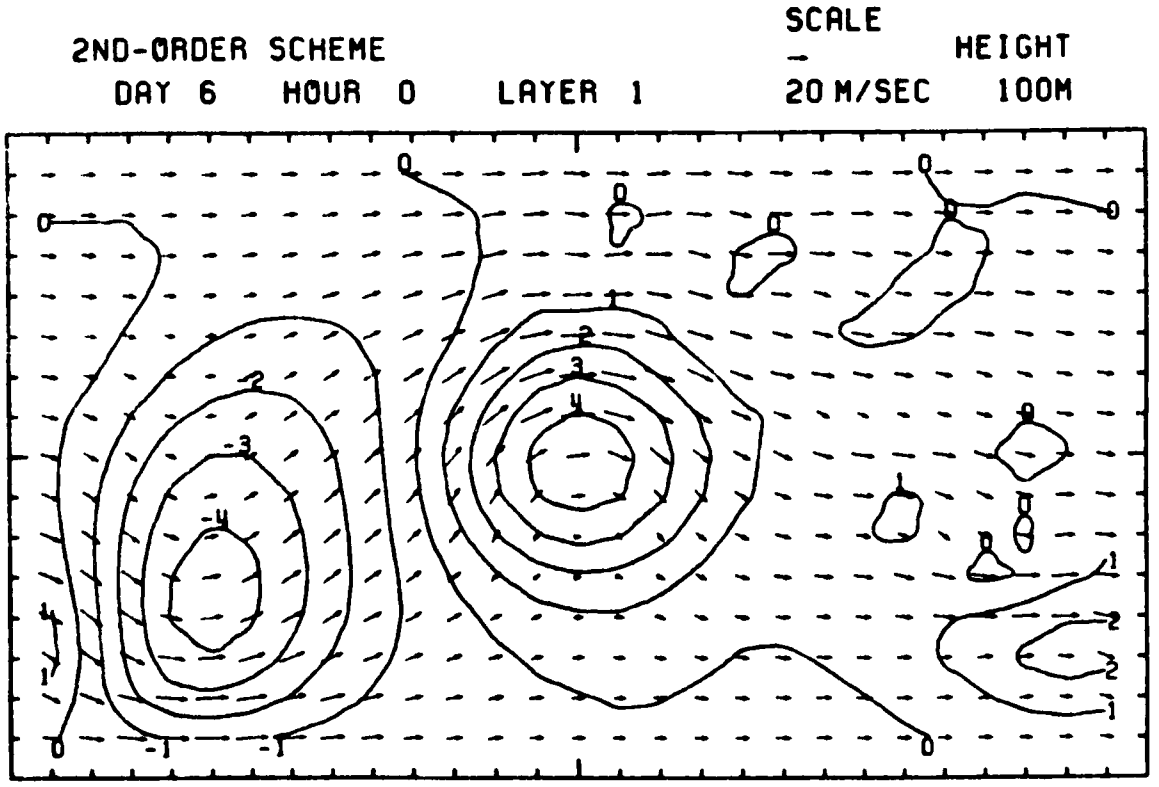
2ND-ORDER SCHEME
DAY 6 HOUR 0 LAYER 1
SCALE
20 M/SEC
HEIGHT
100M

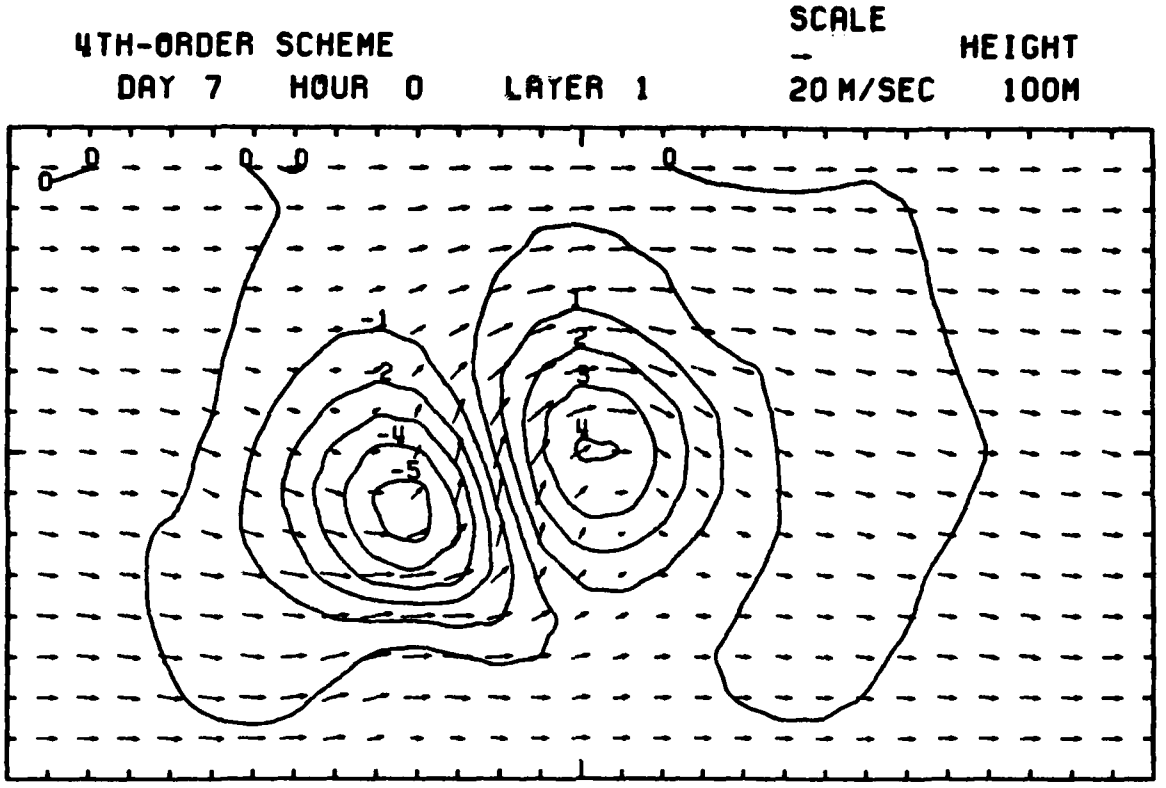
4TH-ORDER SCHEME
DAY 7 HOUR 0 LAYER 1
SCALE
20 M/SEC
HEIGHT
100M

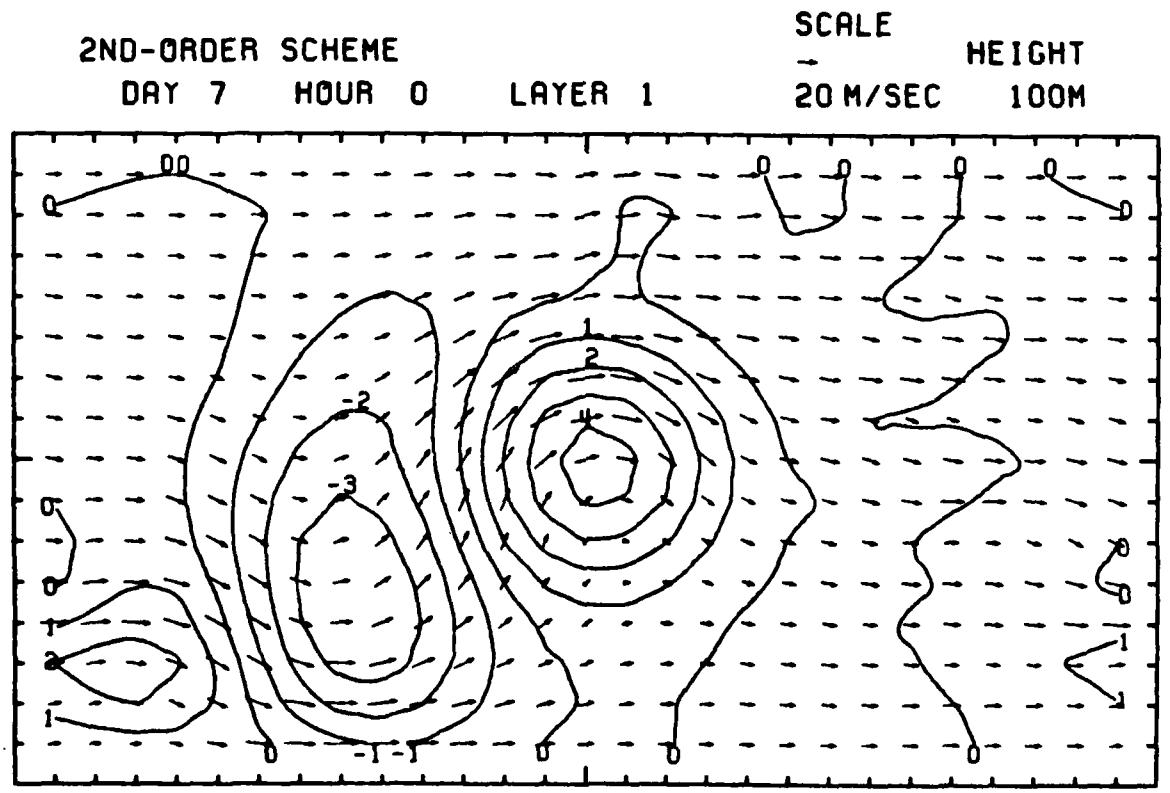
2ND-ORDER SCHEME
DAY 7 HOUR 0 LAYER 1
SCALE
20 M/SEC
HEIGHT
100M

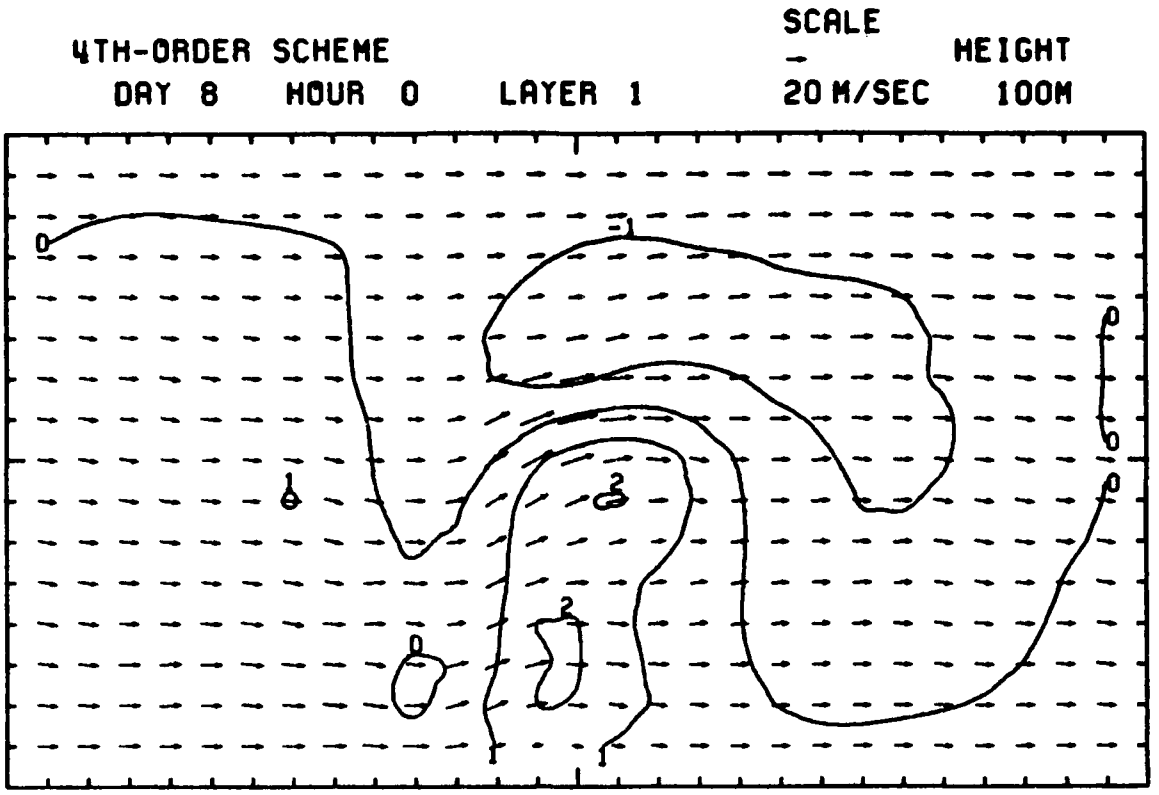
4TH-ORDER SCHEME
DAY 8 HOUR 0 LAYER 1
SCALE
20 M/SEC
HEIGHT
100M

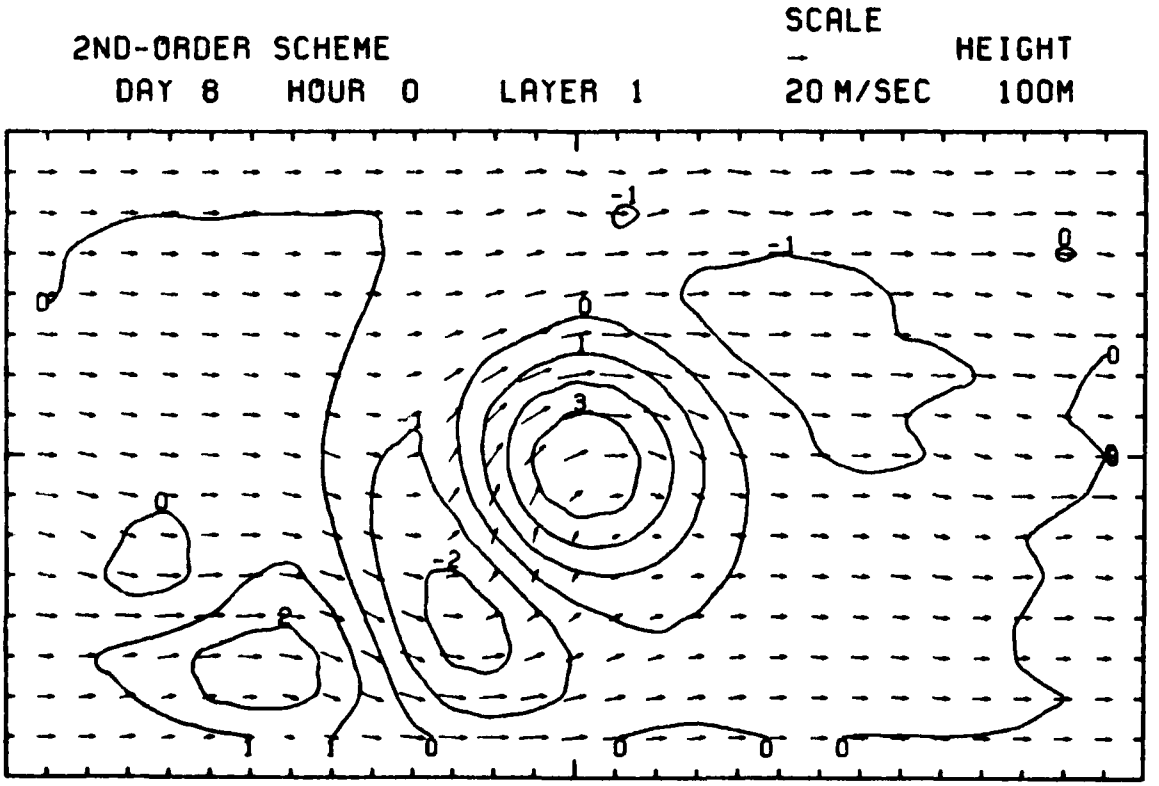
2ND-ORDER SCHEME
DAY 8 HOUR 0 LAYER 1
SCALE
20 M/SEC
HEIGHT
100M

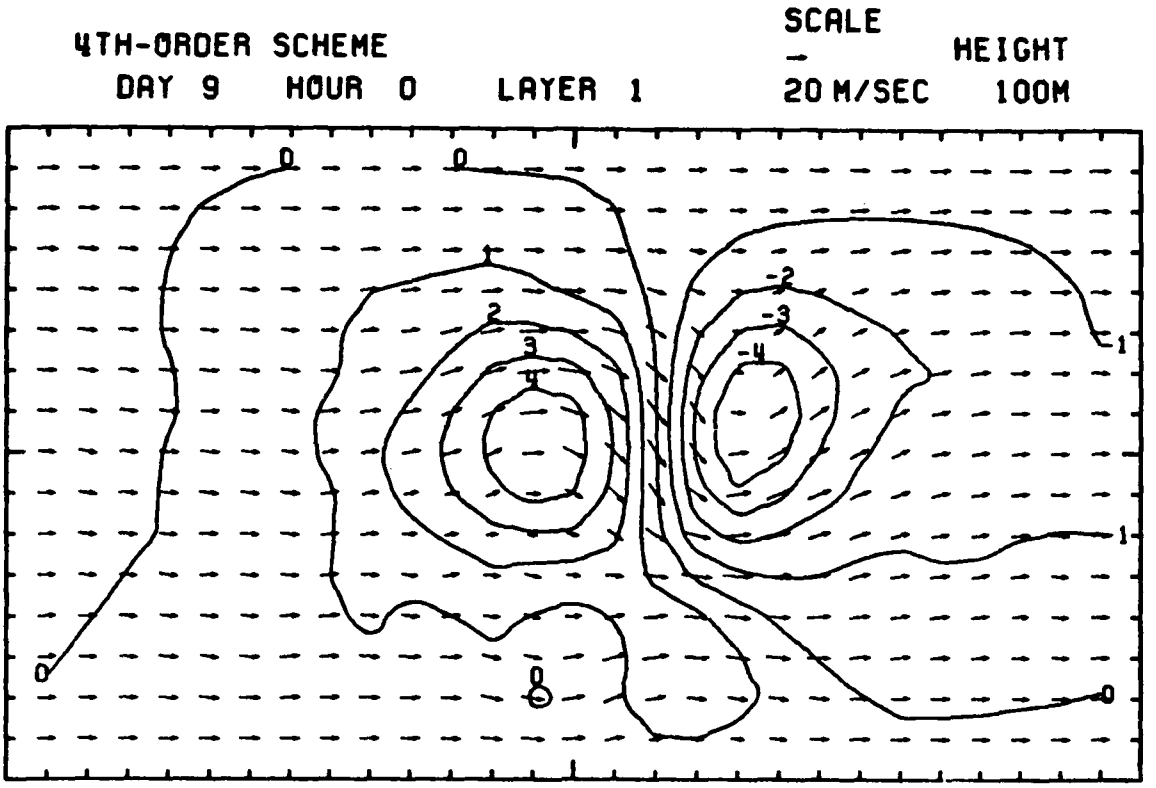
4TH-ORDER SCHEME
DAY 9 HOUR 0 LAYER 1
SCALE
HEIGHT
20 M/SEC 100M

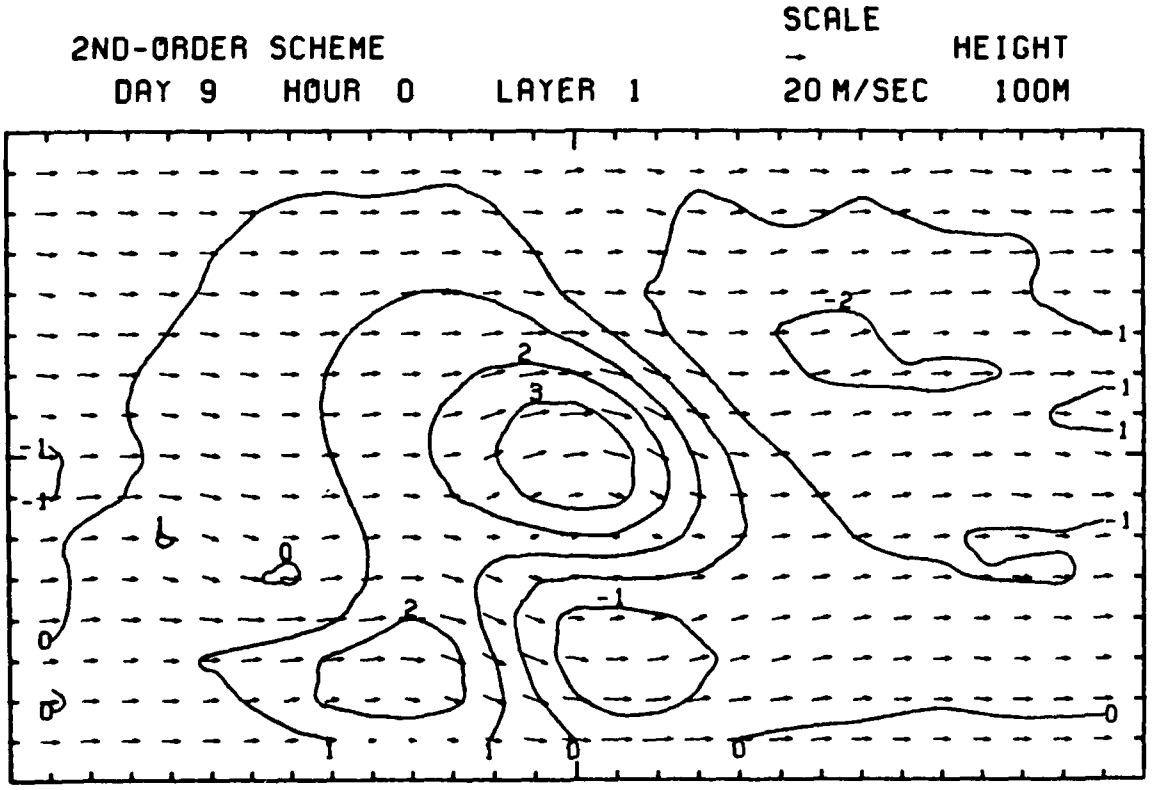
2ND-ORDER SCHEME
DAY 9 HOUR 0 LAYER 1
SCALE
HEIGHT
20 M/SEC 100M

4TH-ORDER SCHEME
DAY 10 HOUR 0 LAYER 1
SCALE — 20 M/SEC
HEIGHT 100M

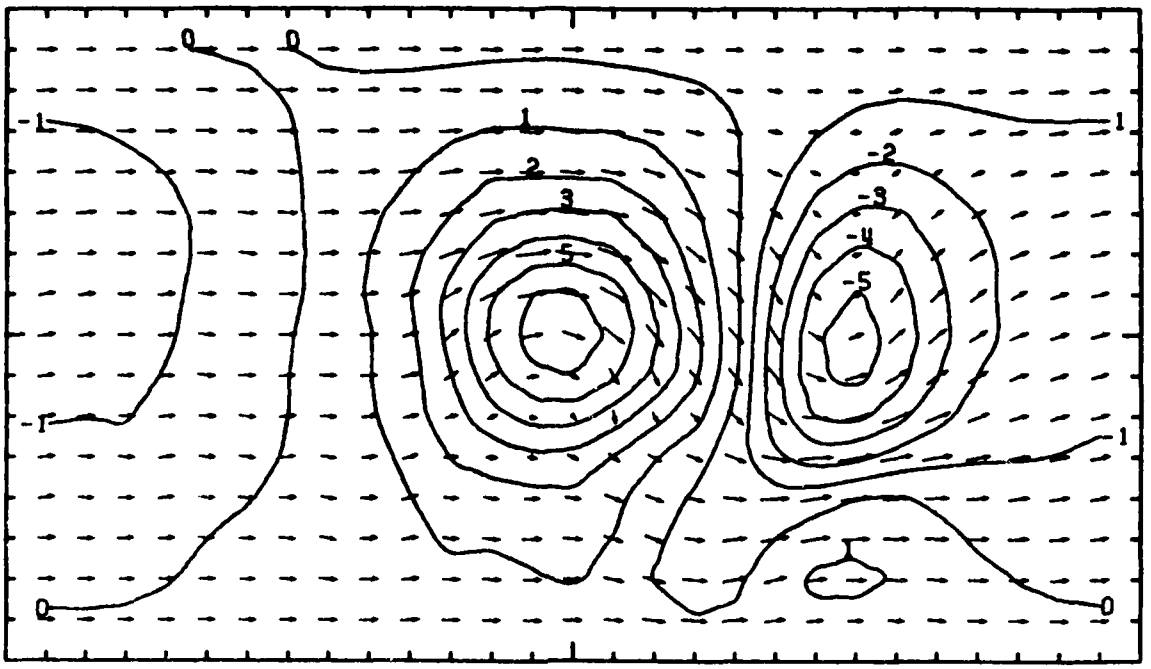

2ND-ORDER SCHEME
DAY 10 HOUR 0 LAYER 1
SCALE — 20 M/SEC
HEIGHT 100M

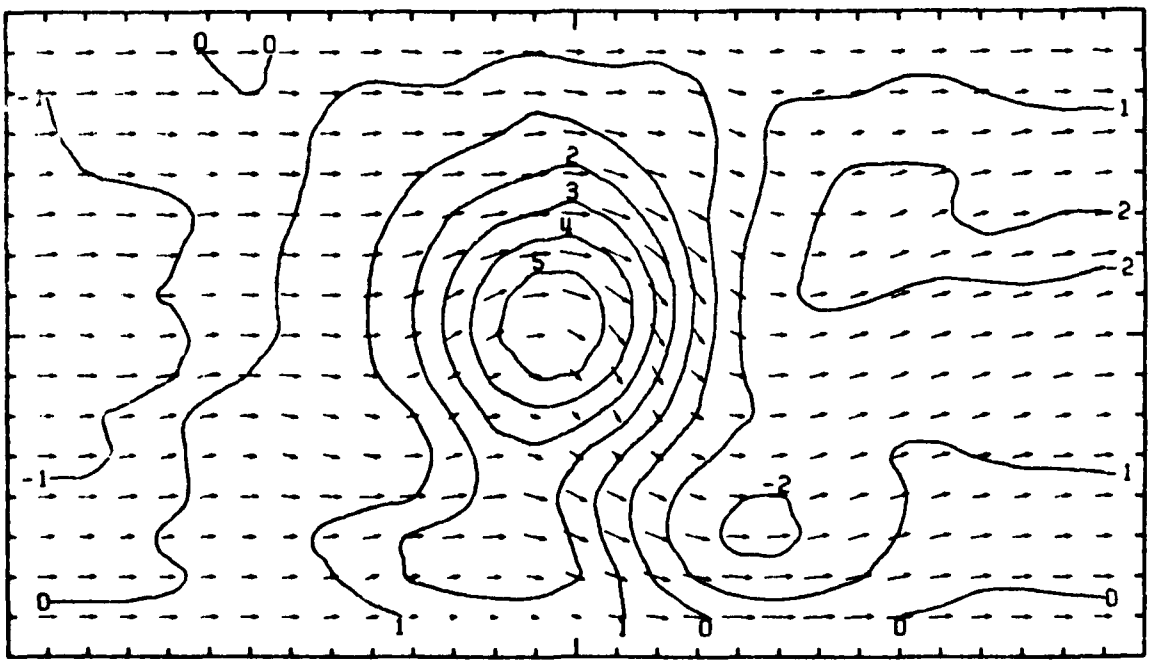

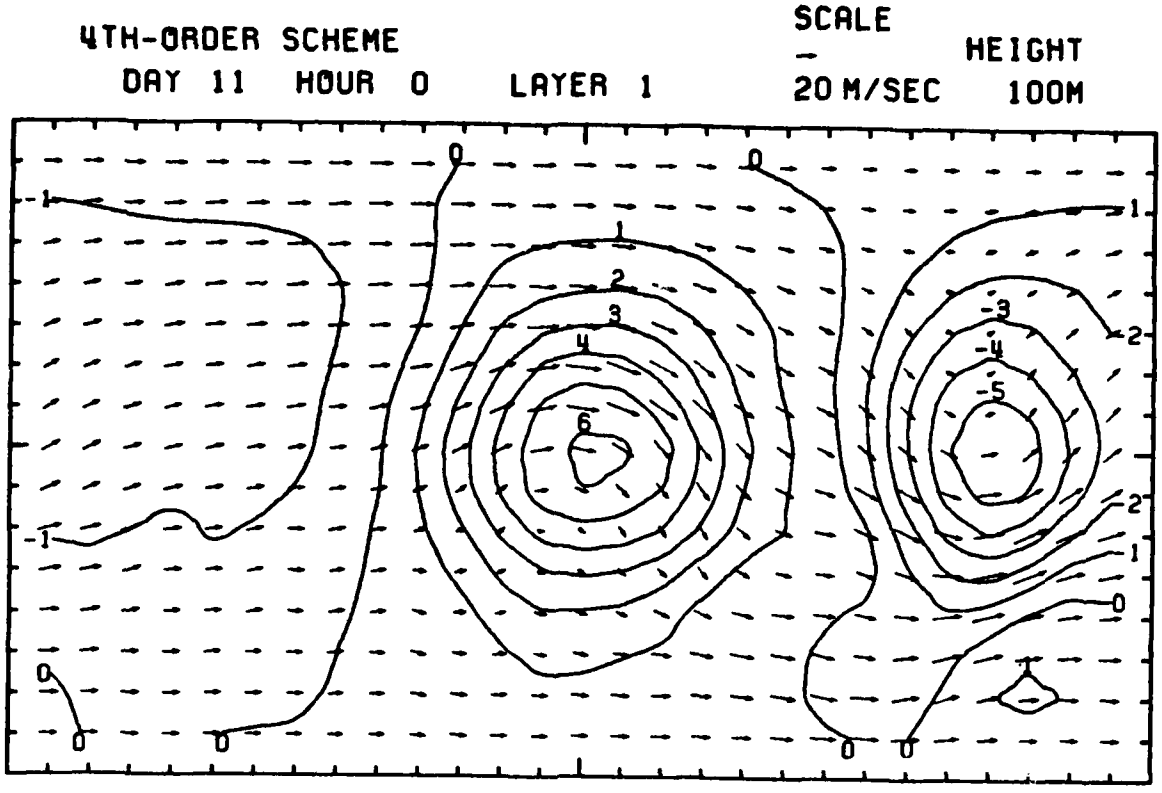
4TH-ORDER SCHEME
DAY 11 HOUR 0 LAYER 1
SCALE
–
20 M/SEC
HEIGHT
100M

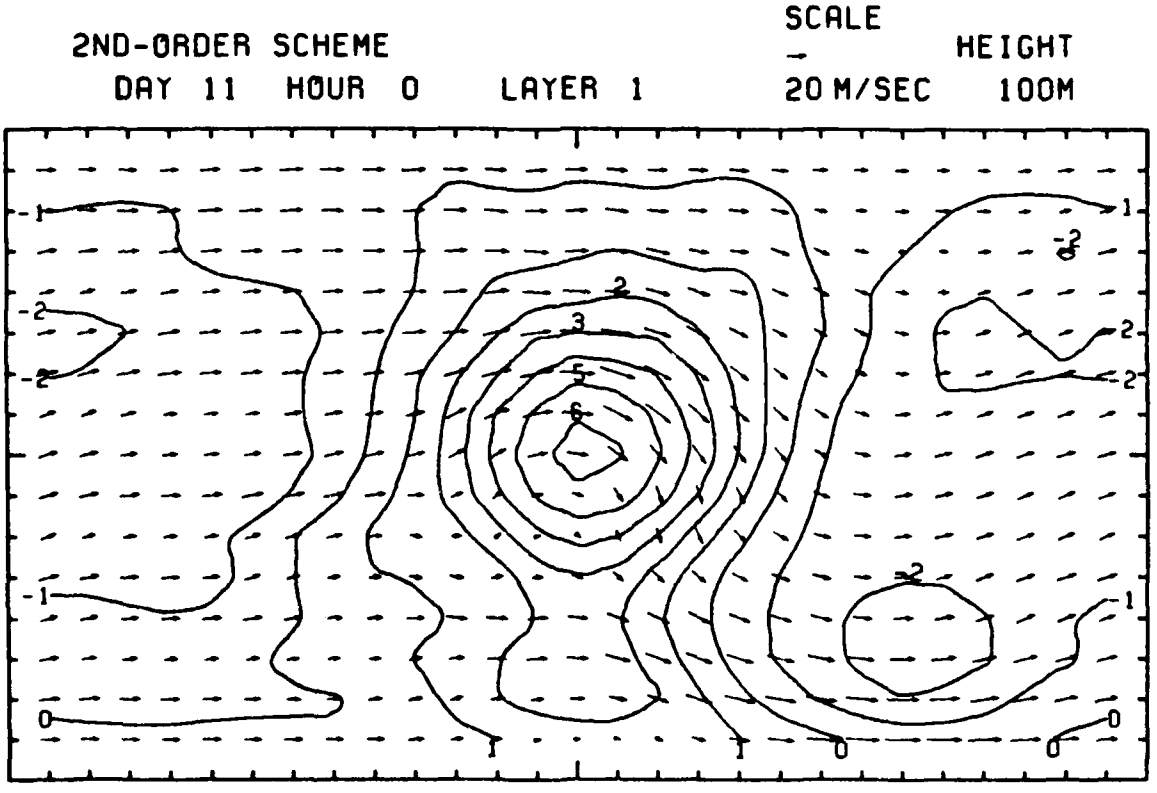
2ND-ORDER SCHEME
DAY 11 HOUR 0 LAYER 1
SCALE
–
20 M/SEC
HEIGHT
100M

4TH-ORDER SCHEME
DAY 12 HOUR 0 LAYER 1

SCALE
–
20 M/SEC

HEIGHT
100M

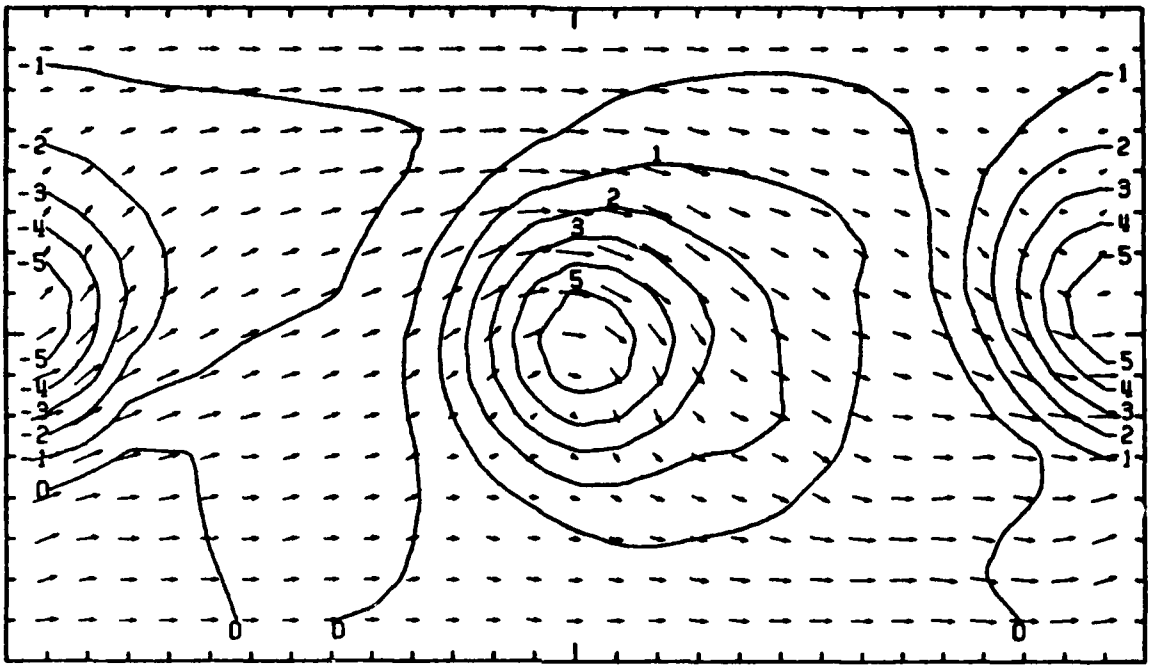

2ND-ORDER SCHEME
DAY 12 HOUR 0 LAYER 1

SCALE
–
20 M/SEC

HEIGHT
100M

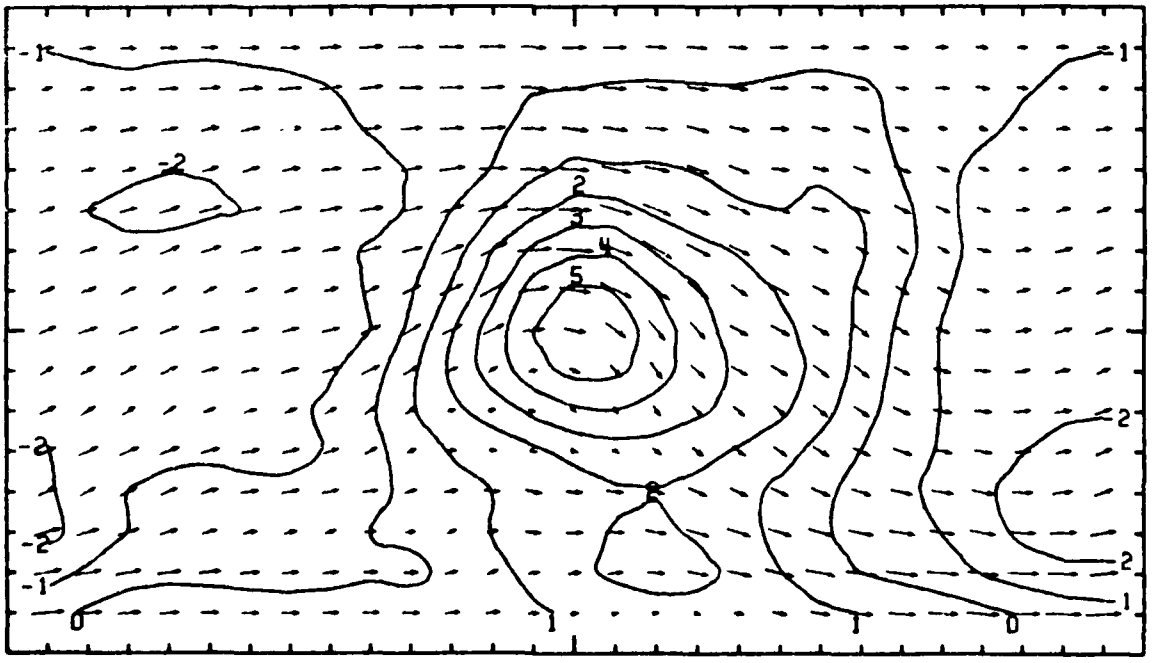

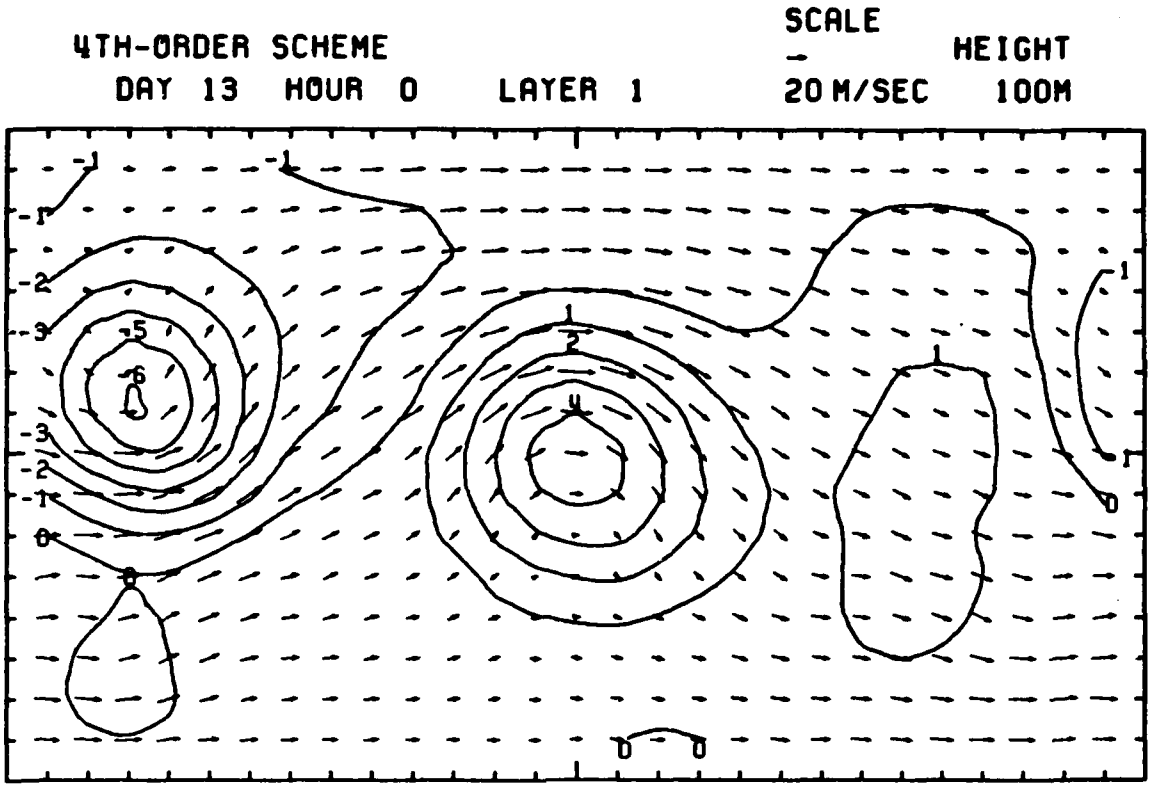
4TH-ORDER SCHEME
DAY 13 HOUR 0 LAYER 1
SCALE
20 M/SEC
HEIGHT
100M

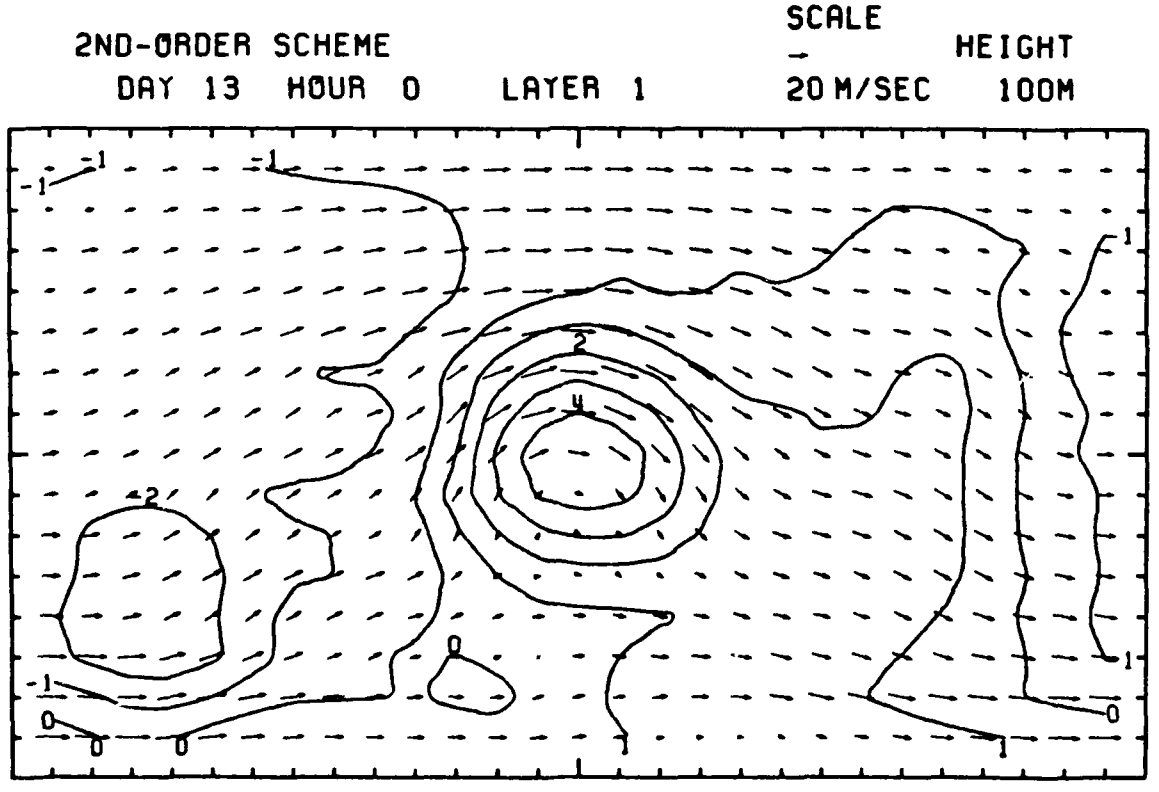
2ND-ORDER SCHEME
DAY 13 HOUR 0 LAYER 1
SCALE
20 M/SEC
HEIGHT
100M

4TH-ORDER SCHEME
DAY 14 HOUR 0 LAYER 1

SCALE
–
20 M/SEC

HEIGHT
100M

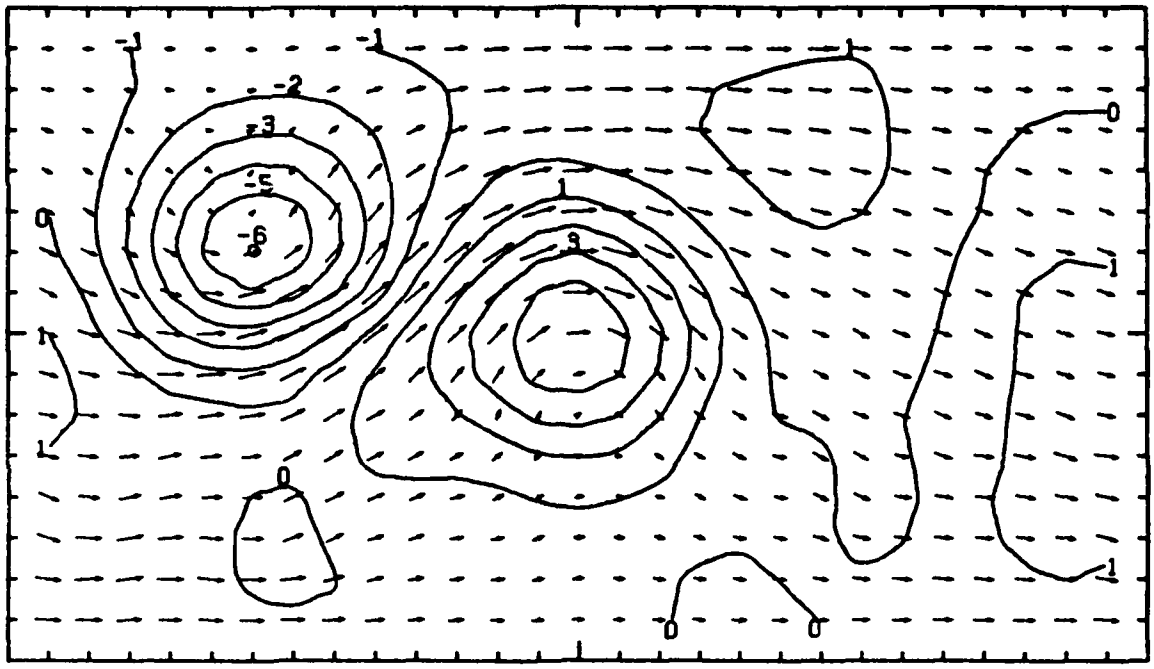

2ND-ORDER SCHEME
DAY 14 HOUR 0 LAYER 1

SCALE
–
20 M/SEC

HEIGHT
100M

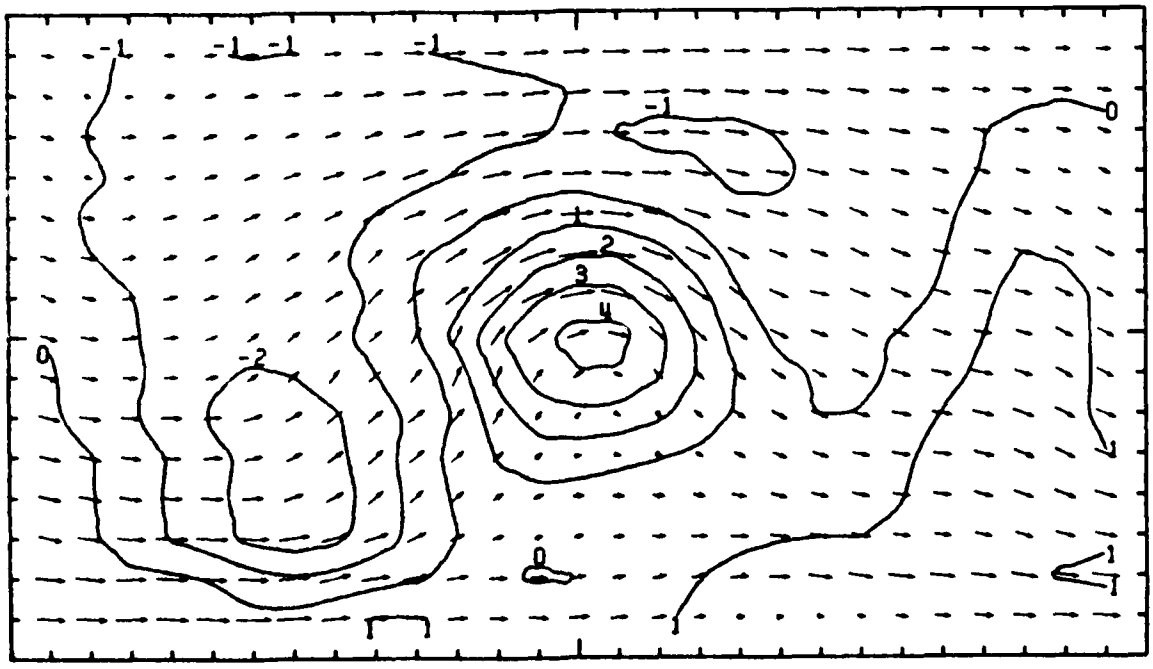

4TH-ORDER SCHEME
DAY 15 HOUR 0 LAYER 1

SCALE
–
20 M/SEC

HEIGHT
100M

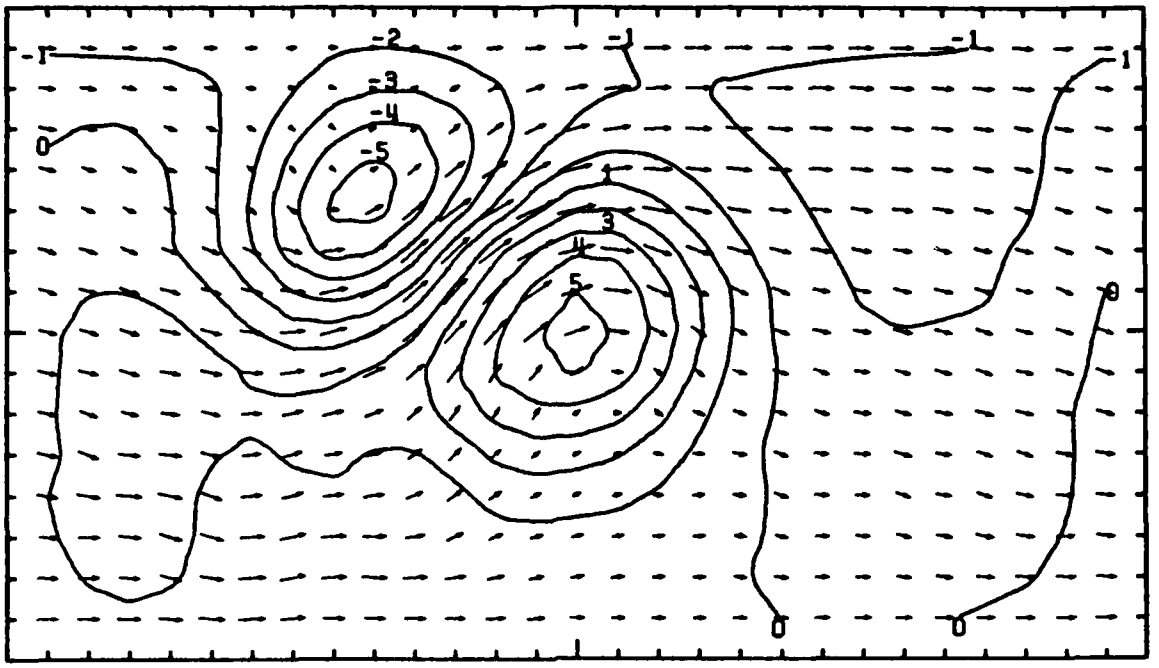

2ND-ORDER SCHEME
DAY 15 HOUR 0 LAYER 1

SCALE
–
20 M/SEC

HEIGHT
100M

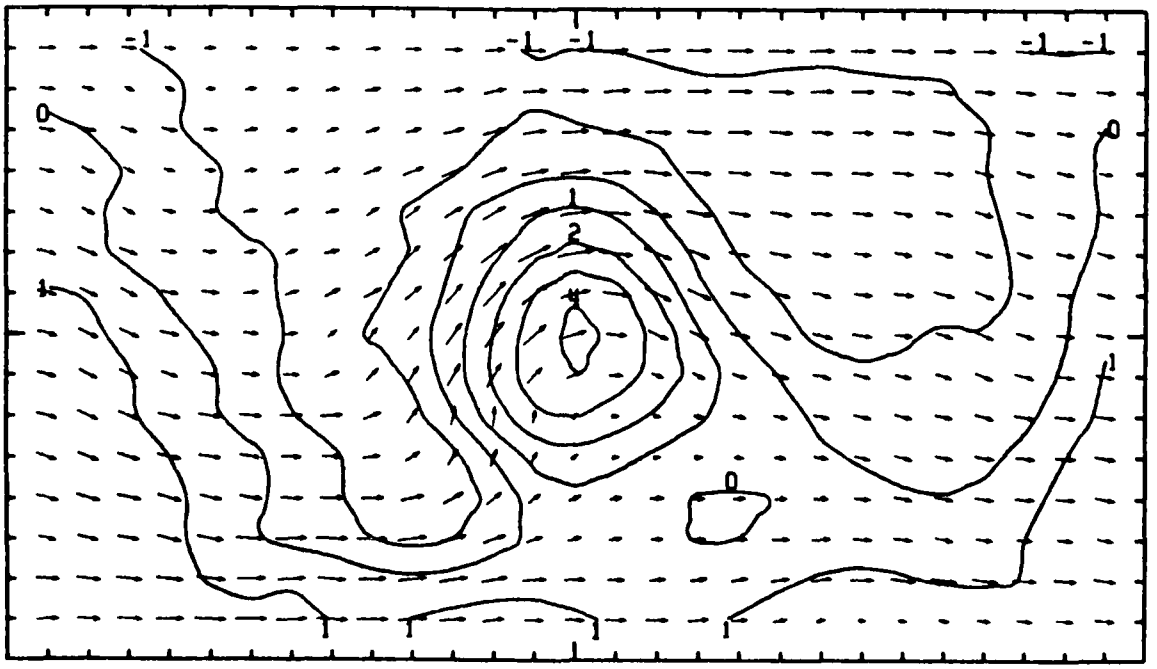

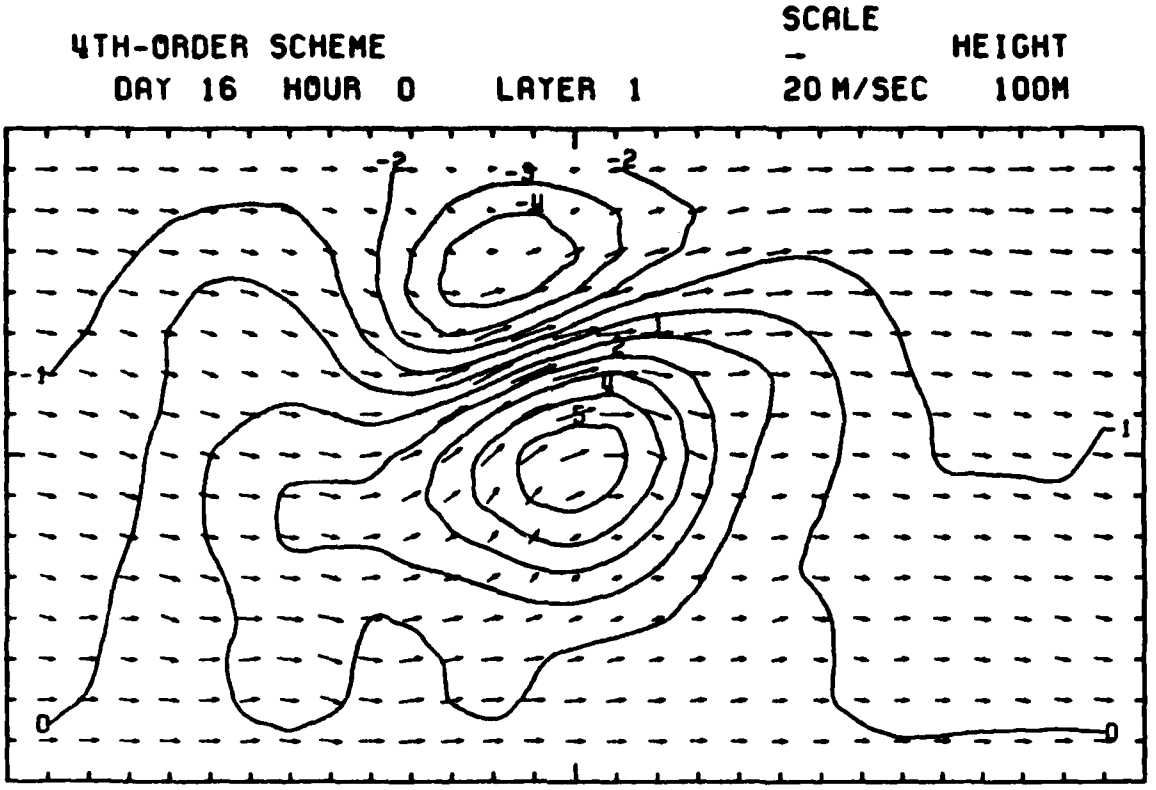
4TH-ORDER SCHEME
DAY 16 HOUR 0 LAYER 1
SCALE
20 M/SEC
HEIGHT
100M

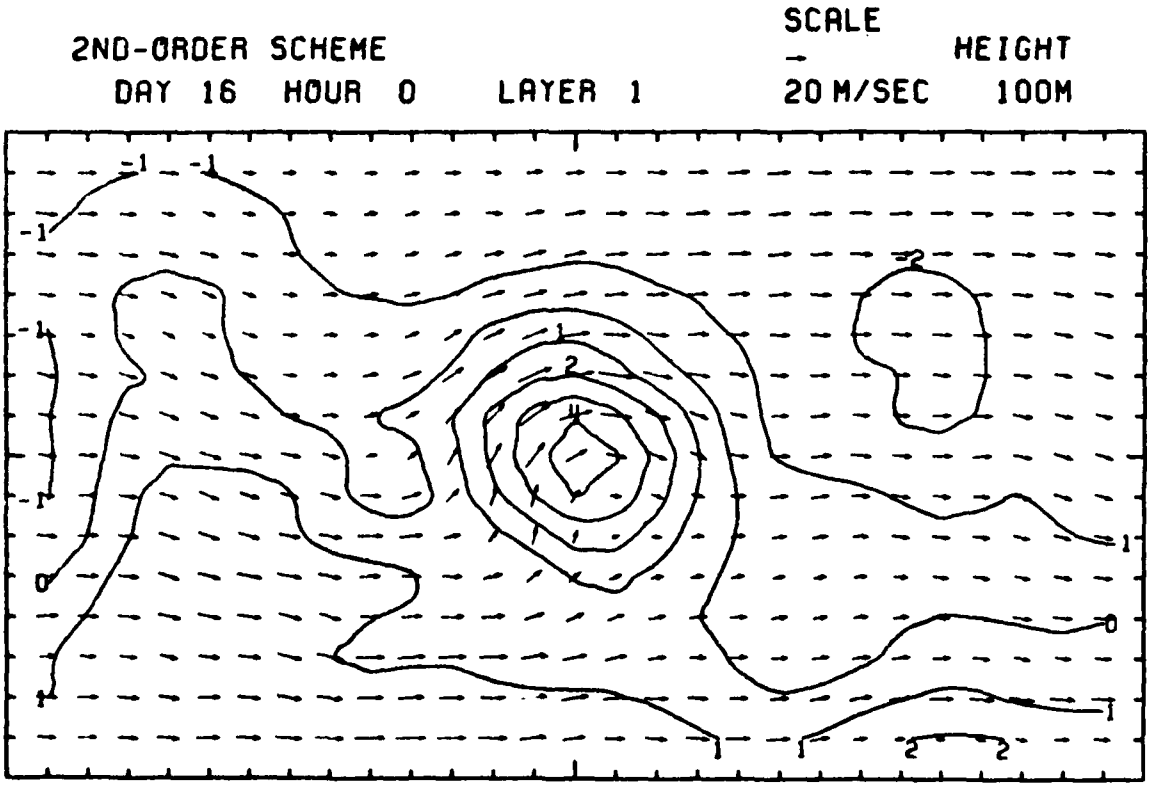
2ND-ORDER SCHEME
DAY 16 HOUR 0 LAYER 1
SCALE
20 M/SEC
HEIGHT
100M

4TH-ORDER SCHEME
DAY 17 HOUR 0 LAYER 1

SCALE
–
20 M/SEC

HEIGHT
100M

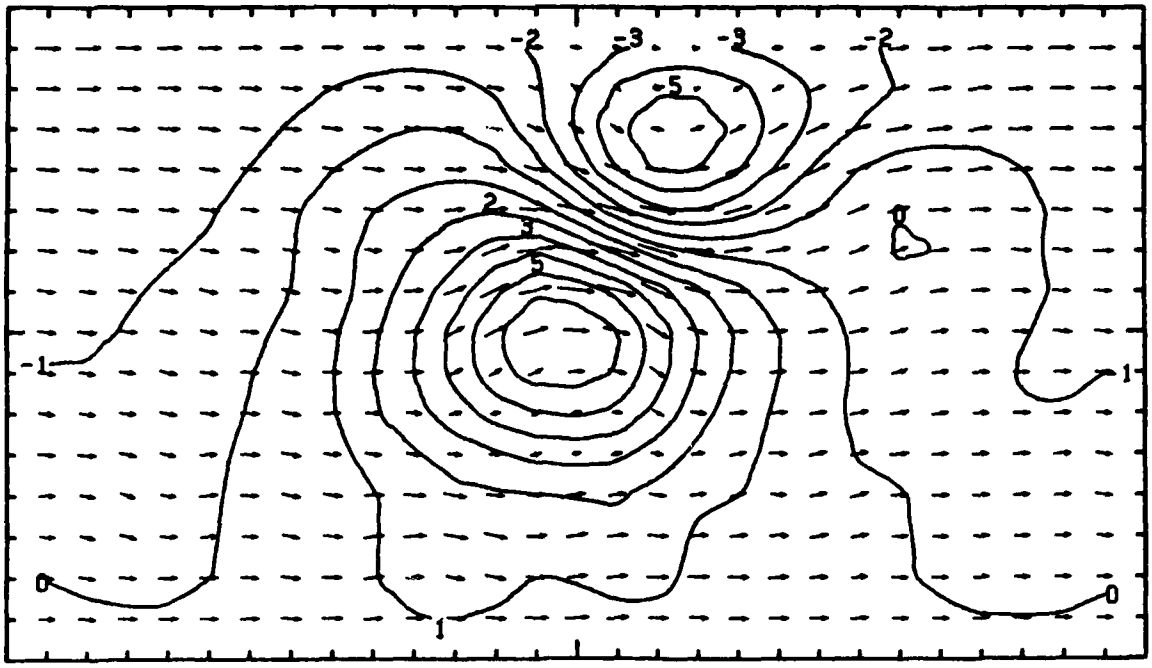

2ND-ORDER SCHEME
DAY 17 HOUR 0 LAYER 1

SCALE
–
20 M/SEC

HEIGHT
100M

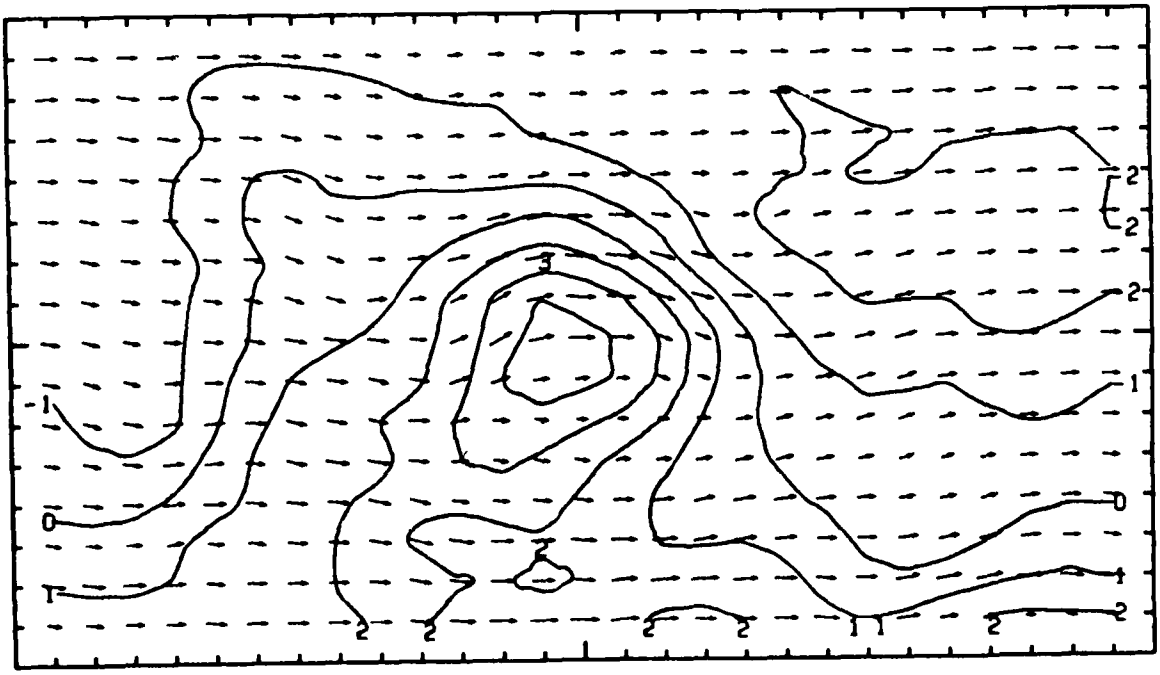

4TH-ORDER SCHEME
DAY 18 HOUR 0 LAYER 1
SCALE — 20 M/SEC
HEIGHT 100M

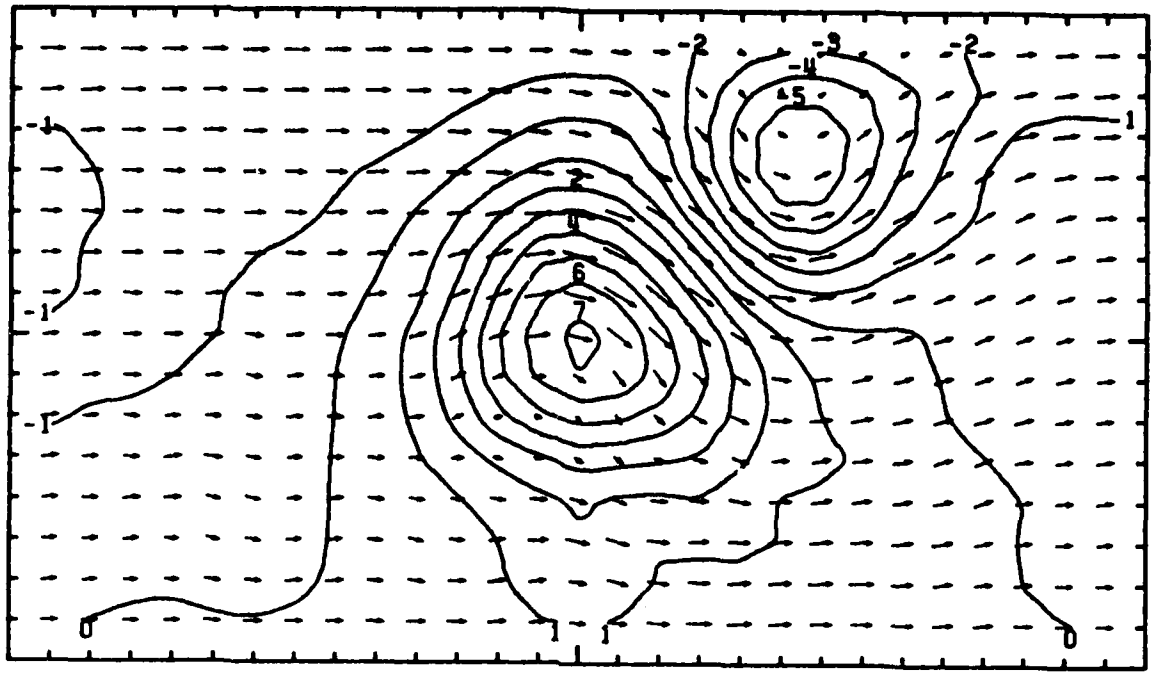

2ND-ORDER SCHEME
DAY 18 HOUR 0 LAYER 1
SCALE — 20 M/SEC
HEIGHT 100M

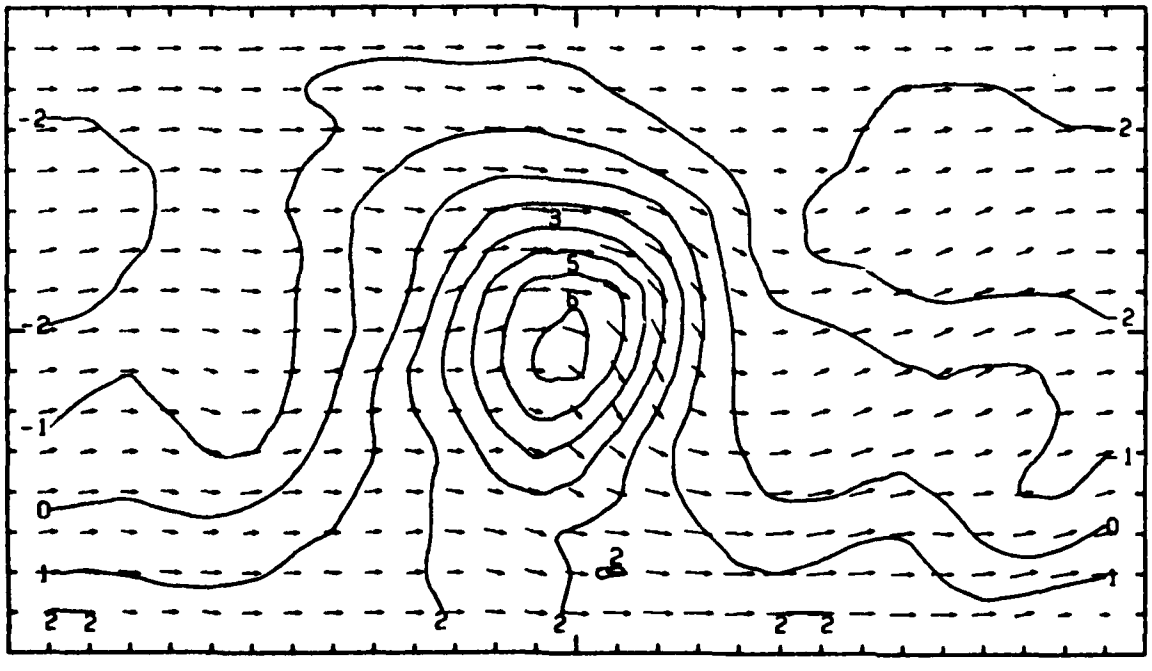

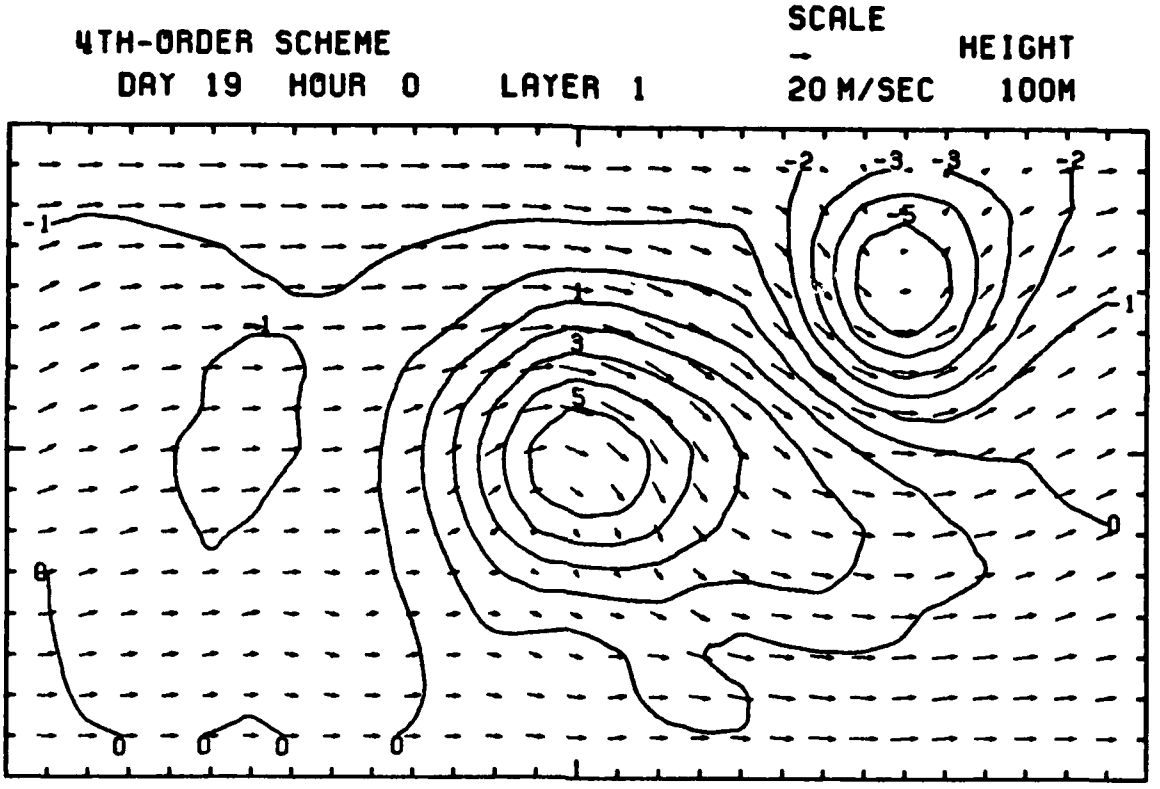
4TH-ORDER SCHEME
DAY 19 HOUR 0 LAYER 1
SCALE
HEIGHT
20 M/SEC 100M

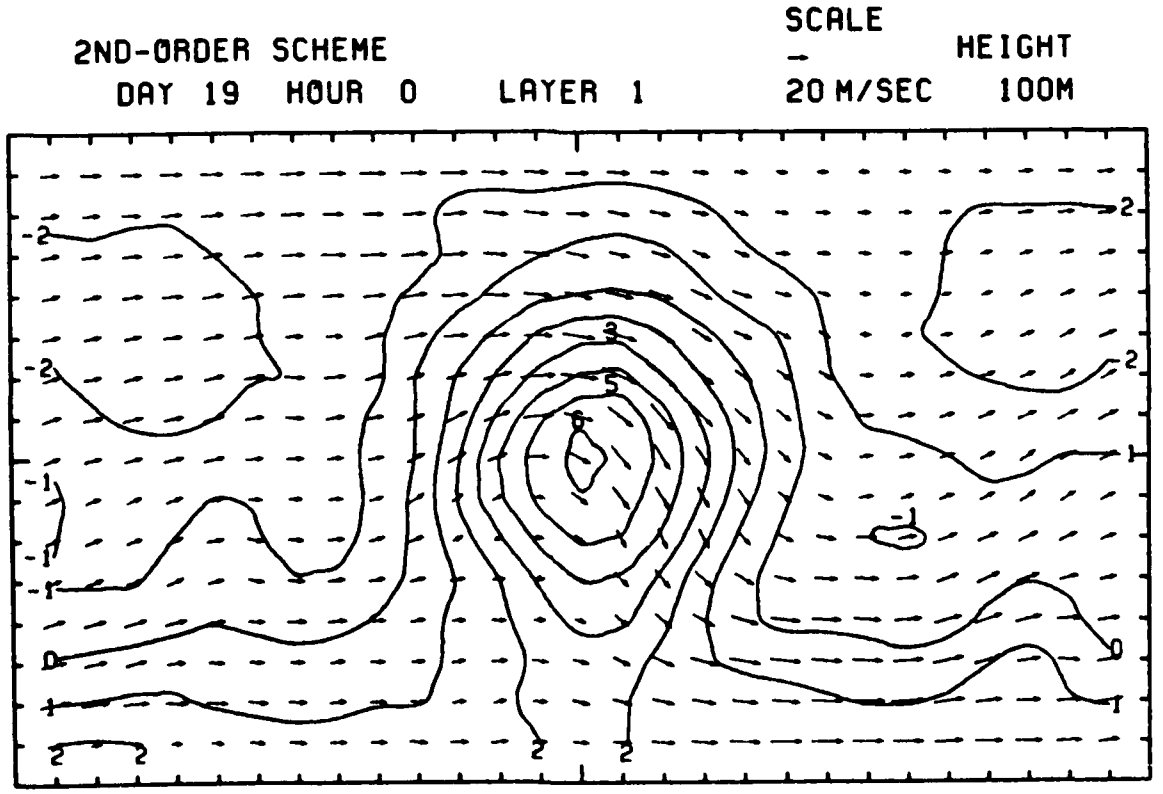
2ND-ORDER SCHEME
DAY 19 HOUR 0 LAYER 1
SCALE
HEIGHT
20 M/SEC 100M

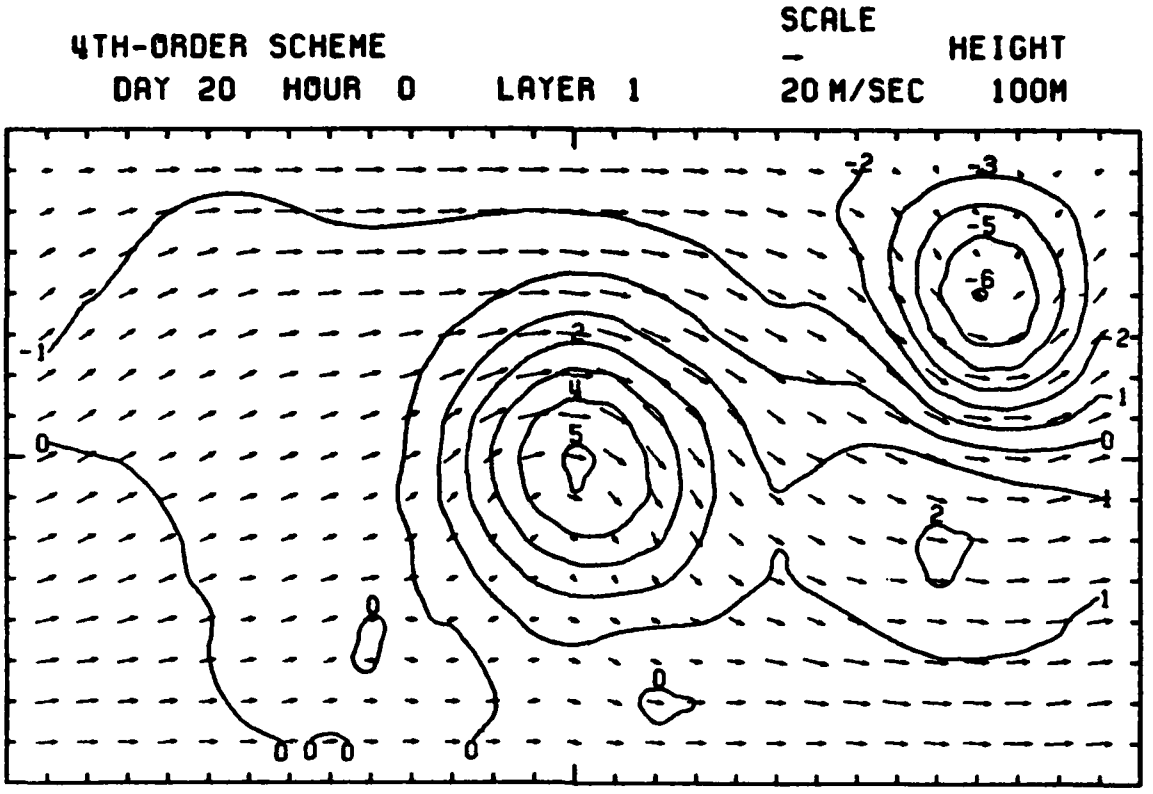
4TH-ORDER SCHEME
DAY 20 HOUR 0 LAYER 1
SCALE
20 M/SEC
HEIGHT
100M

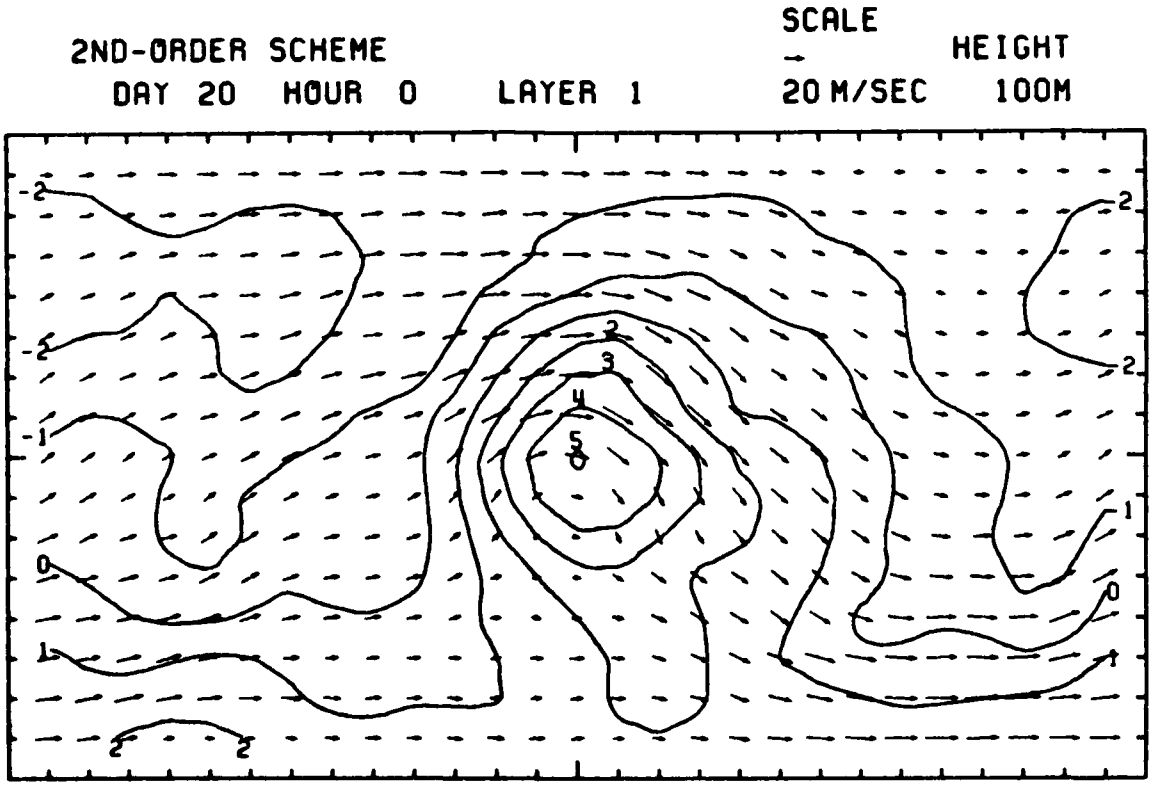
2ND-ORDER SCHEME
DAY 20 HOUR 0 LAYER 1
SCALE
20 M/SEC
HEIGHT
100M

The results of numerical experiments

on the β-plane

Figures 24-43

Day 1, Hour 0 to Day 20, Hour 0

Second- and Fourth-order Schemes

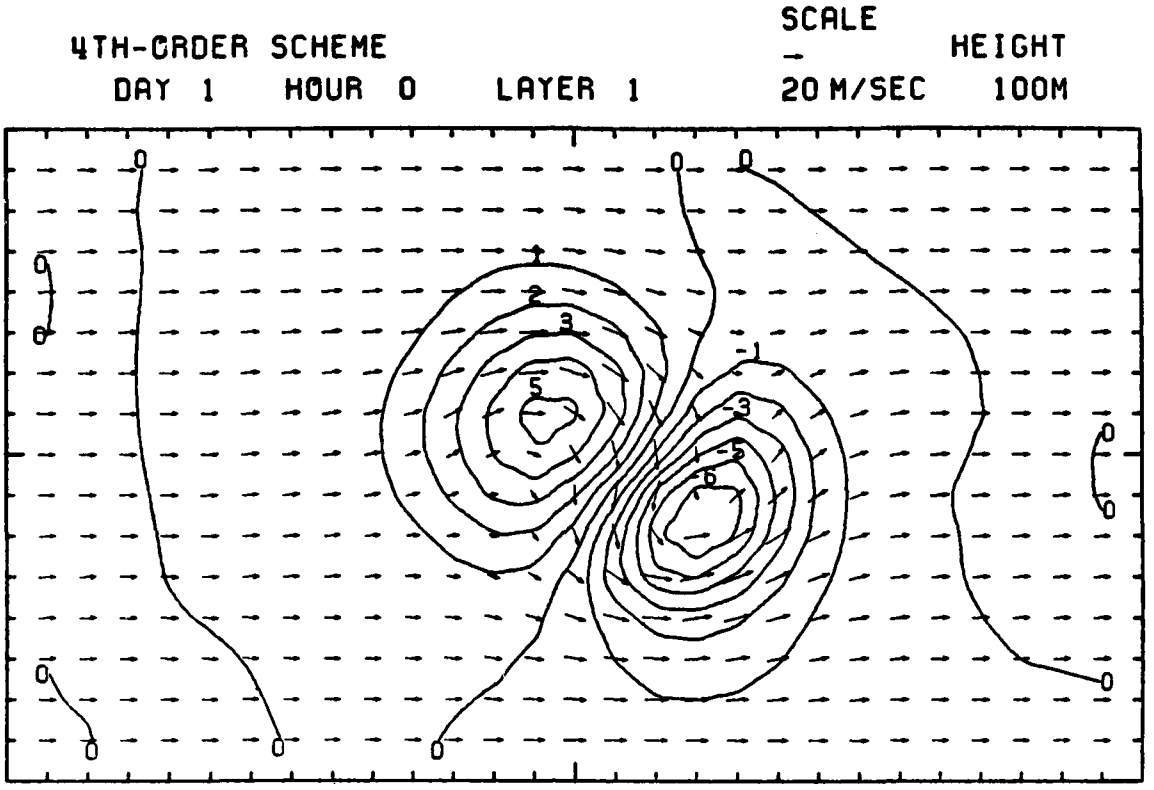
4TH-ORDER SCHEME
DAY 1 HOUR 0 LAYER 1
SCALE
20 M/SEC
HEIGHT
100M

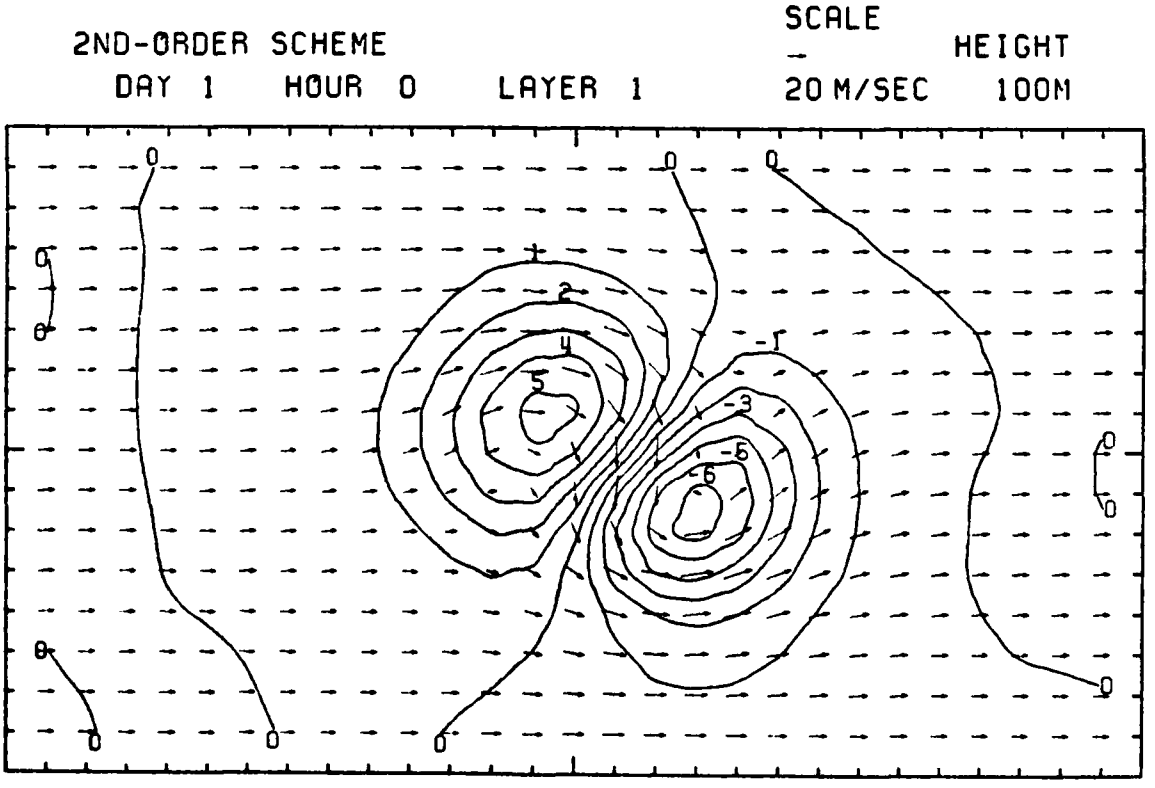
2ND-ORDER SCHEME
DAY 1 HOUR 0 LAYER 1
SCALE
20 M/SEC
HEIGHT
100M

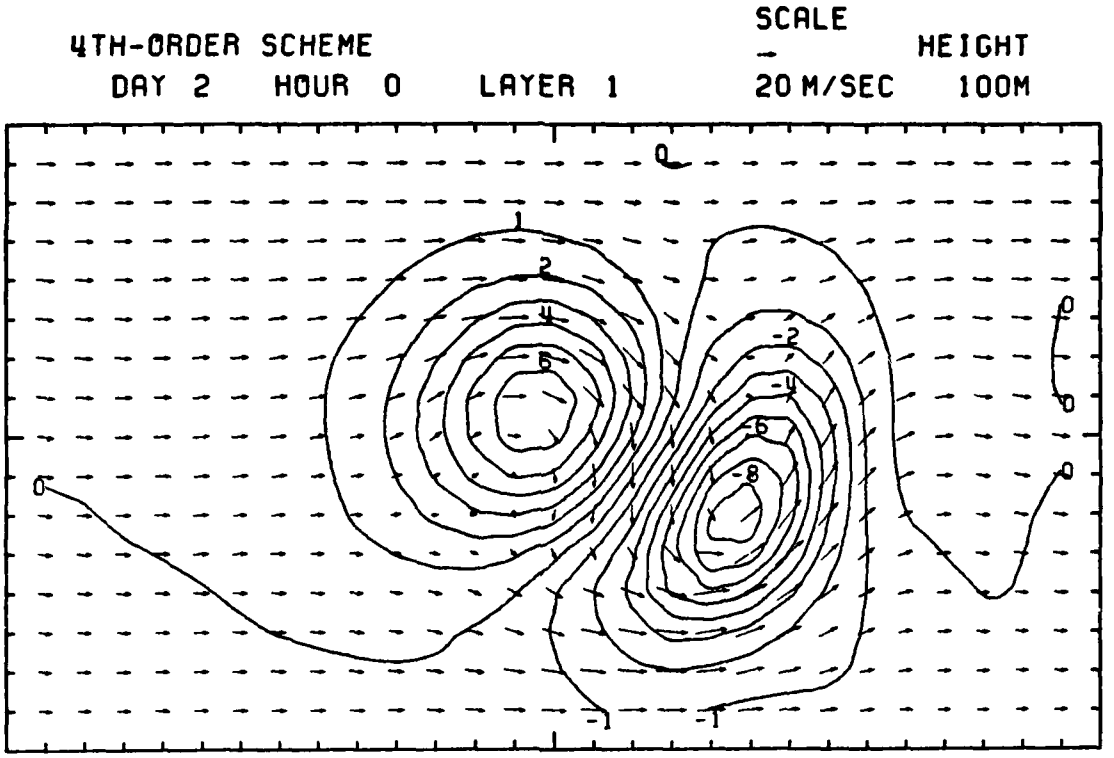
4TH-ORDER SCHEME
DAY 2 HOUR 0 LAYER 1
SCALE
20 M/SEC
HEIGHT
100M

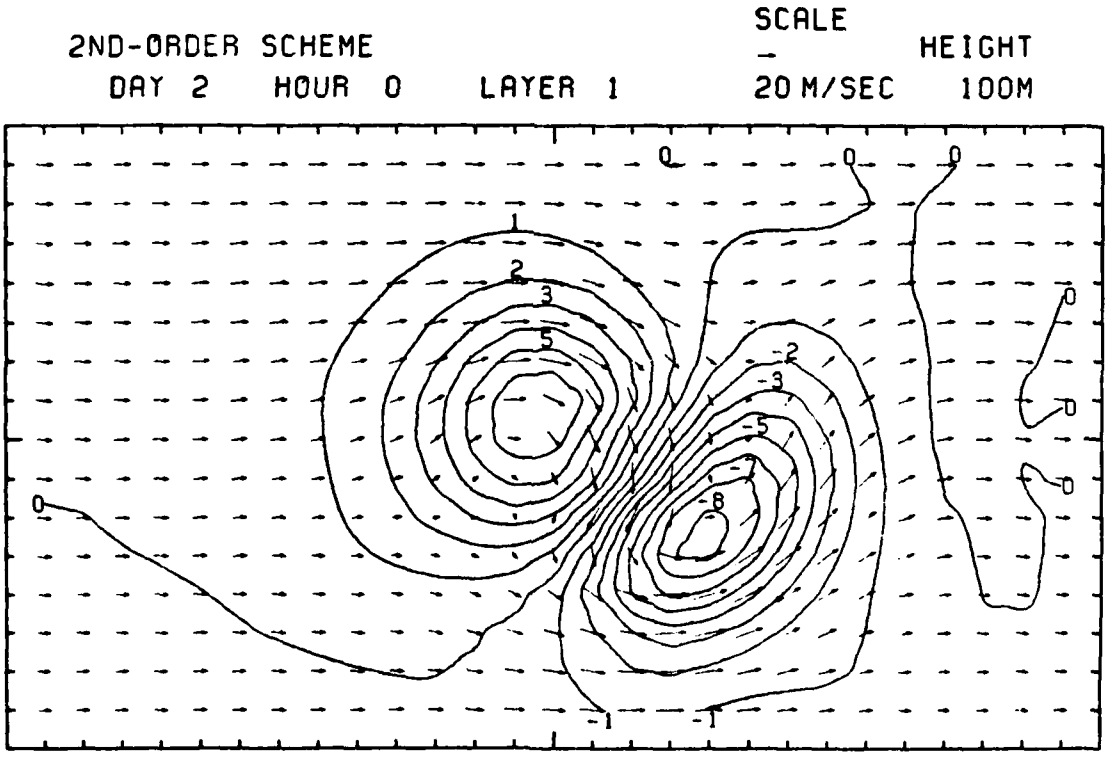
2ND-ORDER SCHEME
DAY 2 HOUR 0 LAYER 1
SCALE
20 M/SEC
HEIGHT
100M

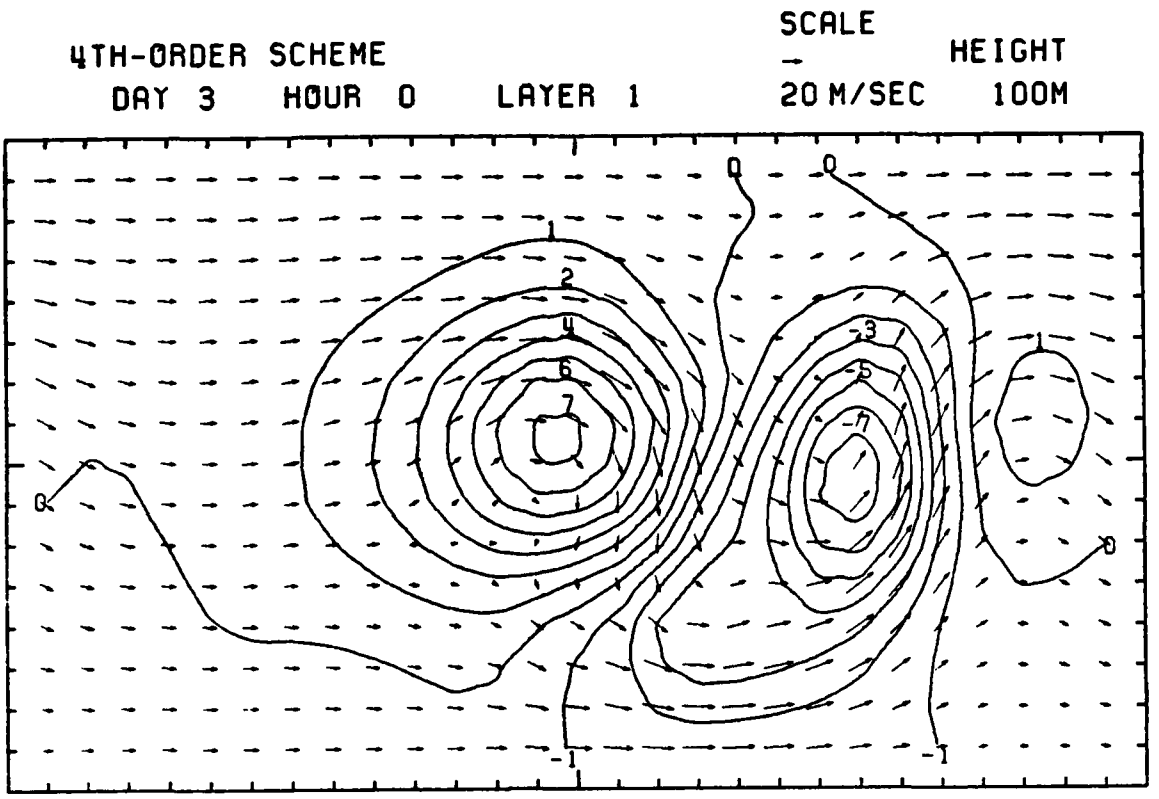
4TH-ORDER SCHEME
DAY 3 HOUR 0 LAYER 1
SCALE
—
20 M/SEC
HEIGHT
100M

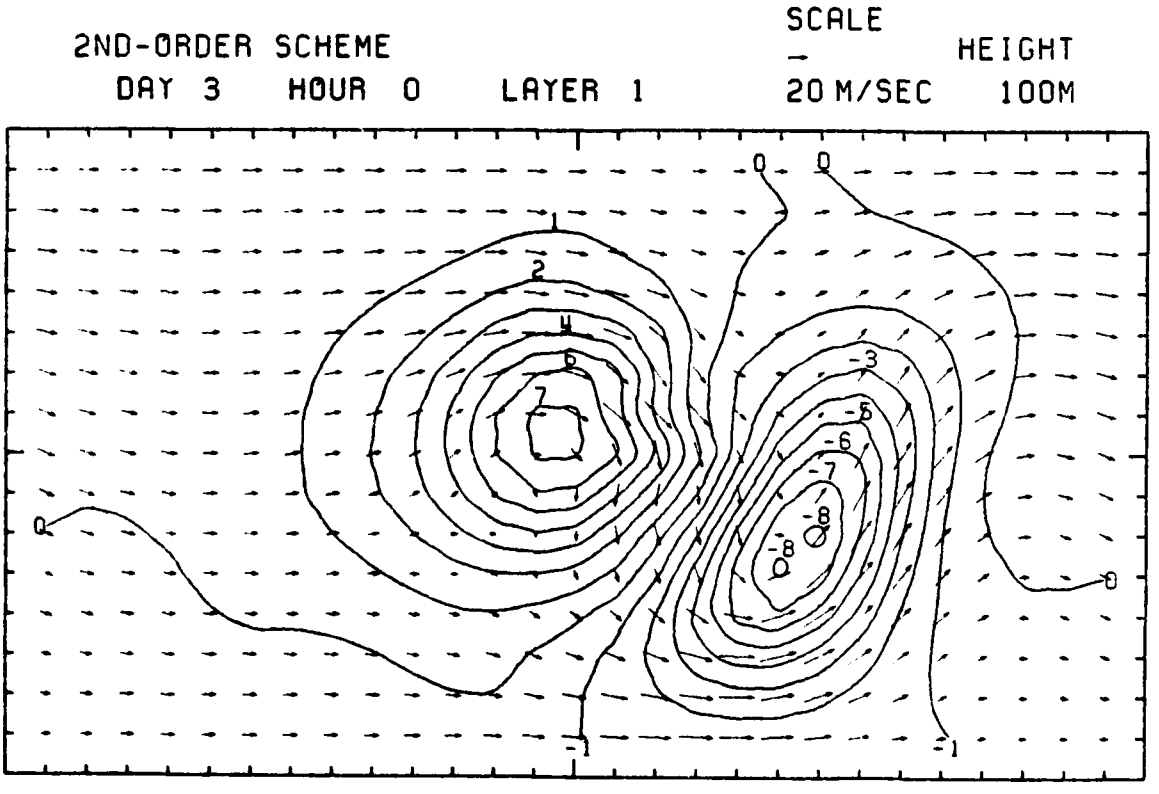
2ND-ORDER SCHEME
DAY 3 HOUR 0 LAYER 1
SCALE
—
20 M/SEC
HEIGHT
100M

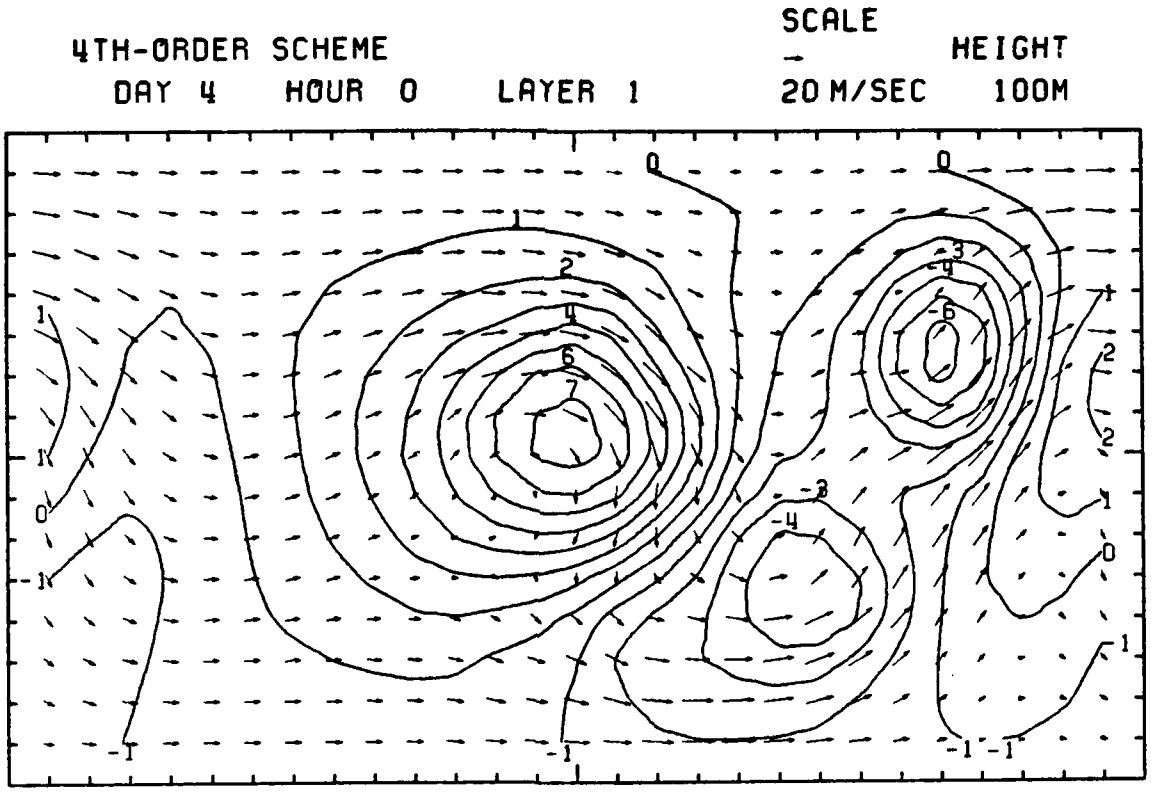
4TH-ORDER SCHEME
DAY 4 HOUR 0 LAYER 1
SCALE
20 M/SEC
HEIGHT
100M

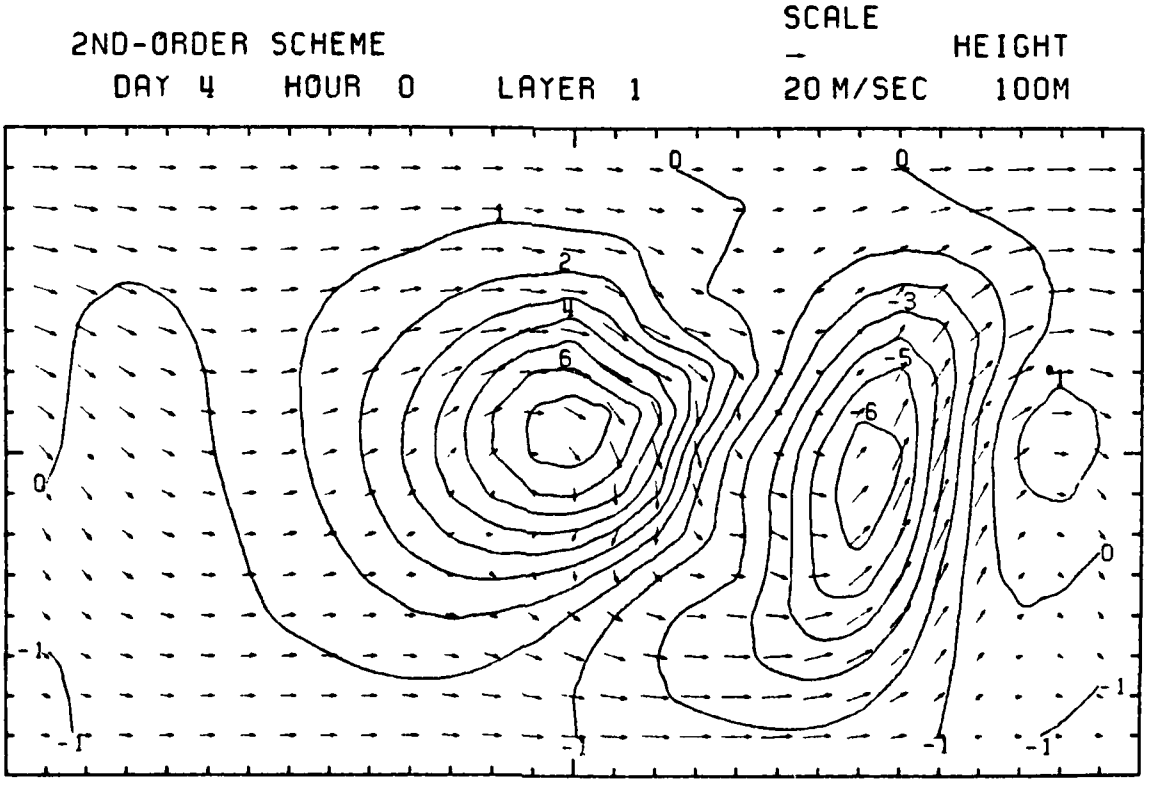
2ND-ORDER SCHEME
DAY 4 HOUR 0 LAYER 1
SCALE
20 M/SEC
HEIGHT
100M

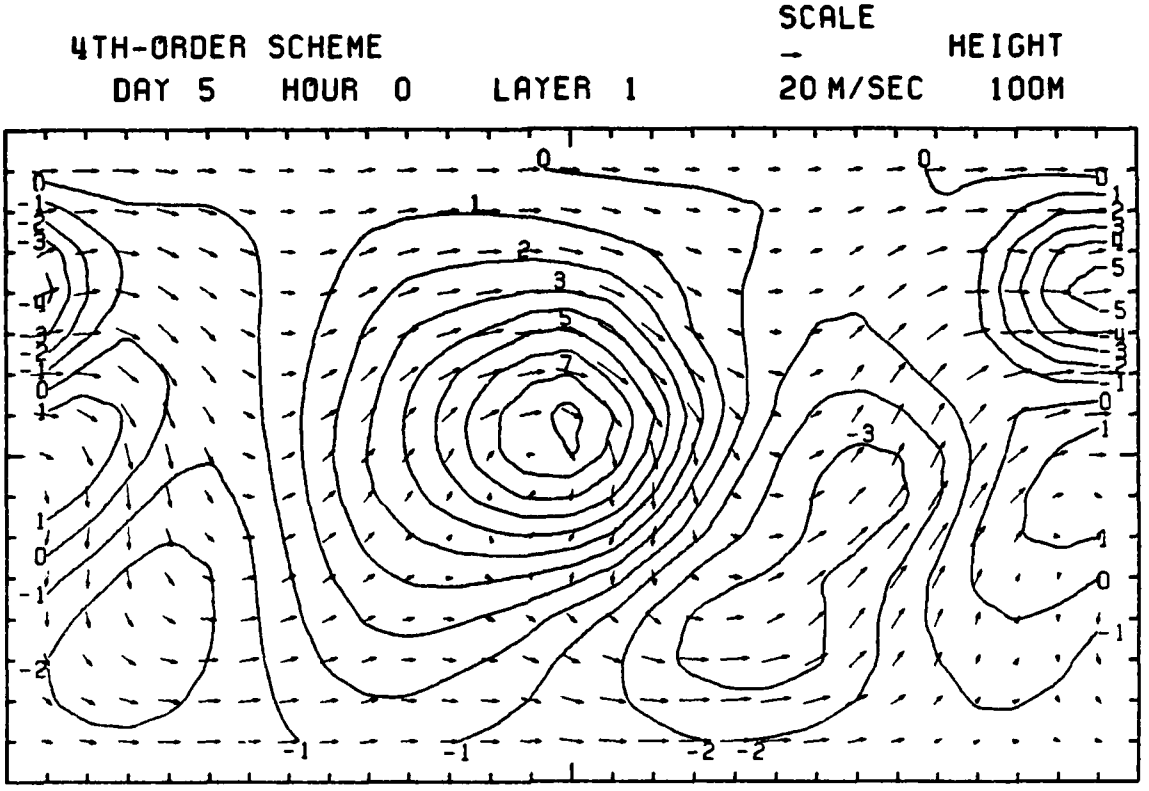
4TH-ORDER SCHEME
DAY 5 HOUR 0 LAYER 1
SCALE
–
20 M/SEC
HEIGHT
100M

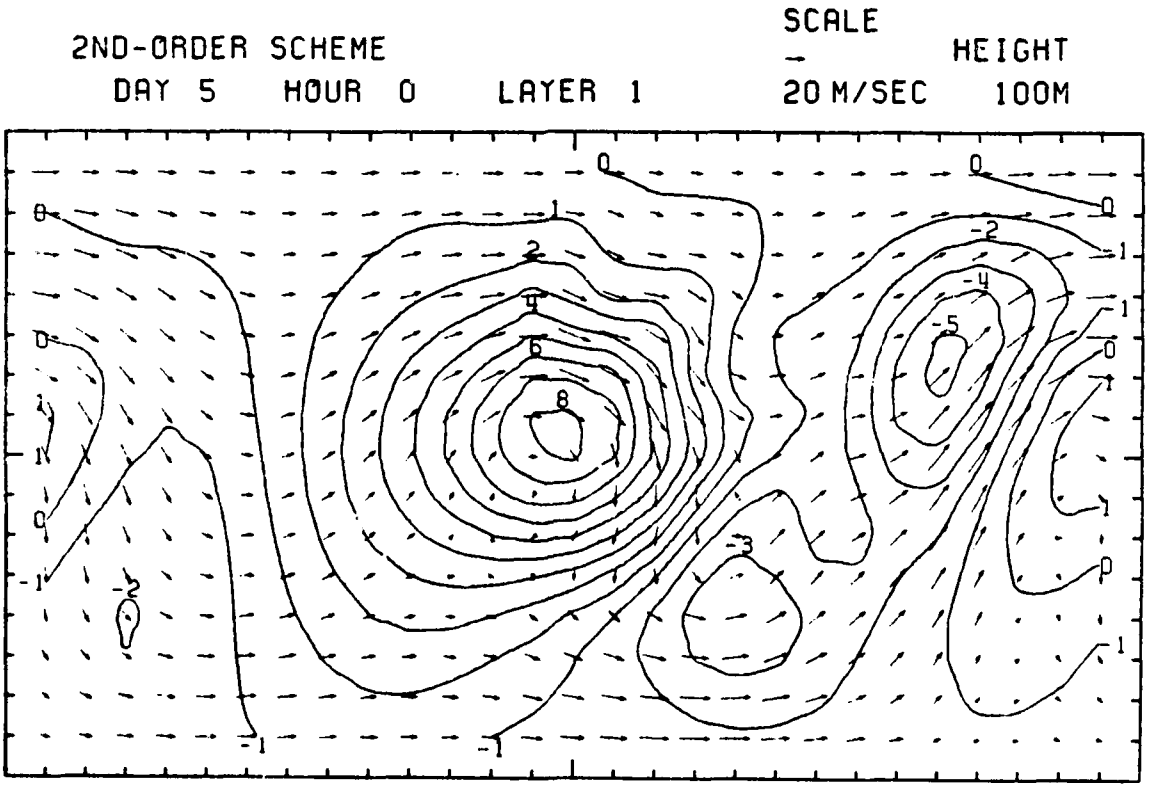
2ND-ORDER SCHEME
DAY 5 HOUR 0 LAYER 1
SCALE
–
20 M/SEC
HEIGHT
100M

4TH-ORDER SCHEME
DAY 6 HOUR 0 LAYER 1

SCALE
—
20 M/SEC

HEIGHT
100M

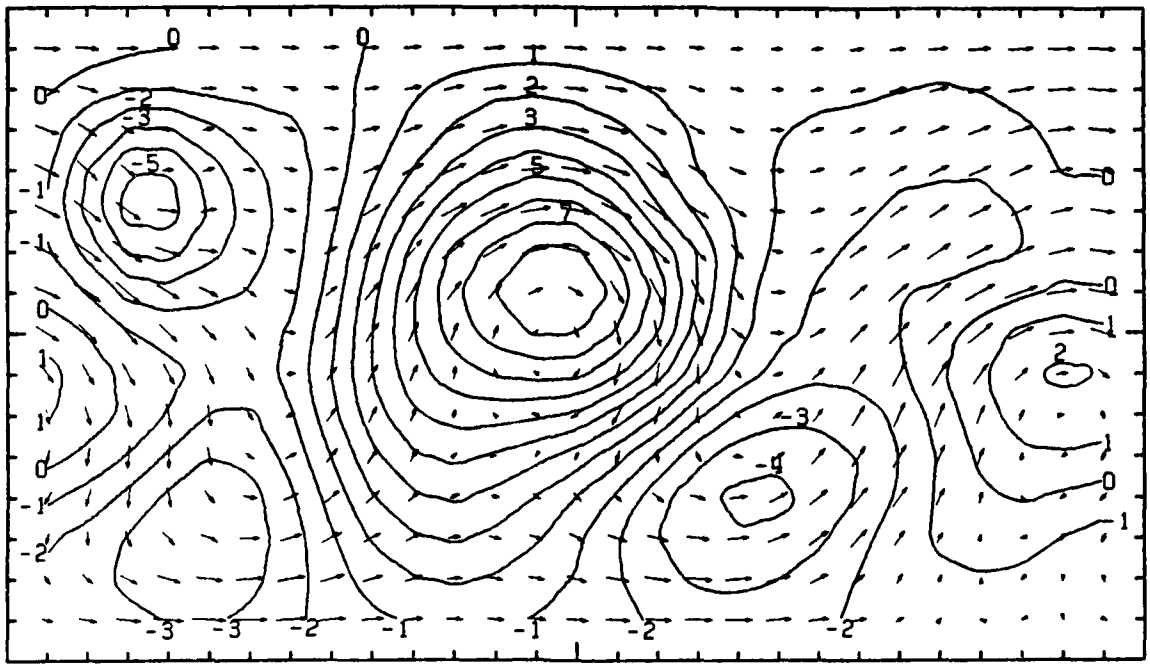

2ND-ORDER SCHEME
DAY 6 HOUR 0 LAYER 1

SCALE
—
20 M/SEC

HEIGHT
100M

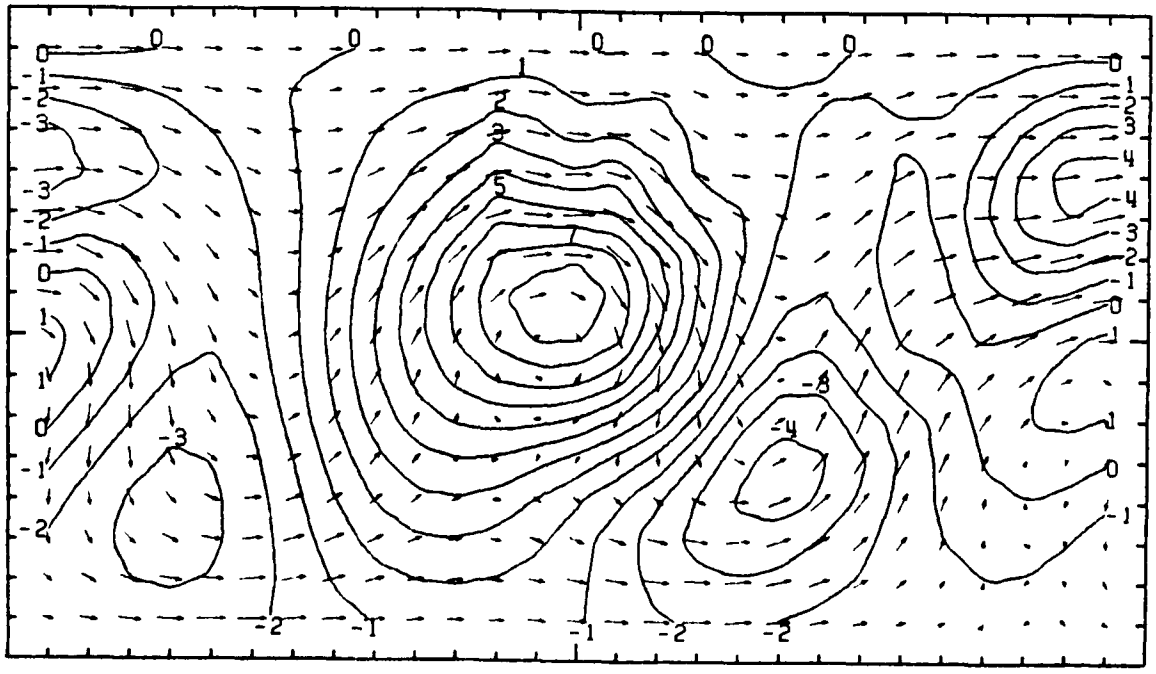

4TH-ORDER SCHEME
DAY 7 HOUR 0 LAYER 1
SCALE — 20 M/SEC
HEIGHT 100M

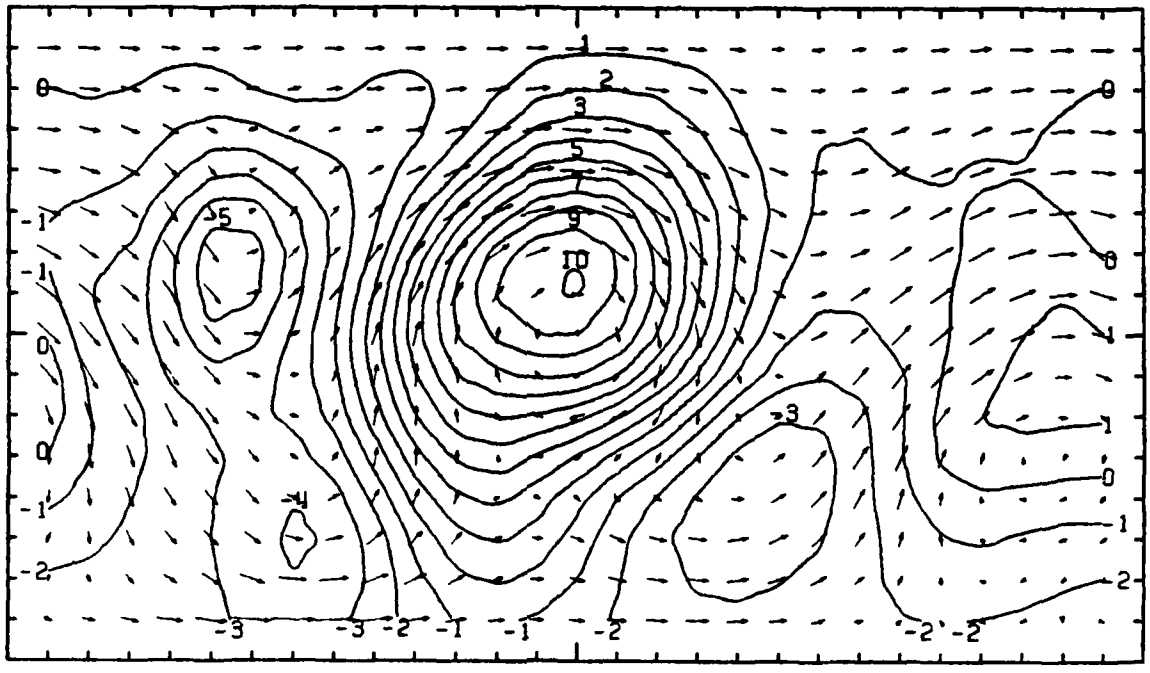

2ND-ORDER SCHEME
DAY 7 HOUR 0 LAYER 1
SCALE — 20 M/SEC
HEIGHT 100M

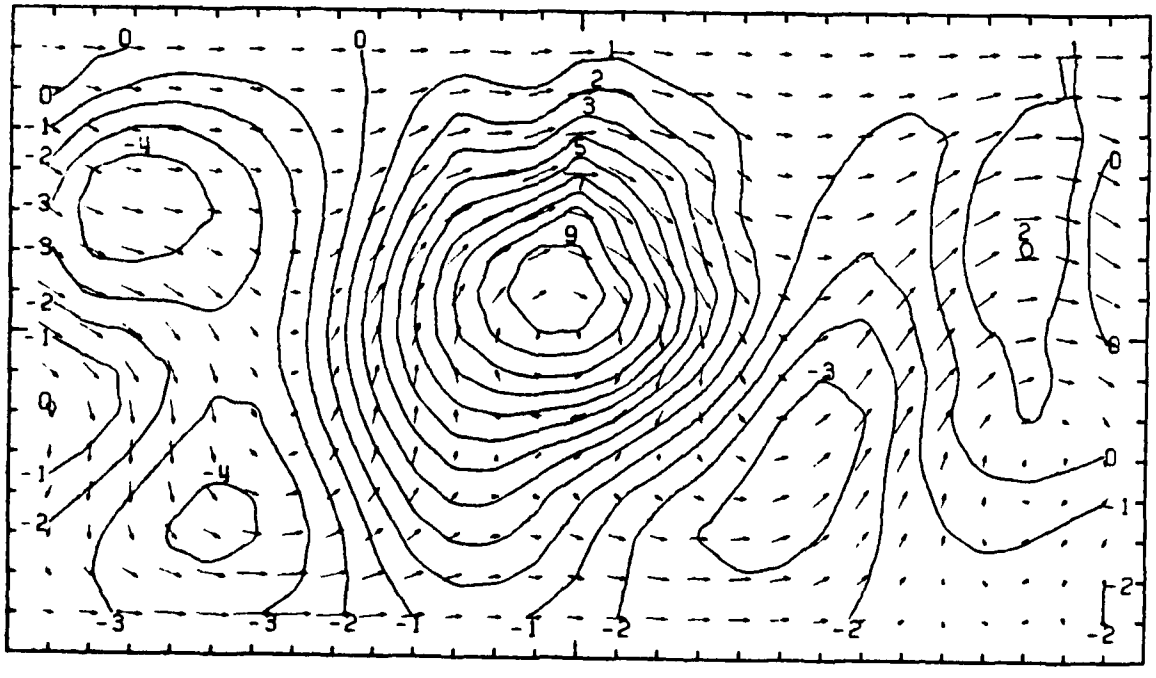

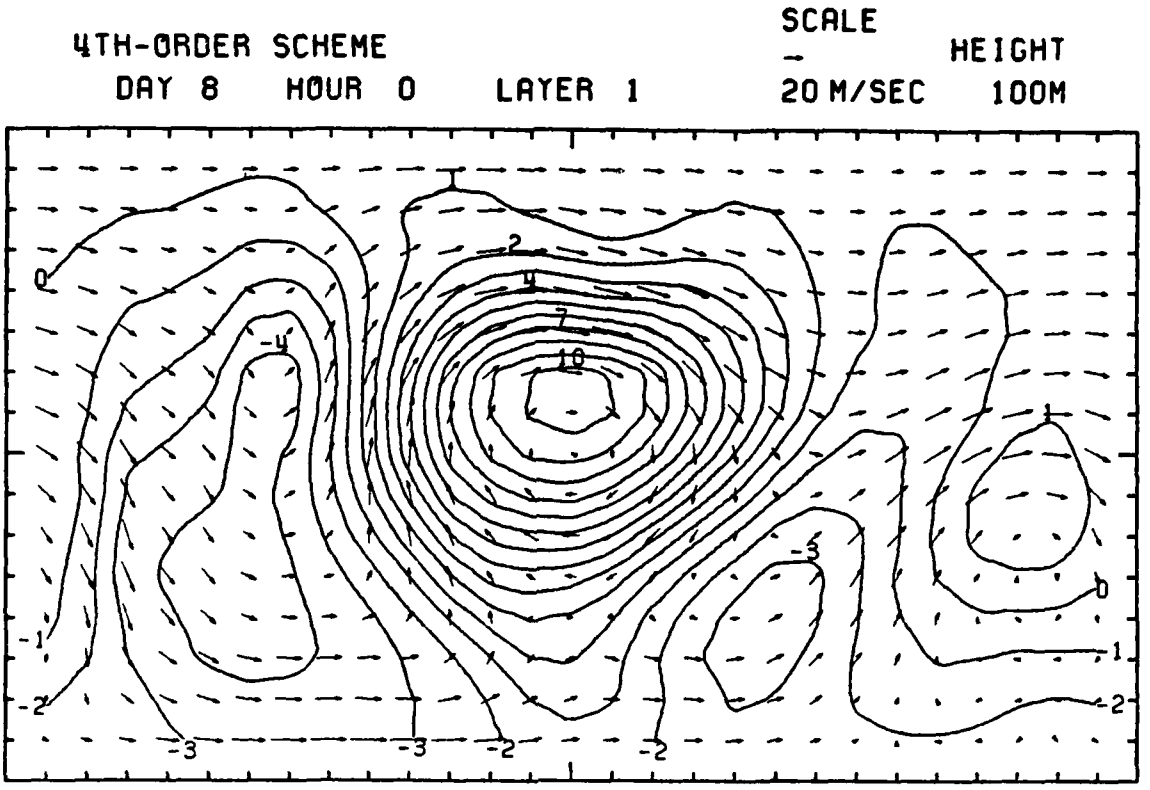
4TH-ORDER SCHEME
DAY 8 HOUR 0 LAYER 1
SCALE
–
20 M/SEC
HEIGHT
100M

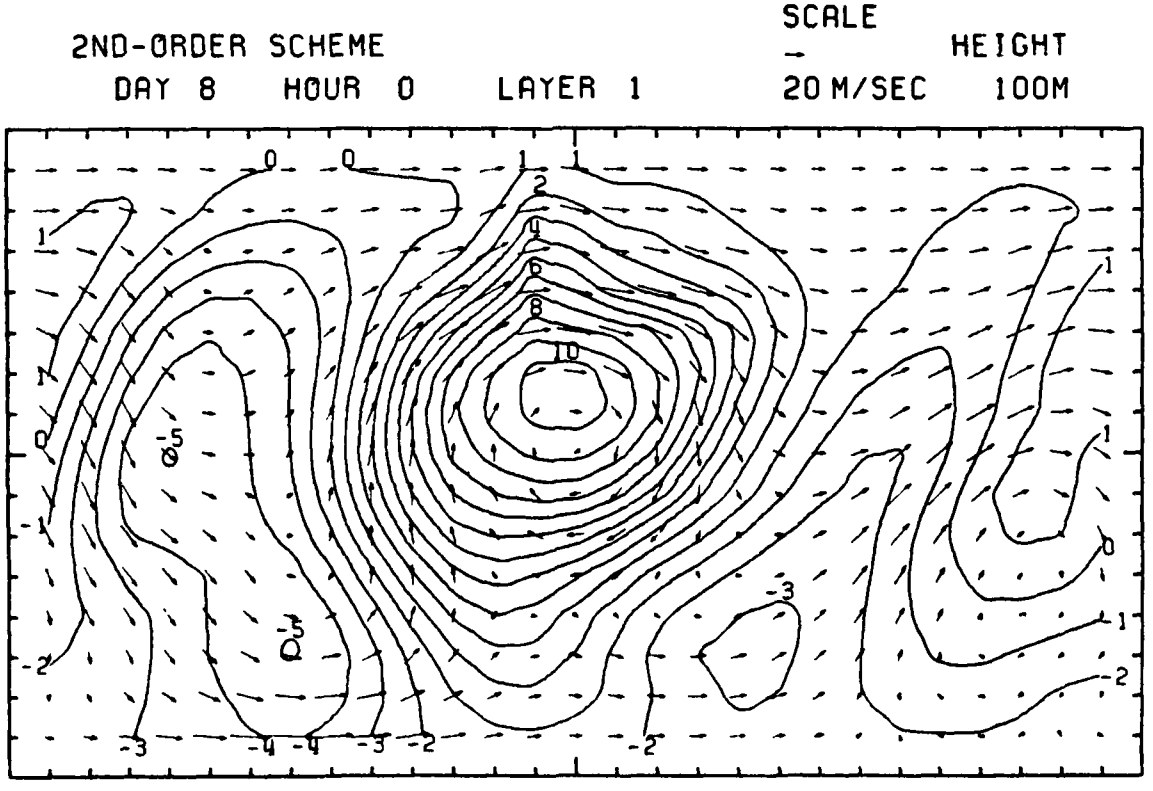
2ND-ORDER SCHEME
DAY 8 HOUR 0 LAYER 1
SCALE
–
20 M/SEC
HEIGHT
100M

4TH-ORDER SCHEME
DAY 9 HOUR 0 LAYER 1

SCALE — 20 M/SEC

HEIGHT 100M

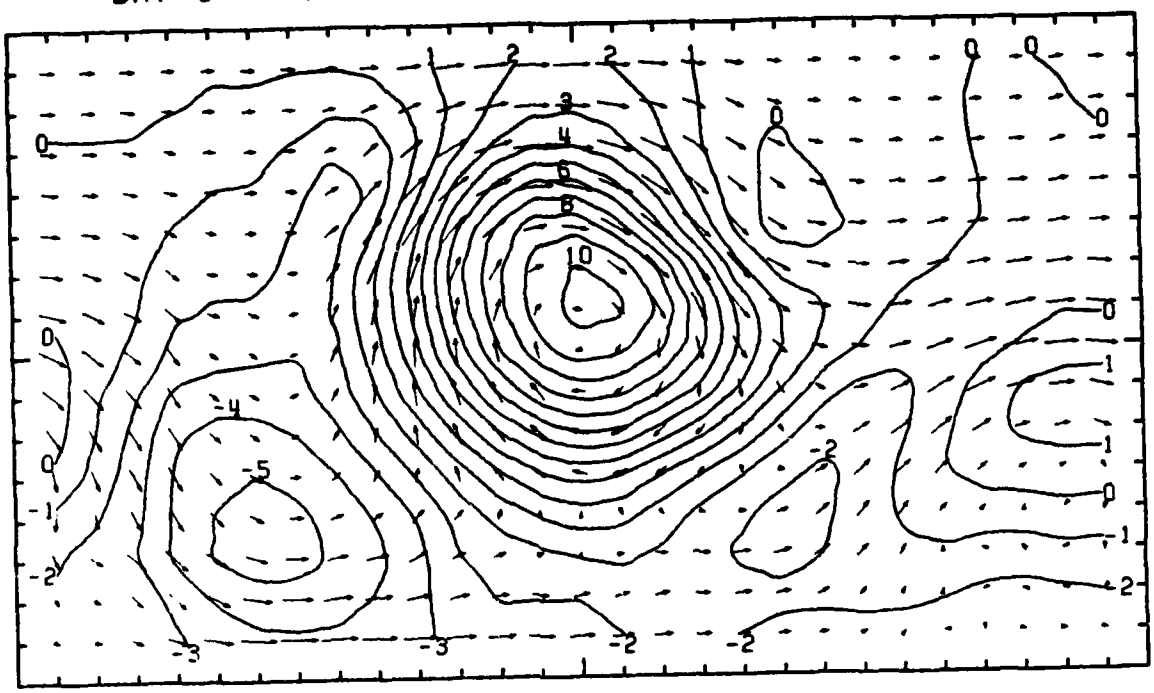

2ND-ORDER SCHEME
DAY 9 HOUR 0 LAYER 1

SCALE — 20 M/SEC

HEIGHT 100M

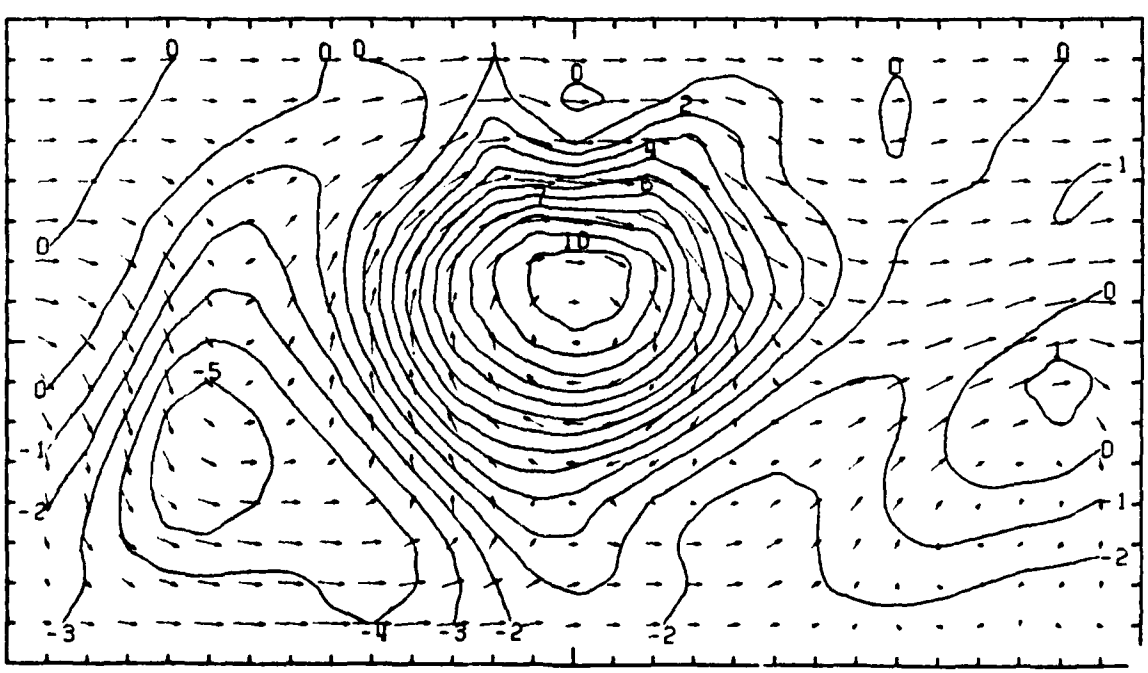

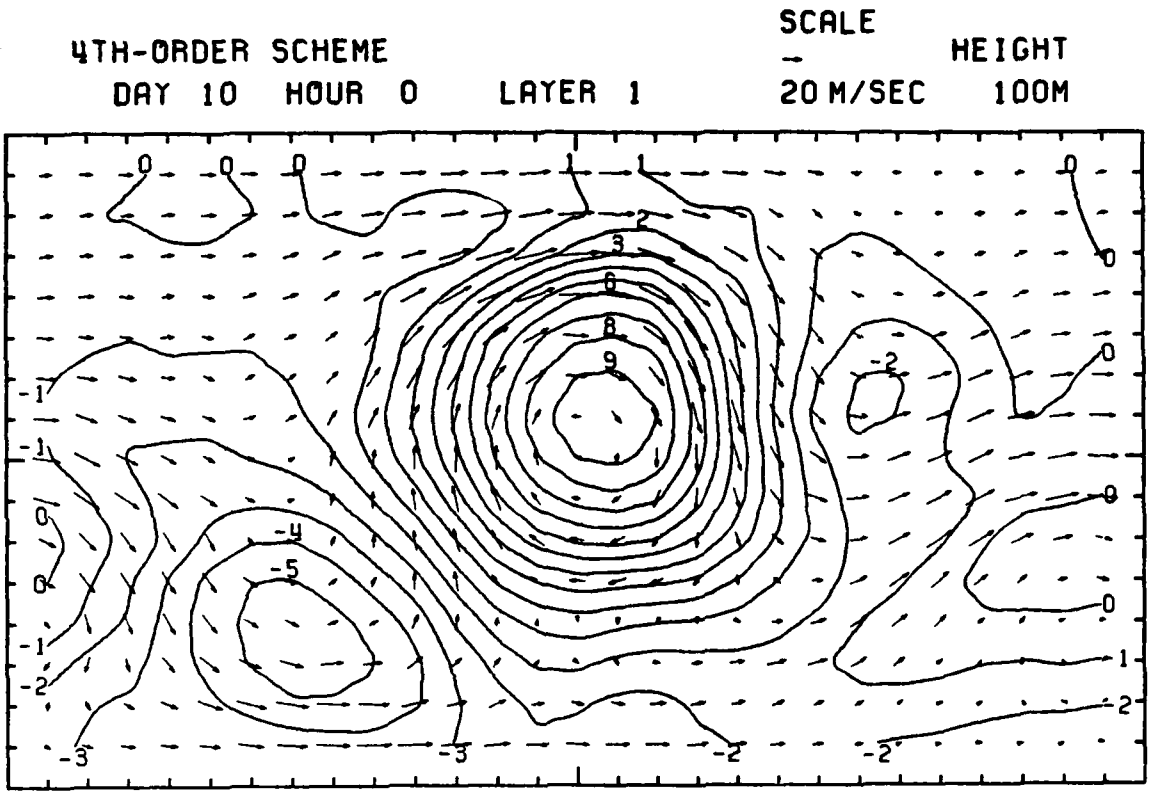
4TH-ORDER SCHEME
DAY 10 HOUR 0 LAYER 1
SCALE
20 M/SEC
HEIGHT
100M

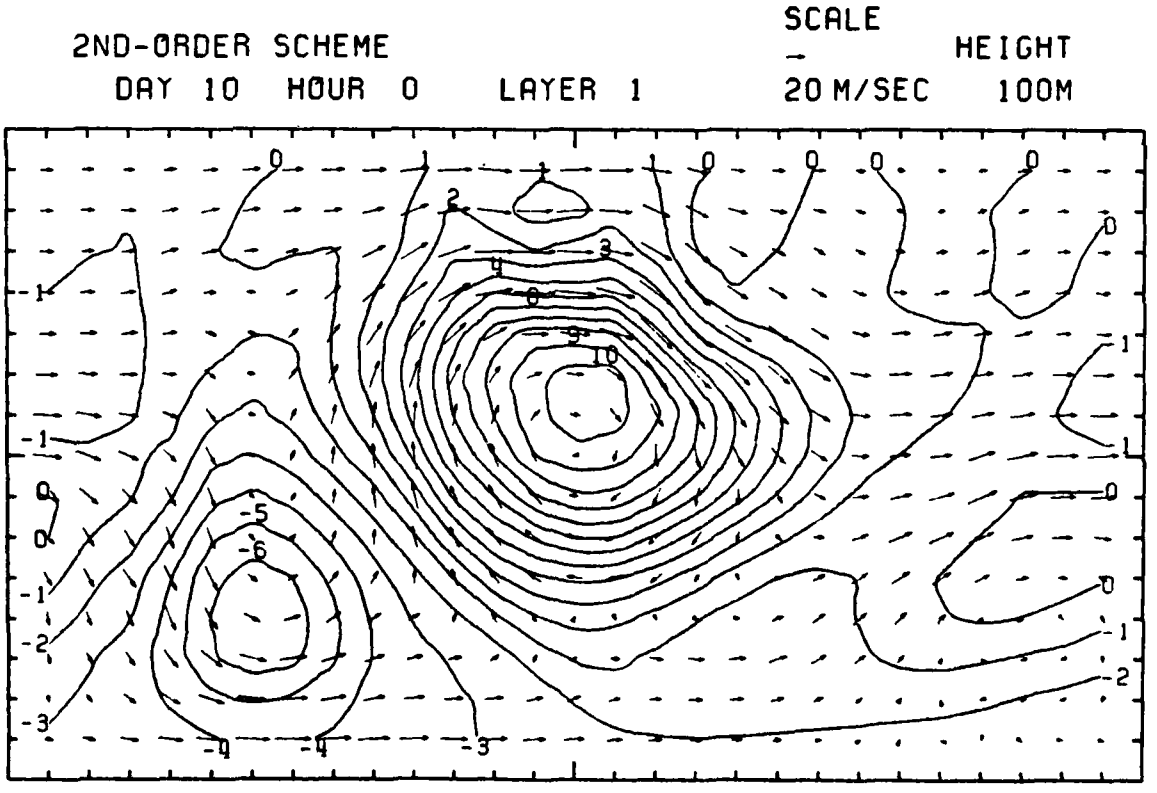
2ND-ORDER SCHEME
DAY 10 HOUR 0 LAYER 1
SCALE
20 M/SEC
HEIGHT
100M

4TH-ORDER SCHEME
DAY 11 HOUR 0 LAYER 1

SCALE
–
20 M/SEC

HEIGHT
100M

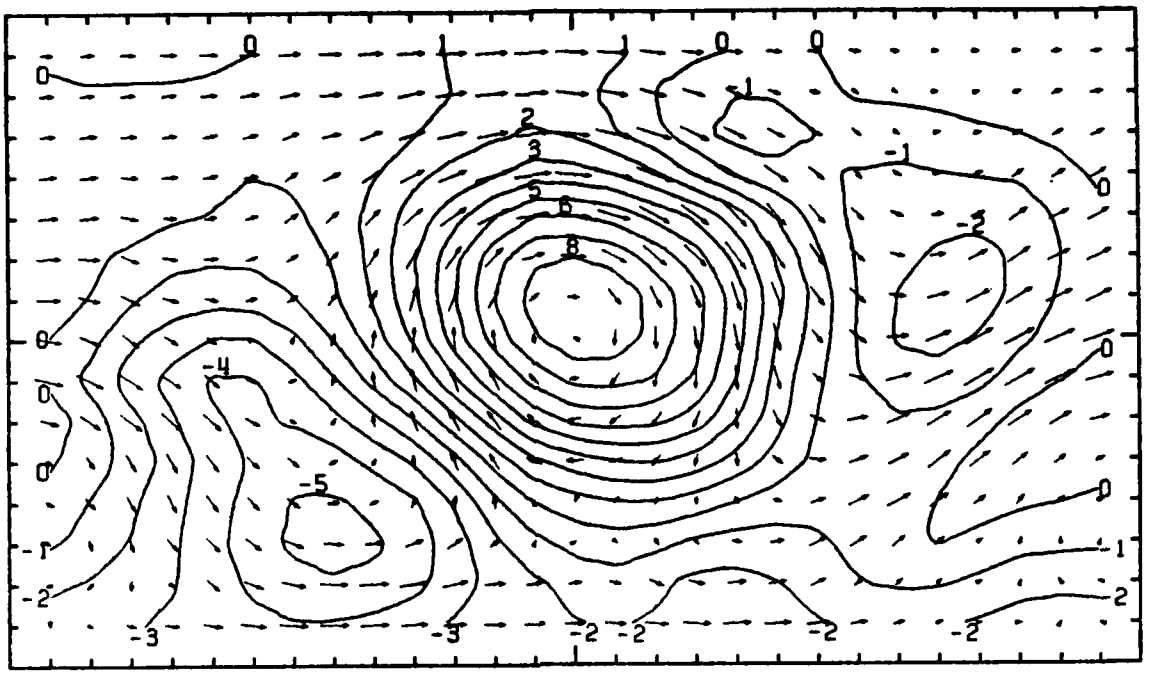

2ND-ORDER SCHEME
DAY 11 HOUR 0 LAYER 1

SCALE
–
20 M/SEC

HEIGHT
100M

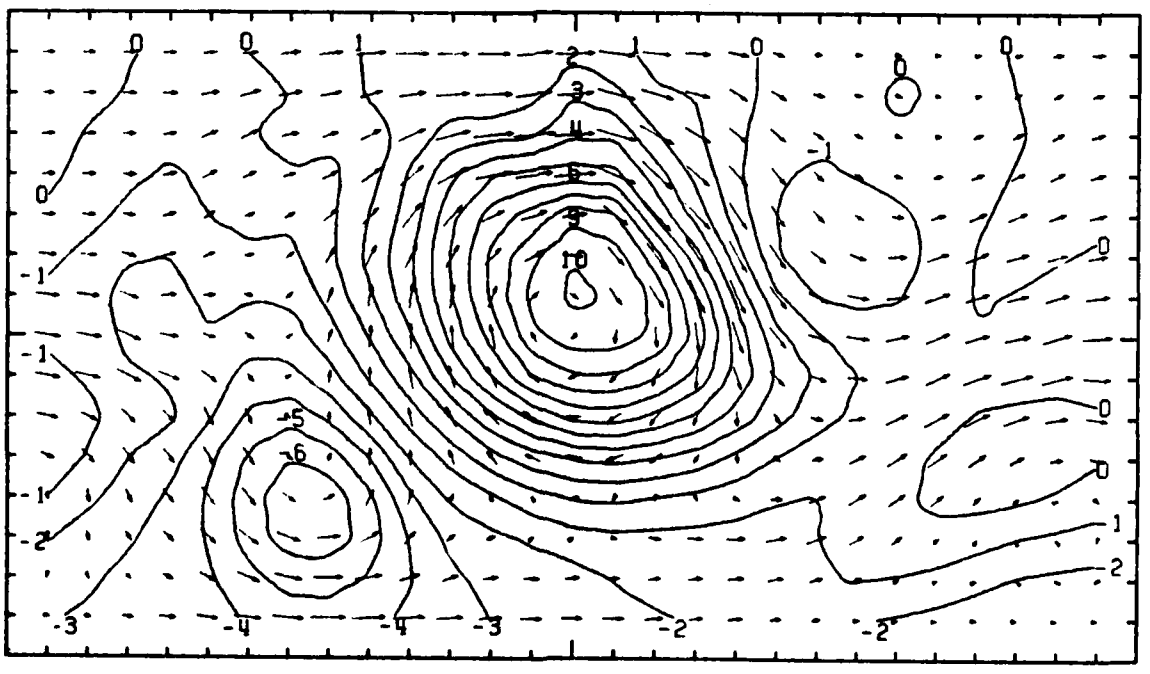

4TH-ORDER SCHEME
DAY 12 HOUR 0 LAYER 1

SCALE
—
20 M/SEC

HEIGHT
100M

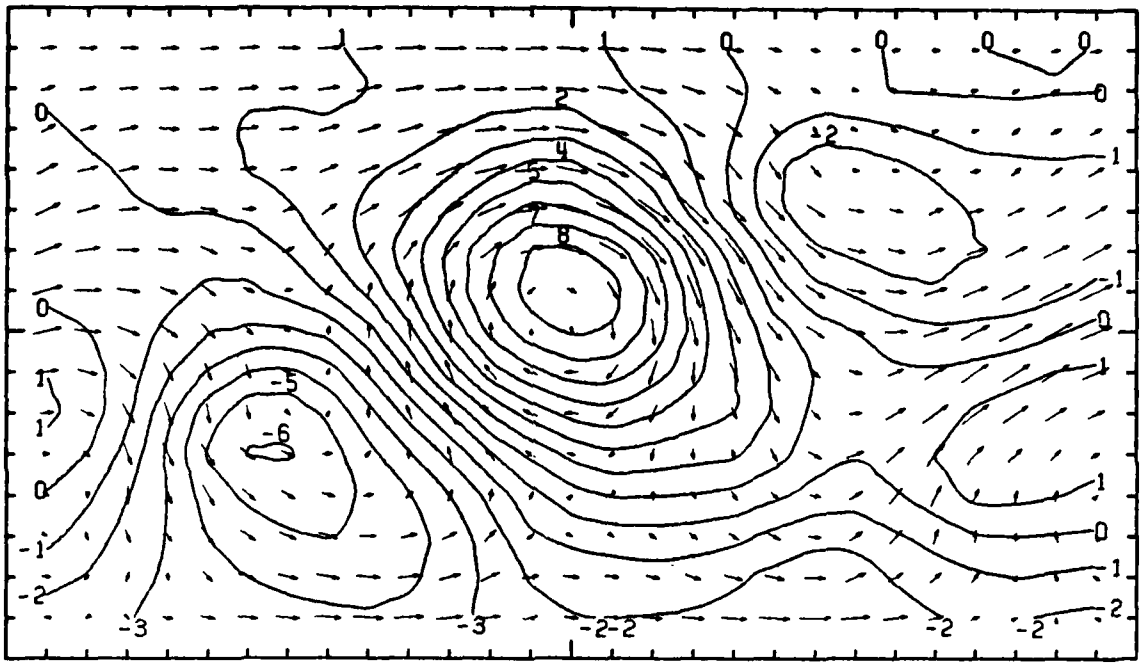

2ND-ORDER SCHEME
DAY 12 HOUR 0 LAYER 1

SCALE
—
20 M/SEC

HEIGHT
100M

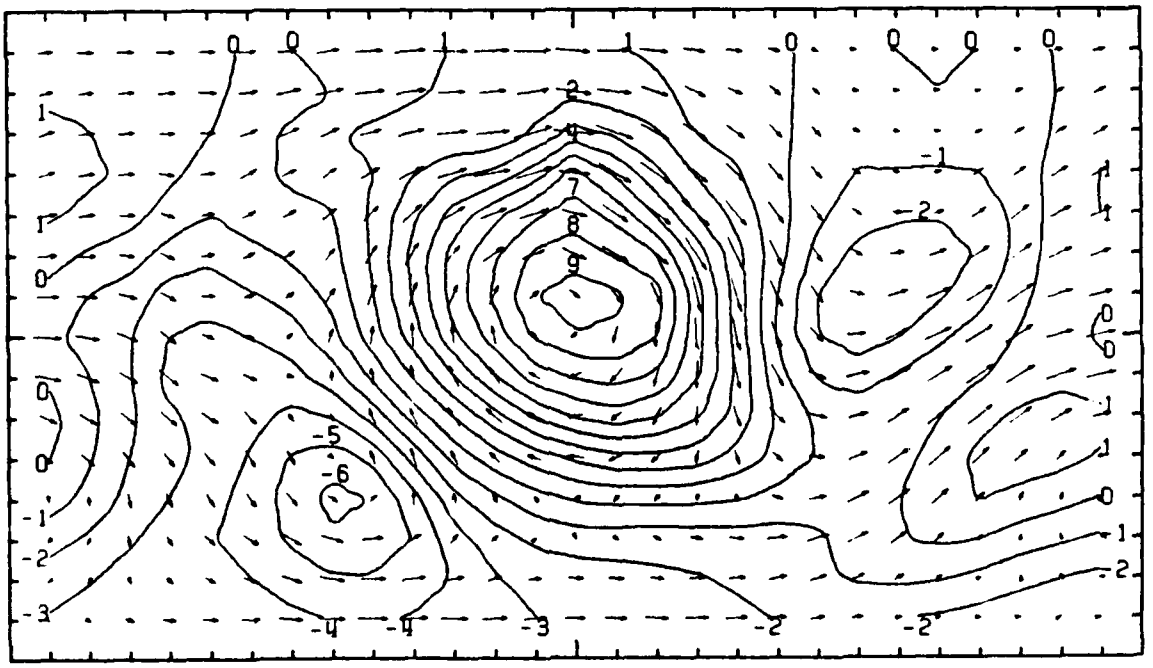

4TH-ORDER SCHEME
DAY 13 HOUR 0 LAYER 1
SCALE — 20 M/SEC
HEIGHT 100M

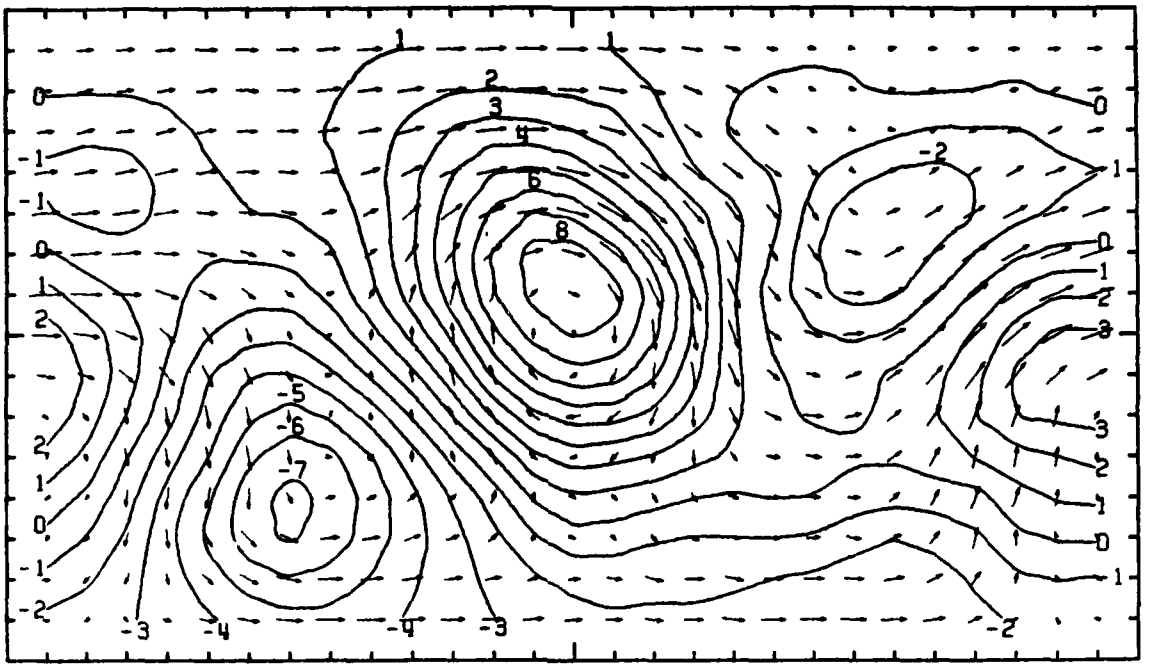

2ND-ORDER SCHEME
DAY 13 HOUR 0 LAYER 1
SCALE — 20 M/SEC
HEIGHT 100M

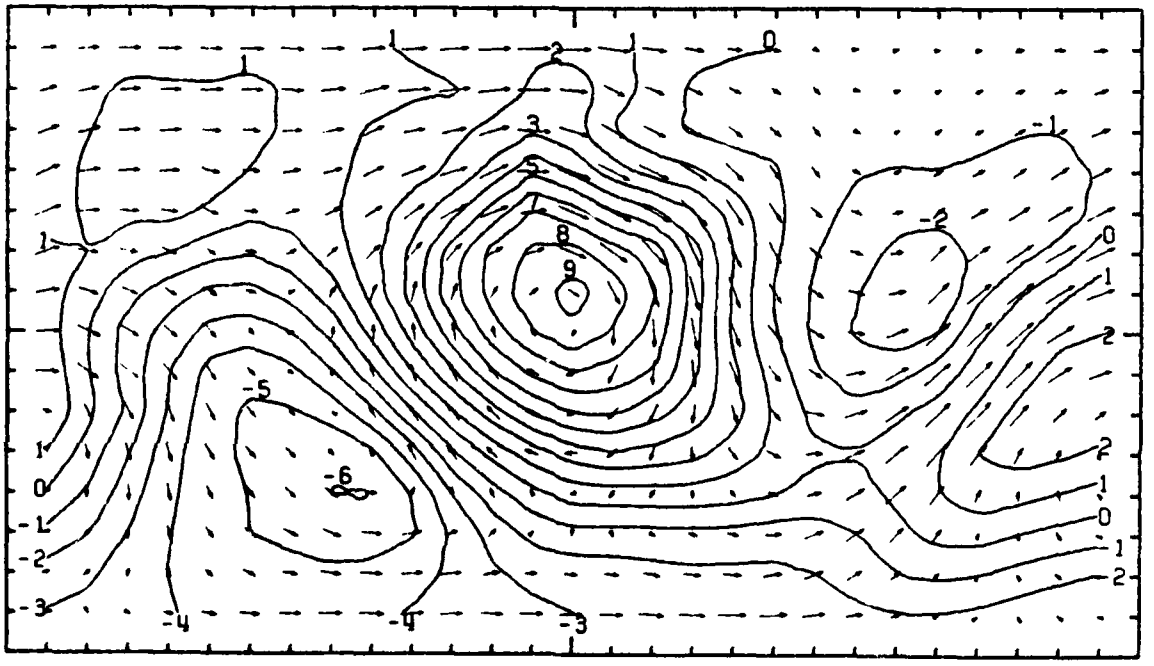

4TH-ORDER SCHEME
DAY 14 HOUR 0 LAYER 1

SCALE
—
20 M/SEC

HEIGHT
100M

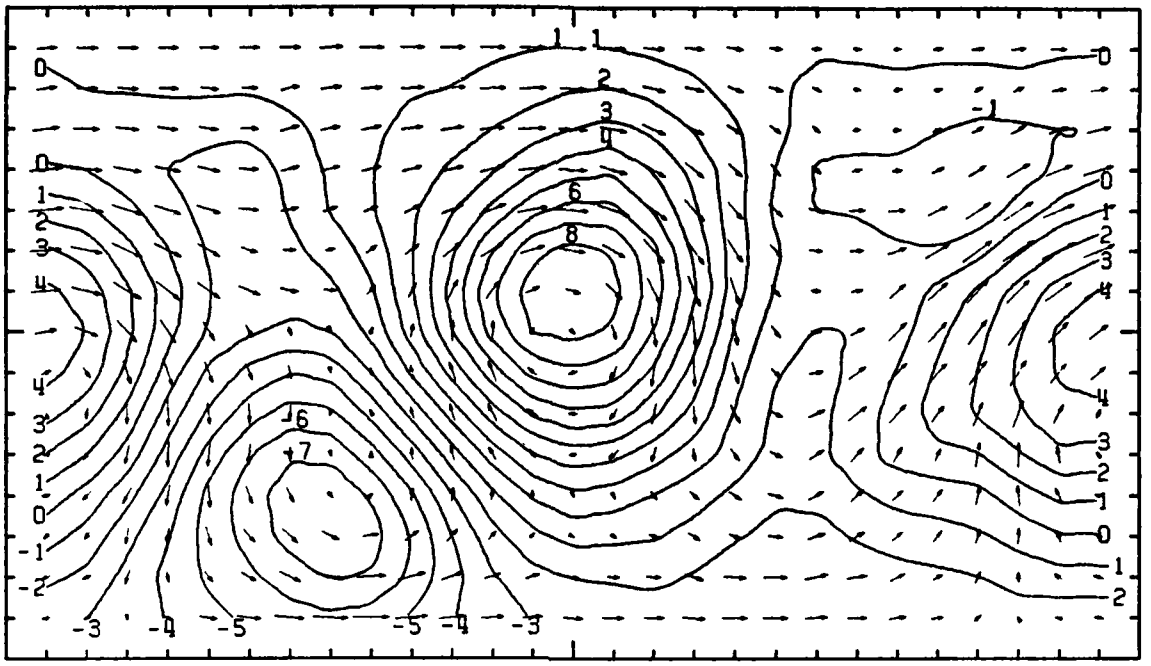

2ND-ORDER SCHEME
DAY 14 HOUR 0 LAYER 1

SCALE
—
20 M/SEC

HEIGHT
100M

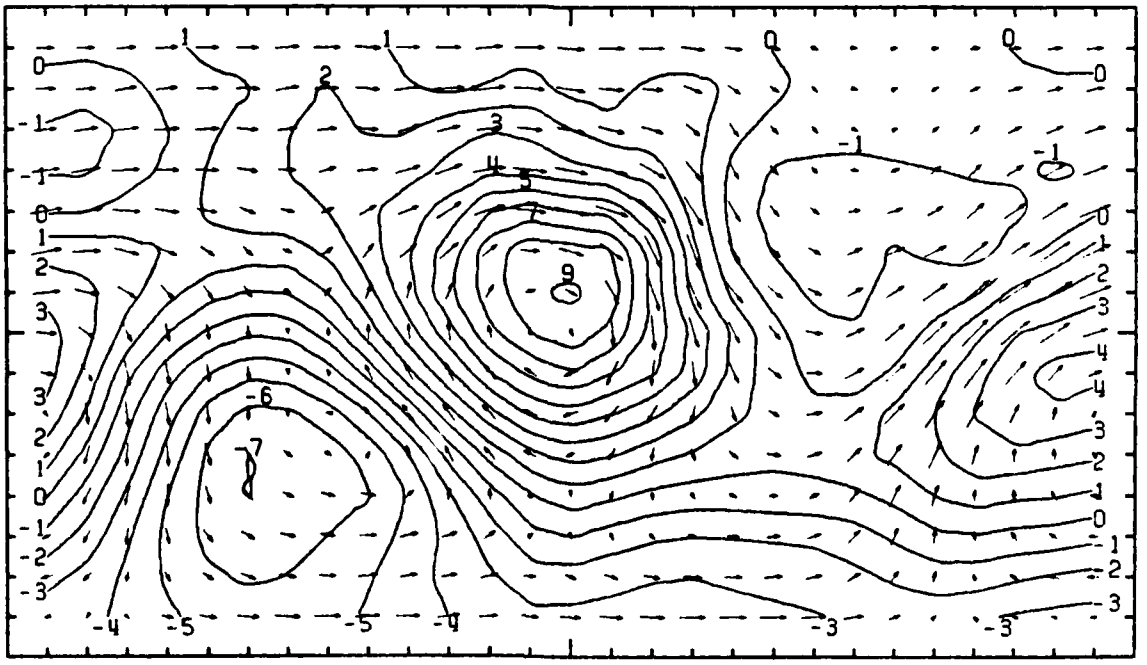

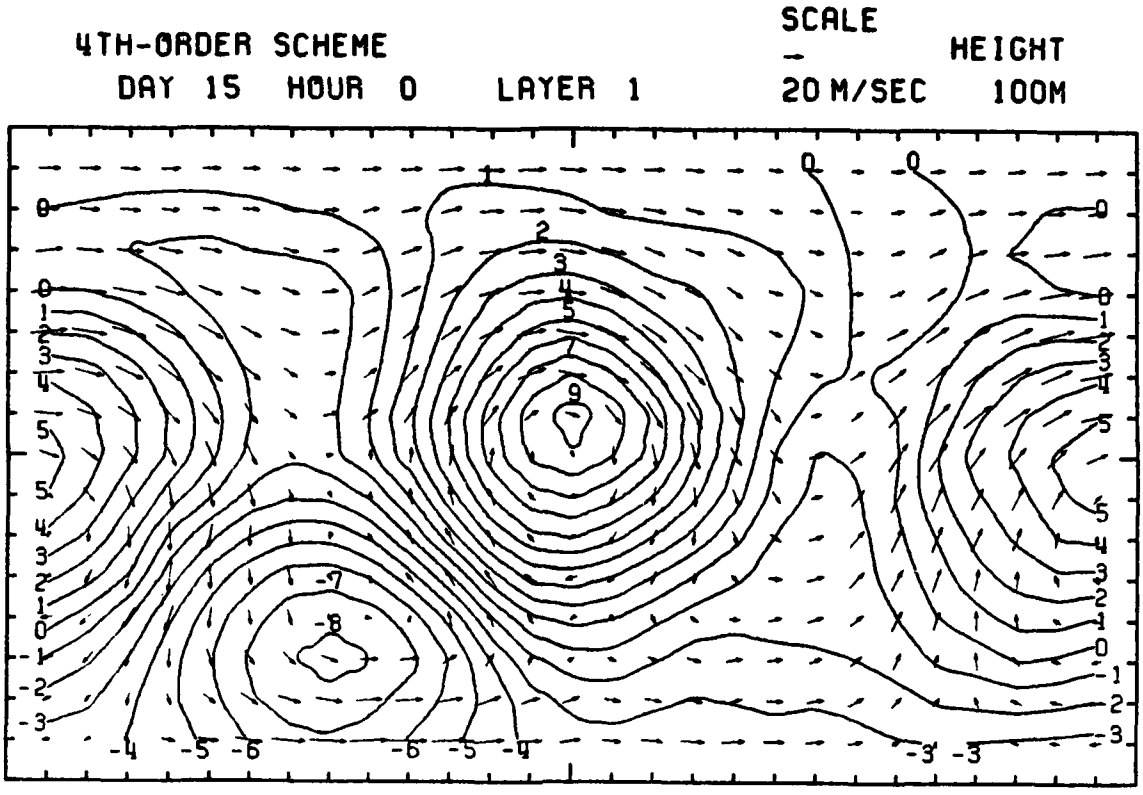
4TH-ORDER SCHEME
DAY 15 HOUR 0 LAYER 1
SCALE
HEIGHT
20 M/SEC 100M

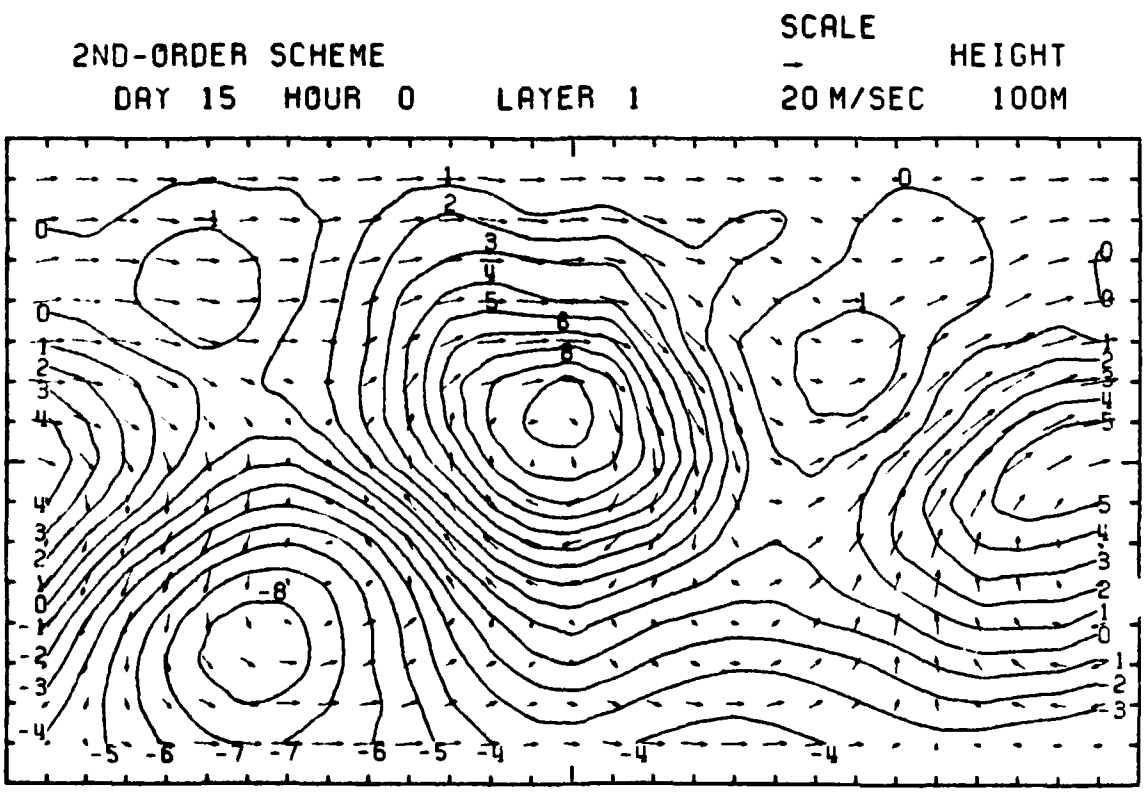
2ND-ORDER SCHEME
DAY 15 HOUR 0 LAYER 1
SCALE
HEIGHT
20 M/SEC 100M

4TH-ORDER SCHEME
DAY 16 HOUR 0 LAYER 1
SCALE
–
20 M/SEC
HEIGHT
100M

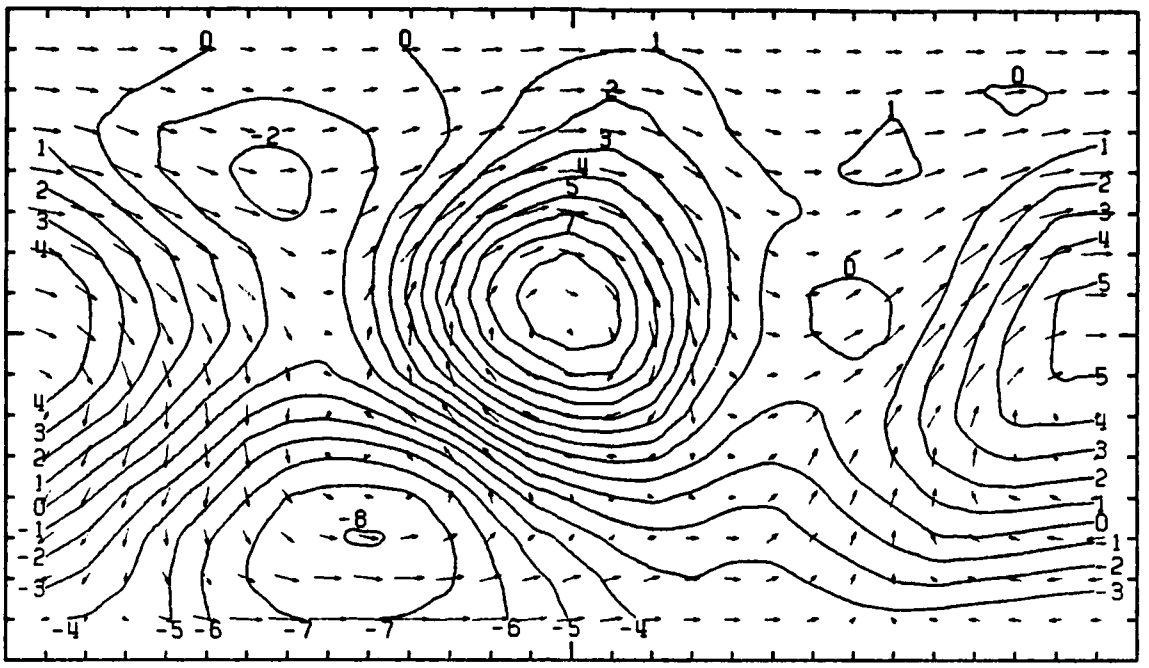

2ND-ORDER SCHEME
DAY 16 HOUR 0 LAYER 1
SCALE
–
20 M/SEC
HEIGHT
100M

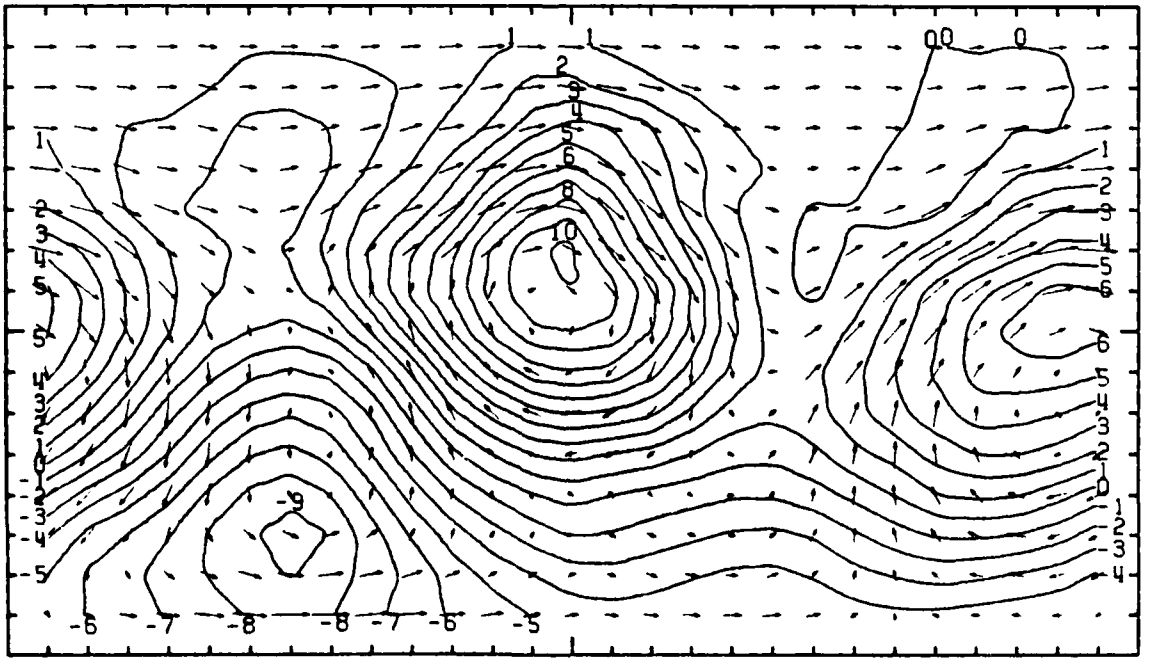

4TH-ORDER SCHEME
DAY 17 HOUR 0 LAYER 1

SCALE
—
20 M/SEC

HEIGHT
100M

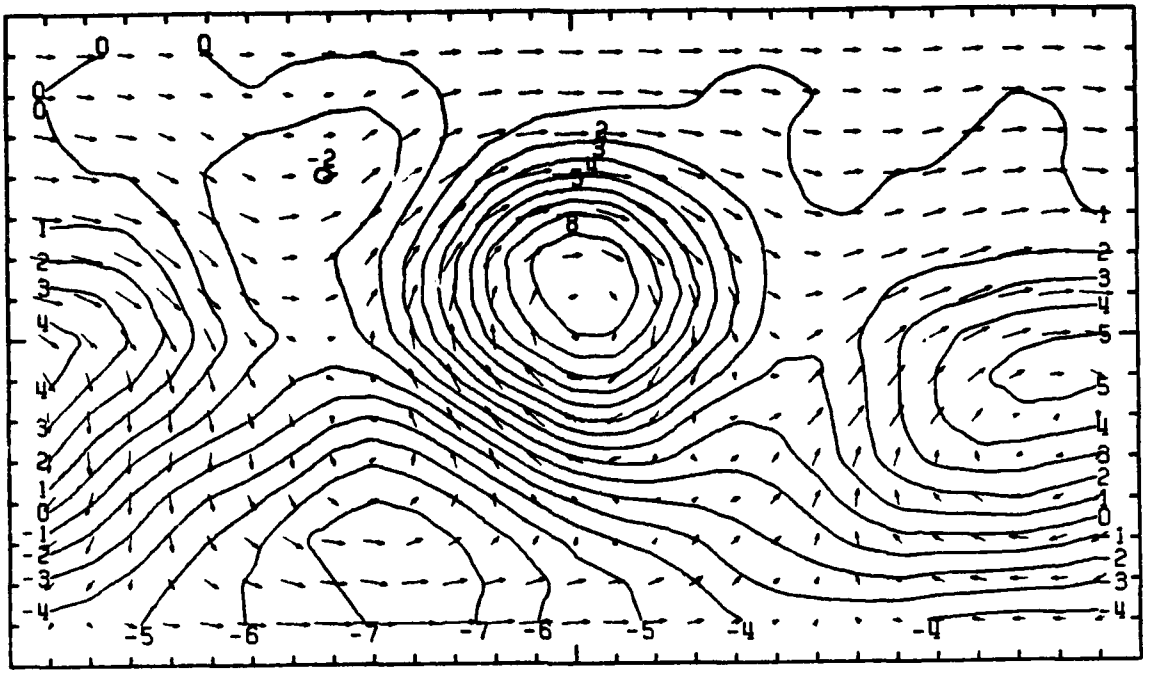

2ND-ORDER SCHEME
DAY 17 HOUR 0 LAYER 1

SCALE
—
20 M/SEC

HEIGHT
100M

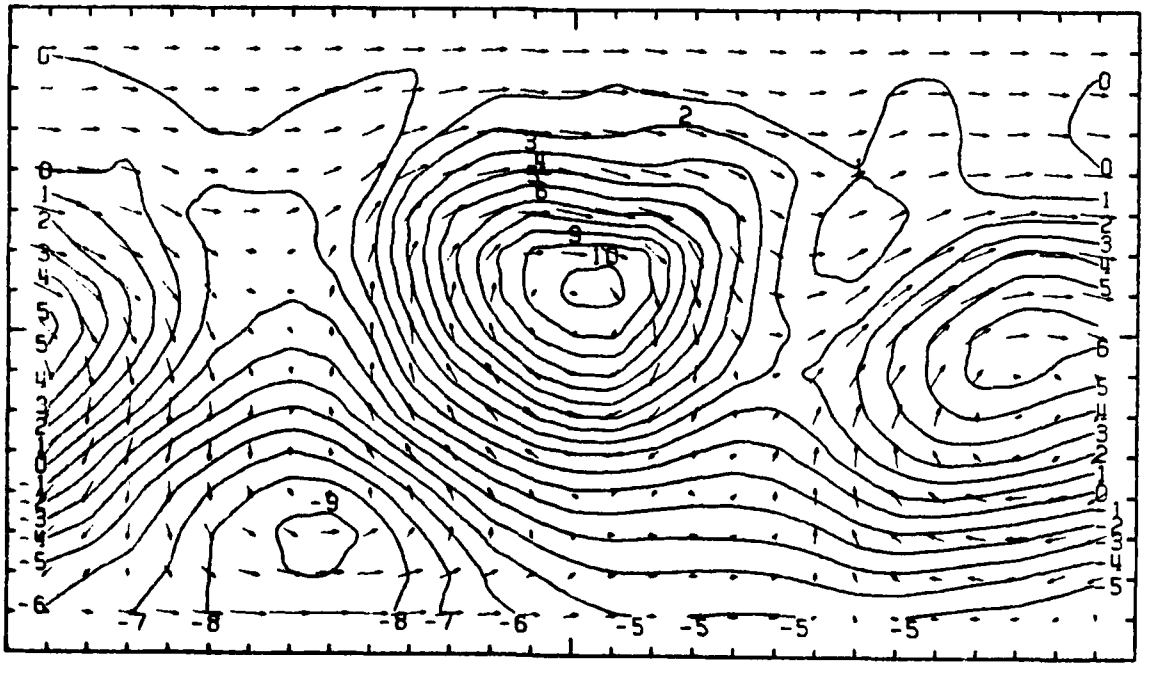

4TH-ORDER SCHEME
DAY 18 HOUR 0 LAYER 1

SCALE
— HEIGHT
20 M/SEC 100M

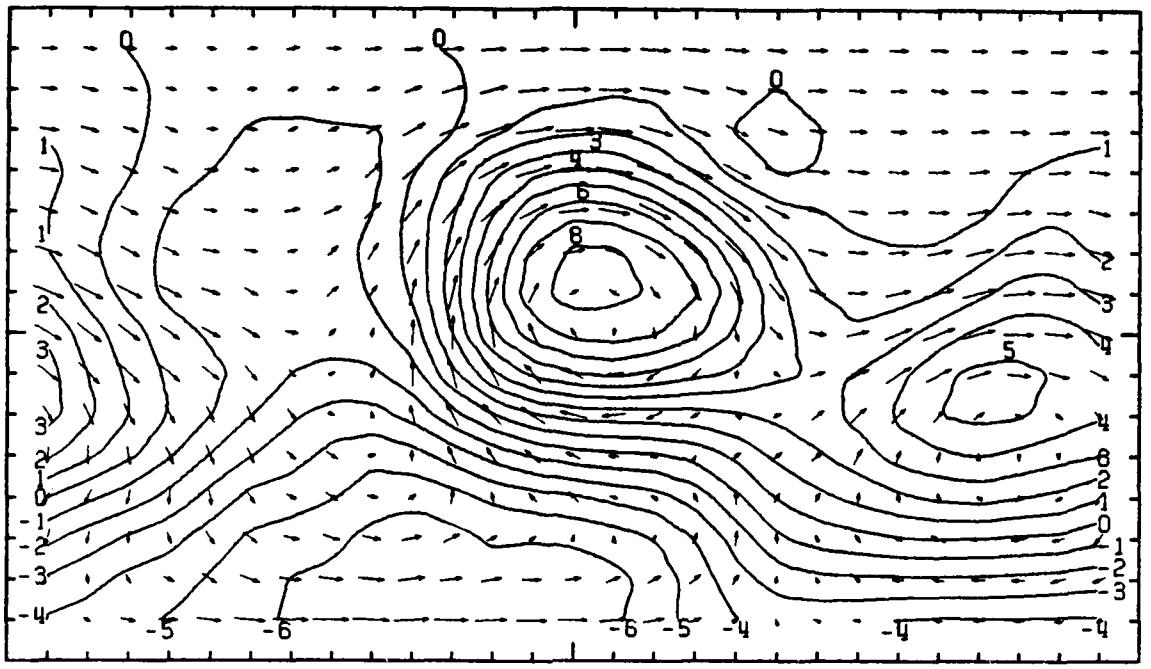

2ND-ORDER SCHEME
DAY 18 HOUR 0 LAYER 1

SCALE
— HEIGHT
20 M/SEC 100M

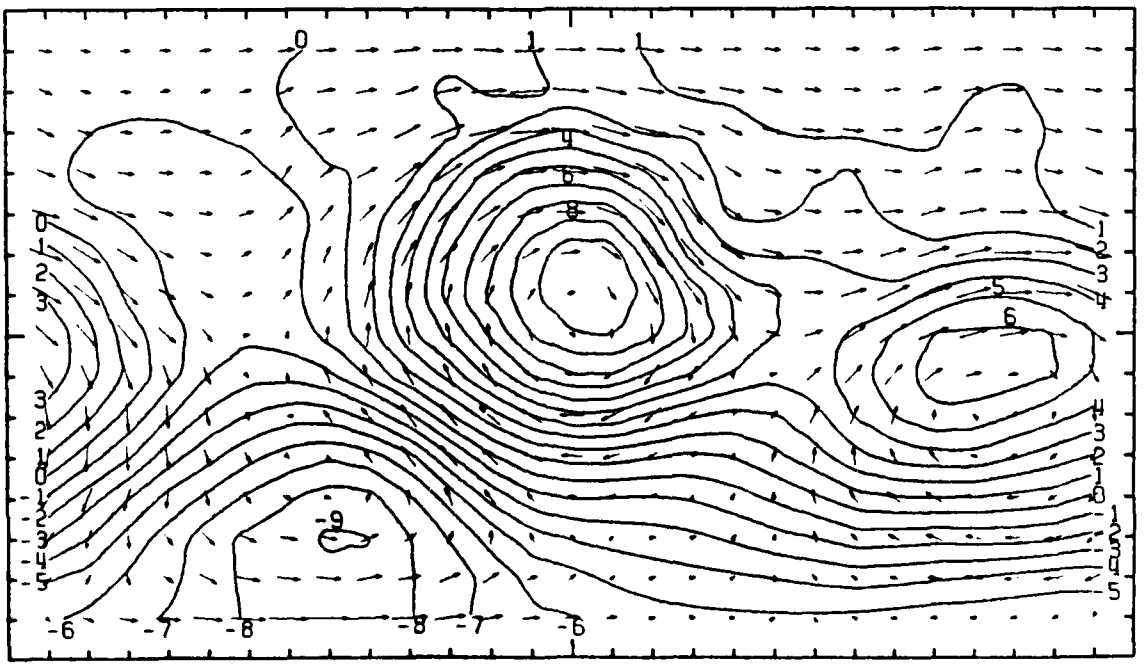

4TH-ORDER SCHEME
DAY 19 HOUR 0 LAYER 1
SCALE
—
20 M/SEC
HEIGHT
100M

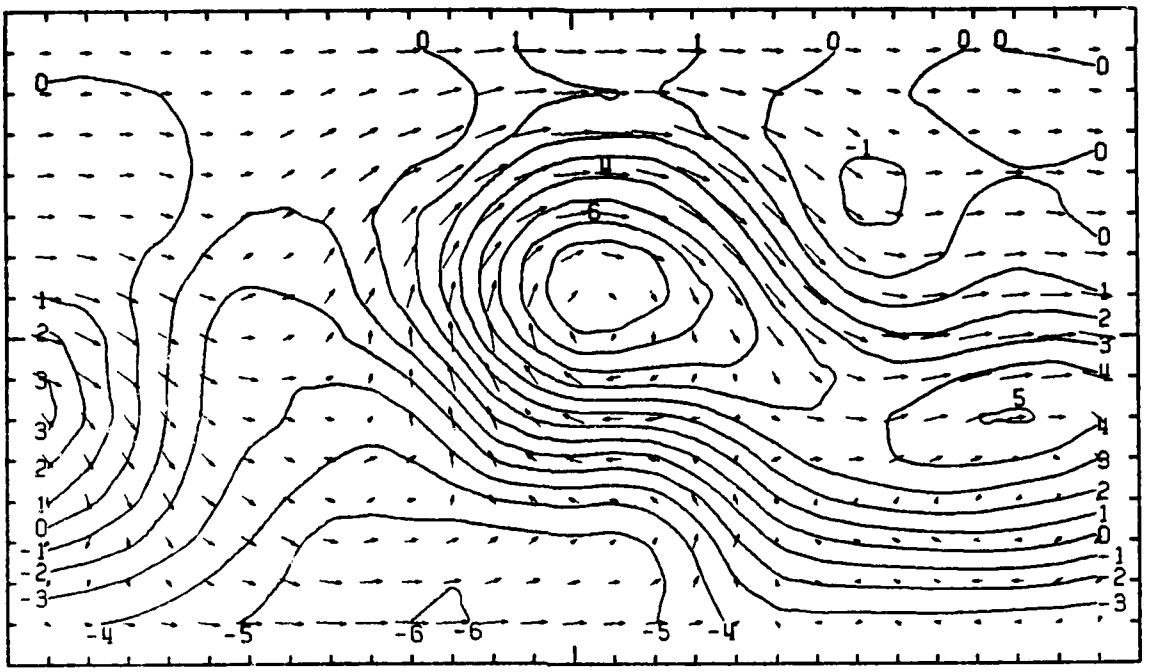

2ND-ORDER SCHEME
DAY 19 HOUR 0 LAYER 1
SCALE
—
20 M/SEC
HEIGHT
100M

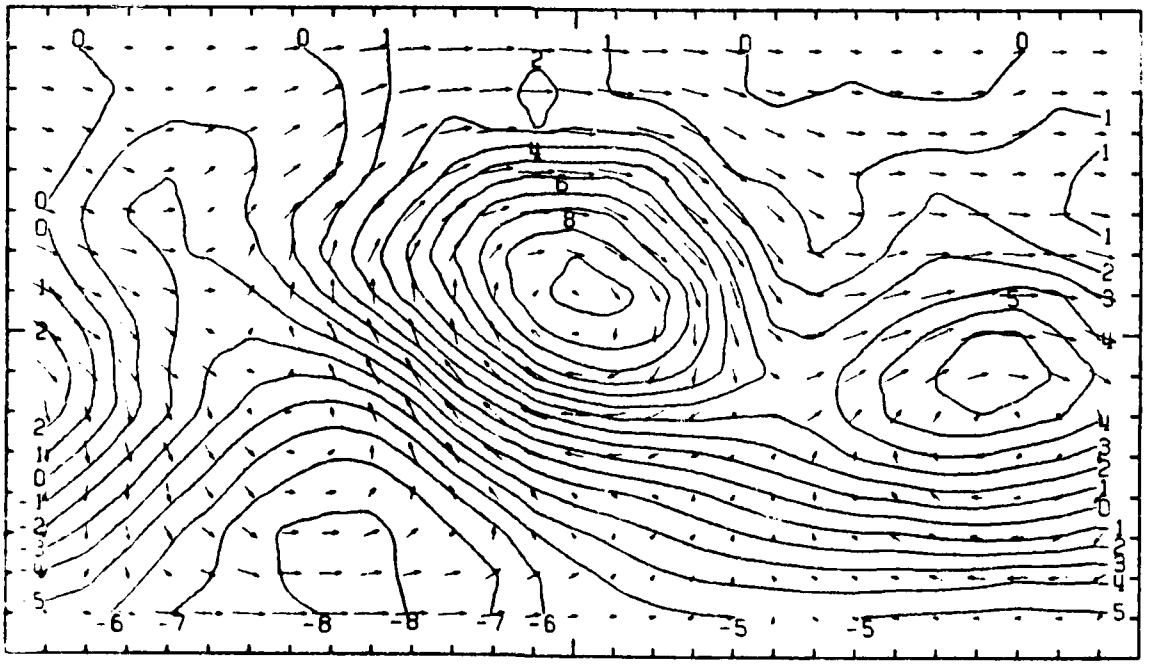

4TH-ORDER SCHEME
DAY 20 HOUR 0 LAYER 1

SCALE
— HEIGHT
20 M/SEC 100M

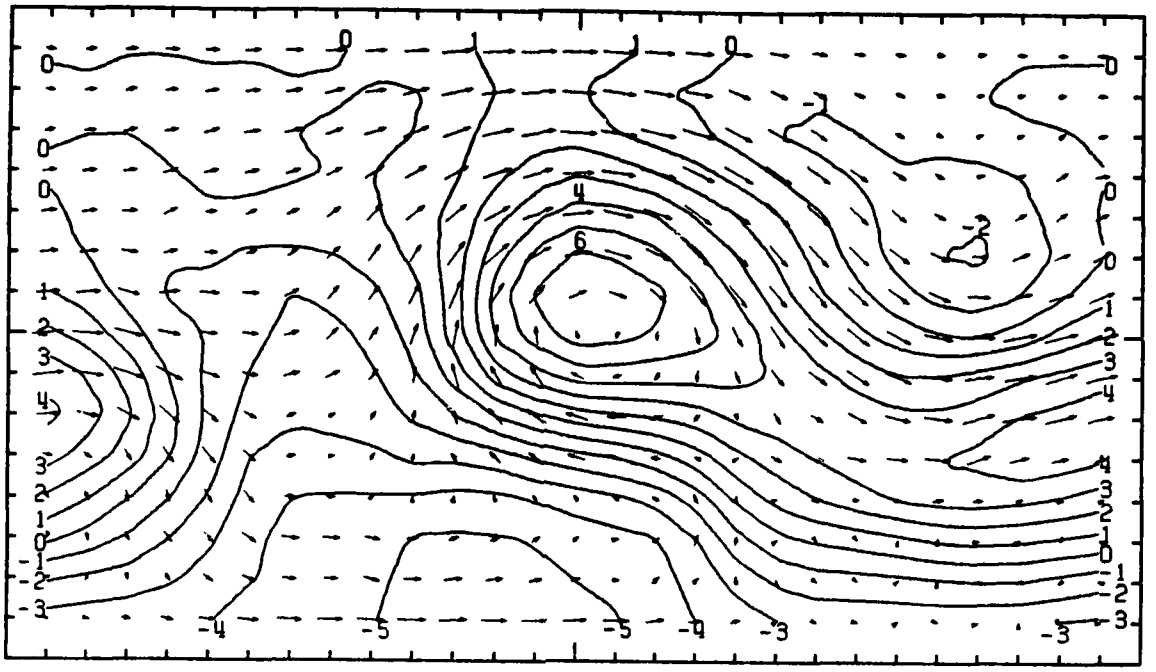

2ND-ORDER SCHEME
DAY 20 HOUR 0 LAYER 1

SCALE
— HEIGHT
20 M/SEC 100M

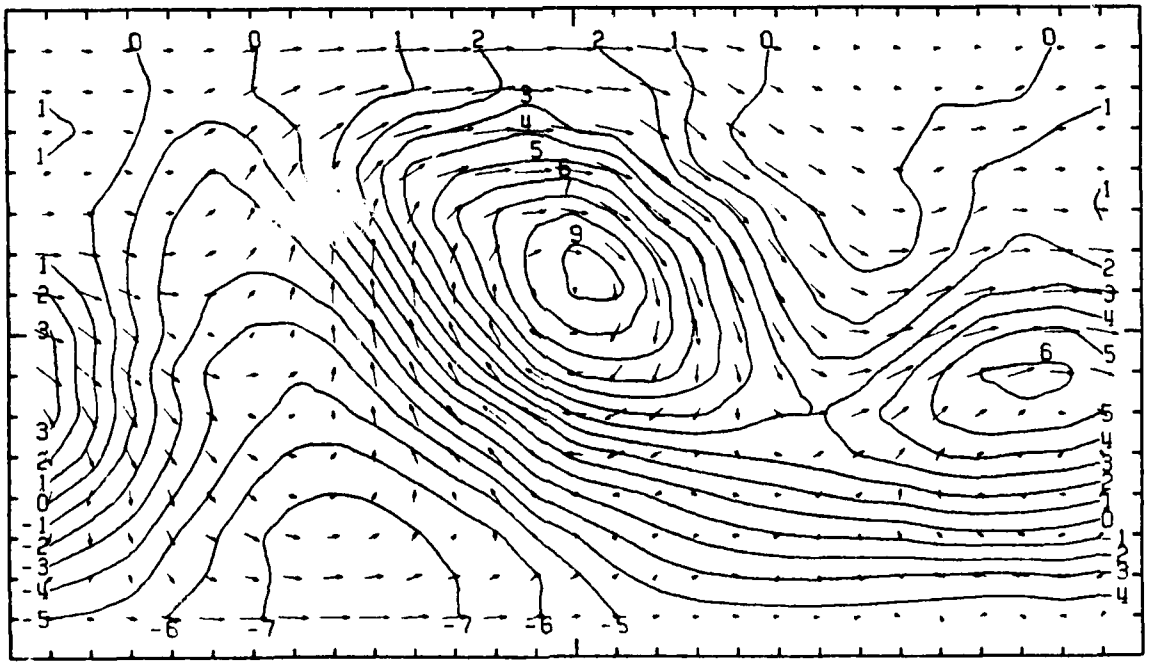

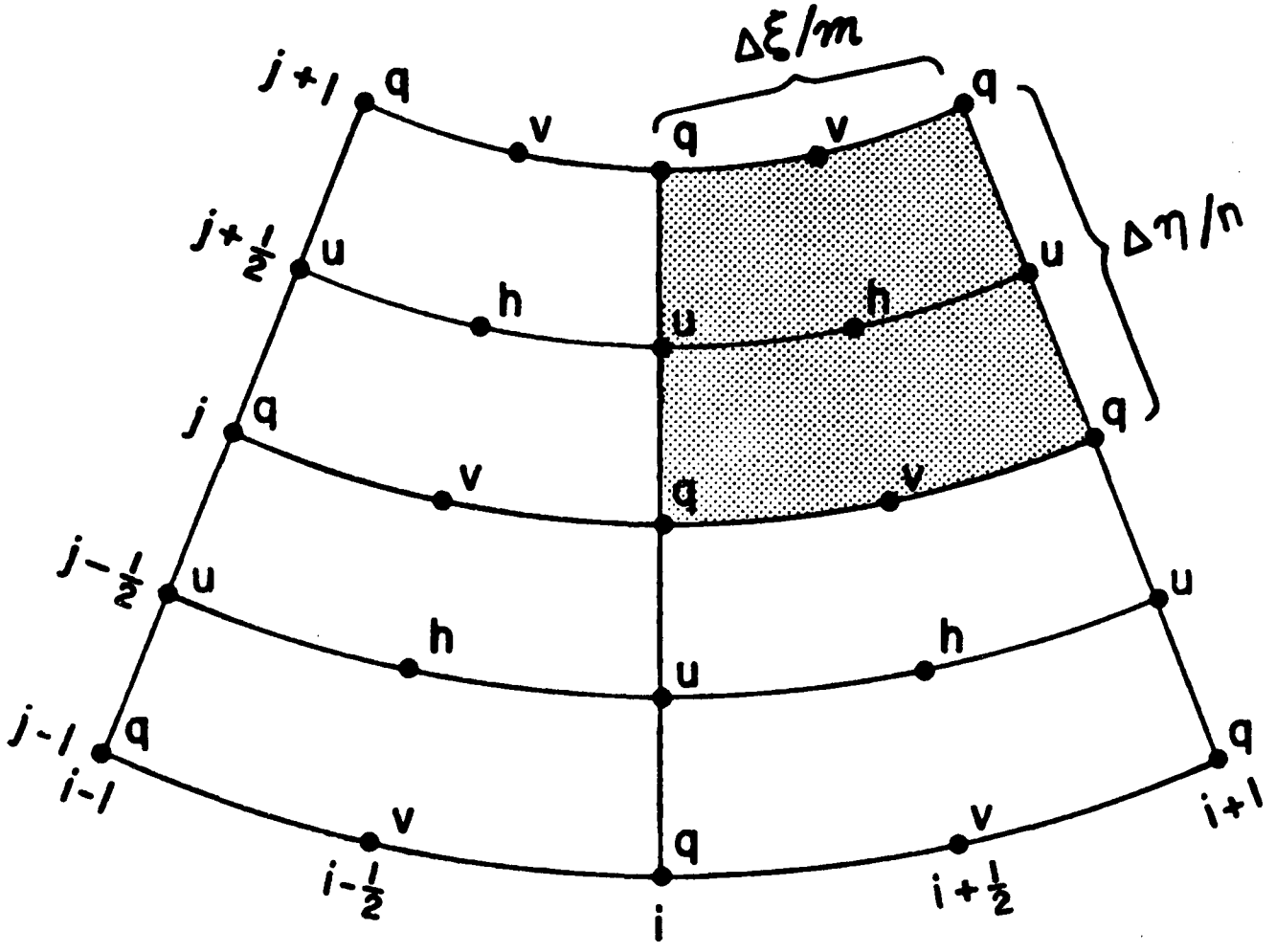

Figure B1.

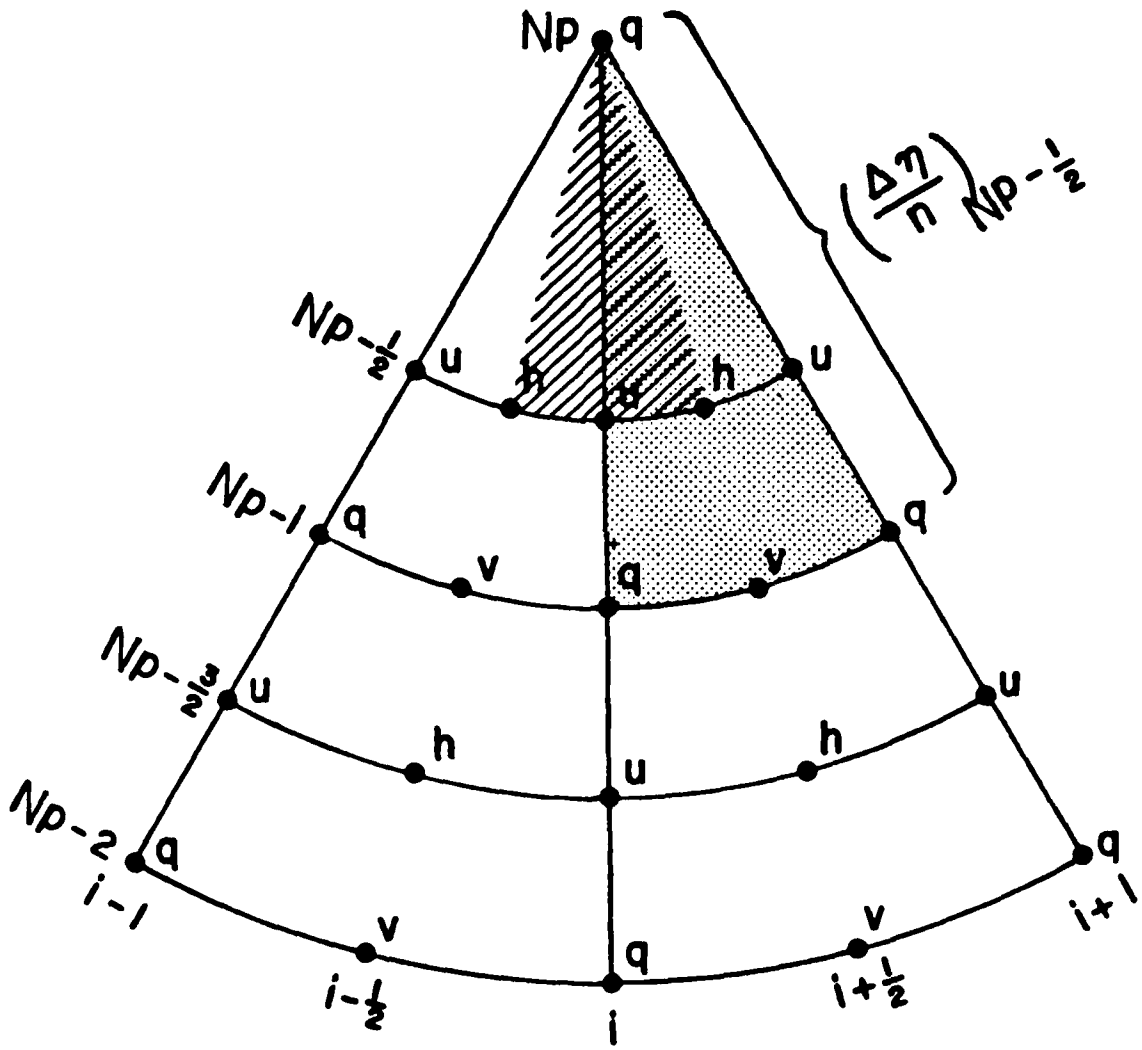
Np
q
$\left(\frac{\Delta\eta}{n}\right)_{Np-\frac{1}{2}}$
$Np-\frac{1}{2}$
u
h
h
u
Np-1
q
v
q
v
q
$Np-\frac{3}{2}$
u
h
u
h
u
Np-2
q
v
q
v
q
i-1
$i-\frac{1}{2}$
i
$i+\frac{1}{2}$
i+1

Figure B2.